Fluorescence in blue light (FLU): Functional analysis of its structural domains for light and dark-dependent control of ALA synthesis

DISSERTATION

zur Erlangung des akademischen Grades

doctor rerum naturalium

(Dr. rer. nat.)

im Fach Biologie

eingereicht an der

Lebenswissenschaftlichen Fakultät

der Humboldt-Universität zu Berlin

von

M.Sc. Zhiwei Hou

Präsidentin der Humboldt-Universität zu Berlin

Prof. Dr.-Ing. Dr. Sabine Kunst

Dekan der Lebenswissenschaftlichen Fakultät

Prof. Dr. Bernhard Grimm

Gutachter/innen: 1. Prof. Dr. Bernhard Grimm

2. Prof. Dr. Christian Schmitz-Linneweber

3. Prof. Dr. Thomas Pfannschmidt

Tag der mündlichen Prüfung: 16.12.2019

Table of contents

Abstract

Fluorescence in blue light (FLU), a negative feedback regulator of chlorophyll biosynthesis, is involved in dark repression of 5-aminolevulinic acid (ALA) synthesis. FLU is part of a complex comprising the enzymes catalyzing the final steps of chlorophyll synthesis. Three functional domains were proposed in the *Arabidopsis* FLU protein: a tetratricopeptide repeat (TPR) domain is at the C-terminus; a transmembrane domain (TM) is at the N-terminus; a coiled-coil domain (linker) is in between. The TPR(FLU) domain interacts with the C-terminal end of glutamyl-tRNA reductase (GluTR), the rate-limiting enzyme of ALA synthesis.

The *flu* mutant cannot grow under light dark conditions due to an over-accumulation of Pchlide in the dark period. It is generally accepted that the major role of FLU is to repress ALA synthesis in the dark. However, ALA synthesis is increased in *flu* relatively to WT even under continuous light, indicating that FLU also plays a role in light. In this study, the regulatory impact of FLU in light was investigated in the light-exposed FLU overexpressing (FLUOE) lines and in WT and *flu* seedlings grown under fluctuating light. FLUOE resulted in repression of ALA synthesis, thereby reduces chlorophyll biosynthesis even in light. The repression is stronger in low and high light than in medium growth light, which indicates that FLU action on ALA synthesis is affected by light intensity. Moreover, less amounts of membrane-associated GluTR was found in the light-exposed *flu* than in WT seedlings, which indicates a portion of GluTR in light to be bound by FLU. Finally, the *flu* mutant grows WT-like under continuous light but showed a pale-green phenotype under fluctuating light growth conditions. In conclusion, FLU not only mediates the repression of ALA synthesis in darkness, but also functions in light, especially under changing light intensities to fine-tuned ALA synthesis for chlorophyll biosynthesis.

The enzyme activity of GluTR was decreased with the TPR(FLU)-domain-containing peptide in an in vitro experiment. It is still questionable whether the synthesis of the TPR(FLU) peptide is sufficient for the GluTR inactivation as it was shown for the endogenous FLU in planta. The role of the functional domains of FLU in the inactivation of ALA synthesis was investigated in *flu* complementation lines which expressed either the TPR(FLU), FLUΔlinker or FLUΔTM peptides. GluTR content increased in all of these complementation lines compared to wild type and the predominant portion of GluTR was always in the same fraction as the truncated FLU peptides. The expression of TPR(FLU) alone or FLUΔlinker in *flu* did not rescue the *flu* phenotype although the interaction between TPR(FLU) and GluTR was demonstrated by pull-down experiments. However, FLUΔTM (TPR and linker domain) expression resulted in a partial complementation, indicating that the linker domain is essential for the inactivation of ALA synthesis. Moreover, in light-exposed plants, the expression of the FLUΔlinker peptide (TPR and TM domain) in *flu* caused a reduced ALA synthesis compared to the *flu* mutant, indicating that binding of GluTR to the membrane represses ALA synthesis. Therefore, not only the TPR(FLU) but also TM and linker domains are required for the inactivation of ALA synthesis. In addition, bimolecular fluorescence complementation and yeast two-hybrid assays revealed interaction of GluTR with PORB. Besides with GluTR, FLU interacts also with PORB

and CHLM. A controlled FLU-induced GluTR inactivation is proposed when both proteins are stabilized in a protein complex consisting of enzymes involved in the last steps of chlorophyll biosynthesis at the plastidic membranes.

In summary, this thesis contributes to the extended knowledge about the function of FLU in light as well as the role of the structural domains of FLU in the inactivation of ALA synthesis.

Keywords: Fluorescence in blue light; ALA synthesis; glutamyl-tRNA reductase; tetrapyrrole biosynthesis; fluctuating light.

Zusammenfassung

Fluorescence in blue light (FLU) ist ein negativer Feedbackregulator der Chlorophyllbiosynthese, welcher an der Dunkelrepression der 5-Aminolävulinsäure (ALA)-Synthese beteiligt ist. FLU ist Teil eines Komplexes, der die Enzyme umfasst, welche an der Katalyse der finalen Schritte der Chlorophyllbiosynthese beteiligt sind. Drei funktionelle Domänen wurden für das *Arabidopsis* FLU Protein postuliert: eine Tetratricopeptid-Wiederholungsdomäne (TPR) befindet sich am C-Terminus; eine Transmembrandomäne (TM) ist am N-Terminus lokalisiert; eine *Coiled-coil*-Domäne (linker) liegt dazwischen. Die TPR-Domäne von FLU Domäne interagiert mit dem C-terminalen Ende der Glutamyl-tRNA Reduktase (GluTR), dem geschwindigkeitsbestimmenden Enzym der ALA-Synthese.

Da die *flu* Mutante in Dunkelphasen Protochlorophyllid (PChlid) akkumuliert, ist die Mutante nicht in der Lage unter Licht Dunkel Bedingungen zu wachsen. Die Repression der ALA-Synthese in Dunkelheit durch FLU wird allgemein als dessen Hauptfunktion angesehen. Dennoch ist die ALA-Synthese in der *flu* Mutante auch unter Dauerlicht relativ zum Wildtyp (WT) erhöht, was auf eine zusätzliche Funktion von FLU im Licht hindeutet. In dieser Arbeit wurde der regulatorische Einfluss von FLU unter Belichtung erforscht. Dies erfolgte in Licht-exponierten FLU Überexpressoren (FLUOE), im WT, sowie in *flu* Keimlingen, welche unter fluktuierendem Licht angezogen wurden. FLUOE verursachten die Repression der ALA-Synthese, folglich beeinflusst FLU die Chlorophyllsynthese auch im Licht. Diese Repression fällt im Niedrig- und Hochlicht stärker aus als bei moderatem Wachstumslicht. Dies lässt darauf schließen, dass die Wirkung von FLU von der Lichtintensität abhängt. Zusätzlich konnten in belichteten *flu* Mutanten geringere Mengen an membranassoziiertem GluTR im Vergleich zum WT detektiert werden. Dies deutet darauf hin, dass ein Teil der GluTR Fraktion auch im Licht von FLU gebunden wird. Auch wächst die *flu* Mutante unter Dauerlicht wildtypartig, zeigt jedoch einen blass-grünen Phänotyp unter fluktuierenden Wachstumsbedingungen. Zusammenfassend ist FLU folglich nicht nur an der Dunkelrepression der ALA-Synthese beteiligt, sondern wirkt ebenfalls in der Lichtphase an der Feinjustierung der ALA-Synthese, besonders unter wechselnden Lichtbedingungen.

Die Enzymaktivität von GluTR wurde mit einem Peptid, das lediglich die TPR(FLU) Domäne enthielt, in einem *in vitro*-Experiment verringert. Es ist immer noch fraglich, ob die Synthese des TPR (FLU) Peptids für die GluTR-Inaktivierung ausreicht, wie dies für das endogene FLU Protein *in planta* gezeigt wurde. Die Rolle der funktionellen Domänen von FLU bei der Inaktivierung der ALA-Synthese wurde in *flu* Komplementierungslinien untersucht, die entweder die TPR(FLU), FLUΔlinker oder FLUΔTM Peptide exprimierten. Der GluTR-Gehalt stieg in allen untersuchten Komplementierungslinien im Vergleich zum Wildtyp an und der überwiegende Anteil von GluTR lag stets in der gleichen Fraktion vor wie die verkürzten FLU-Peptide. Die Expression von TPR(FLU) allein oder von FLUΔlinker in der *flu* Mutante komplementierte den *flu* Phänotyp nicht, obwohl die Interaktion zwischen TPR(FLU) und GluTR durch Pulldown-Experimente nachgewiesen wurde. Die Expression von FLUΔTM (TPR und Linkerdomäne) führte jedoch zu einer partiellen

Komplementierung, was darauf hinweist, dass die Linkerdomäne für die Inaktivierung der ALA-Synthese wesentlich ist. Darüber hinaus verursachte die Expression des FLUΔlinker-Peptids (TPR und TM Domäne) im Hintergrund der *flu* Mutante in lichtexponierten Pflanzen eine verringerte ALA-Synthese im Vergleich zur *flu* Mutante, was darauf hinweist, dass die Bindung von GluTR an die Membran die ALA-Synthese unterdrückt. Daher wird zur Inaktivierung der ALA-Synthese nicht nur die TPR(FLU), sondern auch TM und Linkerdomänen benötigt. Zusätzlich zeigten bimolekulare Fluoreszenzkomplementierungen und Hefe-Zwei-Hybrid-Assays eine Interaktion zwischen GluTR und PORB. Neben GluTR interagiert FLU auch mit PORB und CHLM. Es wird vorgeschlagen, dass die kontrollierte FLU-induzierte GluTR-Inaktivierung dann stattfindet, wenn beide Proteine in einem Proteinkomplex stabilisiert werden, der aus Enzymen besteht, die an den letzten Schritten der Chlorophyll-Biosynthese an den plastidären Membranen beteiligt sind.

Zusammenfassend trägt diese Arbeit zur Erweiterung des Wissen über die Funktion von FLU im Licht sowie über die Rolle der funktionellen Domänen von FLU bei der Inaktivierung der ALA-Synthese bei.

Schlagworte: Fluoreszenz in blauem Licht; ALA-Synthese; Glutamyl-tRNA-Reduktase; Tetrapyrrol-Biosynthese; schwankendes Licht.

Abbreviations

AB, acrylamide-bisacrylamide

ABA, Abscisic Acid

ABRC, Arabidopsis Biological Resource Center

ALA, 5-aminolevulinic acid

ALAD, ALA dehydratase

ALAS, ALA synthase

APRs, aggregation-prone regions

APS ammonium persulfate

AVT, AtGenExpress Visualization Tool

BCA, bicinchoninic acid

BSA, bovine serum albumin

CAB domain, Chlorophyll a/b binding domain

CaMV, Cauliflower mosaic virus

CCA1, Circadian clock-associated1

cDNA, complementary DNA

Chl, chlorophyll

Chlide, chlorophyllide

CHLM, MgP methyltransferase

Clp, Caseinolytic peptidase

CLSM, confocal laser-scanning microscope

COP1, constitutive photomorphogenic 1

Copro III, coproporphyrinogen III

CPOX, Copro III oxidase

cpSRP, chloroplast signal recognition particle

ddH_2O, double distilled water

DMSO, dimethyl sulfoxide

DNA, desoxyribonucleic acid

dNTP, deoxyribonucleoside triphosphate

DPOR, dark-dependent Pchlide reductase

DTT, dithiothreitol

ECL, enhanced chemiluminescence

EDTA ethylenediaminetetraacetic acid

EDTA, Ethylenediaminetetraacetic acid

et al. ET ALTERA

EX1, Executer 1

FAD, flavin adenine dinucleotide

FeCh, Ferrochelatase

FLP, FLU-like protein

FLU, Fluorescence in blue light

FLU, Fluorescent in blue light

FMN, flavin mononucleotide

FW, fresh weight

GBP, GluTR binding protein

GFP, green fluorescent protein

GLK, Golden2-like

GluRS, Glutamyl-tRNA synthetase

GluTR, glutamyl-tRNA reductase

GRX, glutathione/glutaredoxin

GSA, glutamate 1-semialdehyde

GSAT, GSA aminotransferase

GUN4, Genomes Uncoupled 4

HA, human influenza hemagglutinin

HBD, heme-binding domain

HL, high light

HO, heme oxygenase

HPLC, high-performance liquid chromatography

HRP, Horseradish peroxidase

IPTG, isopropyl-β-d-thiogalactoside

ITC, isothermal titration calorimetry

kDa, kilo Dalton

LB, Lysogeny broth

LHC, light-harvesting complexes

M, molar

MgP, Mg protoporphyrin IX

Min, minutes

MME, MgP monomethylester

MS, mass spectrometry

MS, Murashige & Skoog Medium

NADH, reduced nicotinamide adenine dinucleotide

NADP, nicotinamide adenine dinucleotide phosphate

NASC, Nottingham Arabidopsis Stock Centre

NBT, nitro blue tetrazolium

NPQ, non-photochemical quenching

NTR, NADPH-dependent TRX-reductase

PBG, porphobilinogen

PBS, phosphate-buffered saline

PCD, programmed cell death

PCR, polymerase chain reaction

PGR 7, proton gradient regulation 7

PhANGs, Photosynthesis associated nuclear genes

PIFs, Phytochrome-interacting factors

PLP, pyridoxal phosphate

PMP, pyridoxamine phosphate

POR, protochlorophyllide oxidoreductase

PPOX, protoporphyrinogen IX oxidase

Proto IX, protoporphyrin IX

qRT-PCR, quantitative real-time PCR

RNA, ribonucleic acid

ROS, reactive oxygen species

Rpm, rounds per minute

RT, room temperature

SAM, S-adenosyl-L-methionine

TAE, Tris-acetate-EDTA

TBE, Tris-borate-EDTA

TBS, tetrapyrrole biosynthesis

TBST, Tris-buffered saline incl. Tween

TCA, trichloroacetic acid

T-DNA, transferred DNA of the Ti plasmid of A. tumefaciens

TE buffer, Tris-hydrochloride buffer

TEMED, tetramethylethylenediamine

TM, transmembrane domain

TPR, tetratricopeptide repeat

Tris, Tris(hydroxymethyl)aminomethane

UPM1, dependent methyltransferase

Uro III, uroporphyrinogen III

UROD, Uro III decarboxylase

UROS, Uro III synthase

WT, wild type

xg, times gravitational force

YFP, yellow fluorescent protein

1 Introduction

Tetrapyrroles are biomolecules consisting of four pyrroles. They are among the most ubiquitous molecules. Four classes of tetrapyrroles, namely chlorophyll (Chl), heme, siroheme, and phytochromobilin, play essential roles in higher plants (Grimm, 1998; Battersby, 2000; Grimm, 2003; Grimm et al., 2007; Tanaka and Tanaka, 2007; Tanaka et al., 2011). Chl is the most abundant pigment in plants. Around 10^9 tons of Chl are produced annually, mainly in the oceans (Rüdiger, 1997; Eckhardt et al., 2004; Grimm et al., 2007). They conduct principal light energy capture in light-harvesting complexes (LHC) and energy transfer to the reaction centers of photosystem I and II. Five distinctive types of Chl exist in oxygenic photosynthetic organisms, namely Chl a, b, c, d, and the recently discovered f (Chen et al., 2010). All these types contain an identical macrocyclic ring with a central Mg iron, but with some modified side chains or hydration states, which contribute to the modified absorption properties that allow photosynthetic organisms to broaden the light absorption range at different wavelengths (Strain et al., 1963; Suzuki et al., 1997). Chl a is found in nearly all oxygenic photosynthetic organisms as the major pigment. Higher plants contain Chl a as the major pigment and Chl b as the accessory pigment (Grimm et al., 2007; Tanaka and Tanaka, 2007; Chen et al., 2010). Chl d and Chl f are far-red absorbing Chl, enabling photosynthesis under near infrared radiation. In *Acaryochloris marina,* Chl d replaces Chla as the major pigment not only in LHC but also in reaction centers photosystem I and II (Hu et al., 1998).

Heme serves an essential function in photosynthesis and respiration. Plants synthesize different types of heme. Heme b, also named protoheme, is the most abundant heme and the precursor for other types. Heme a and c contain modified side chains, which facilitate the covalent binding to different apoproteins (Hou et al., 2006; Tanaka and Tanaka, 2007). Siroheme is the cofactor of nitrite and sulfite reductase. It plays an important role in nitrogen and sulfate assimilation. S- or N-containing compounds are only produced in plants while animals acquired them in the diet. Phytochromobilin is the chromophore of phytochrome, which mediates the light perception in plants (Quail et al., 1995; Furuya and Schäfer, 1996; Kohchi et al., 2001; Kendrick and Kronenberg, 2012).

1.1 The de novo synthesis of tetrapyrroles in higher plants

The de novo synthesis of tetrapyrroles utilizes glutamate as a substrate in higher plants (Tanaka and Tanaka, 2007). Glutamate is first converted to 5-aminolevulinic acid (ALA), the universal precursor for tetrapyrrole biosynthesis (TBS). Eight molecules of ALA are then synthesized to the first cyclic tetrapyrrole, namely uroporphyrinogen III (Uro III). The synthesis of siroheme deviates from the other TBS pathways after the step of Uro III synthesis. Uro III is also utilized for the synthesis of protoporphyrin IX (Proto IX). Dependent on the insertion of an iron or magnesium cation into the macrocyclic ring, Proto IX is assigned to the heme branch or the Chl branch, respectively (Beale and Weinstein, 1990; Von Wettstein et al., 1995; Reinbothe et al., 1996; Heinemann et al., 2008). Phytochromobilin biosynthesis begins with the breakdown of heme by heme oxygenase (Beale, 1993) (Figure 1.1).

Figure 1.1 TBS pathway in higher plants. TBS in plants utilizes glutamate as the substrates to synthesize four classes of tetrapyrrole end products. 5-Aminolevulinic acid (ALA) is the first molecule committed to TBS and can be used for the synthesis of Uro III, which is an intermediate for the synthesis of Proto IX or siroheme. Proto IX is the branch point of heme and chlorophyll biosynthesis. Phytochromobilin synthesis begins with the break-down of heme. ALAD, ALA dehydratase; CAO, chlorophyllide a oxidase; CBR, chlorophyll b reductase; CHL27, MgP monomethylester cyclase; CHLM, MgP methyltransferase; CPOX, Coproporphyrinogen III oxidase; CS, chlorophyll synthase; FeCh, Ferrochelatase; GluRS, glutamyl-tRNA synthetase; GluTR, glutamyl-tRNA reductase; GSAT, glutamate-1-semialdehyde aminotransferase; MgCh, Mg chelatase; PBGD, PBG deaminase; POR, light-dependent NADPH-protochlorophyllide oxidoreductase; PPOX, protoporphyrinogen IX oxidase; Proto IX, protoporphyrin IX; TBS, tetrapyrrole biosynthesis; Uro III, Uroporphyrinogen III. Solid lines refer to one single enzymatic step while dashed lines refer to several steps.

1.1.1 ALA synthesis

ALA synthesis in different organisms is conducted by two different pathways, namely the C4 or C5 pathway according to the number of carbon atoms of the substrates (Shin et al., 2007). The C4 pathway is mainly found in non-photosynthetic eukaryotic organisms such as animals, yeast, and fungi. ALA is formed in this pathway by condensation of succinyl-coenzyme A with glycine catalyzed by the pyridoxal-P-containing ALA synthase (ALAS). The C5 pathway exists in photosynthetic organisms like plants, algae, cyanobacteria, some photosynthetic bacteria, eubacteria and also some non-photosynthetic prokaryotic bacteria, such as

Escherichia coli (Beale and Weinstein, 1990; Ilag et al., 1994; Von Wettstein et al., 1995). The C5 pathway forms ALA by utilization of glutamate as the substrate by 3 enzymatic reactions. First, glutamate is activated by ligating to a $tRNA^{Glu}$, which is also a common step to protein synthesis. This step is catalyzed by Glutamyl-tRNA synthetase (GluRS). The second step is the reduction of the activated $tRNA^{Glu}$ by the NADPH-dependent glutamyl-tRNA reductase (GluTR) to form glutamate 1-semialdehyde (GSA). Finally, GSA is converted to ALA catalyzed by GSA aminotransferase (GSAT). The C5 pathway is a more ancient pathway than the C4 pathway. The structural analysis of GSAT from cyanobacteria reveals a structural relationship to ALAS, indicating that ALAS might be evolved from GSAT (Schulze et al., 2006a). Succinyl CoA is the substrate for ALAS. It is dominantly synthesized and metabolized in mitochondria (Beevers, 1961; Wellburn, 1975). Interestingly, by introducing ALAS into chloroplasts, higher plants can also utilize ALAS to produce ALA for Chl biosynthesis. Previous experiments have shown that the Chl-deficient transgenic lines, expressing GSAT antisense RNA, returned green when imported with exogenous ALAS from yeast (Zavgorodnyaya et al., 1997). Enzymes and their encoding genes involved in ALA synthesis in higher plants are detailed in the following chapters.

1.1.1.1 GluRS

The reaction catalyzed by GluRS is conducted in two steps. The initial step is to form an enzyme-bound aminoacyl adenylate as an intermediate. An ATP is consumed in this step. Subsequently, the $tRNA^{Glu}$ is acylated with glutamate (Freist et al., 1997). In *Arabidopsis,* GluRS is coded by a single gene, *GluRS* (AT5G26710). The amino acid sequence of GluRS from *Arabidopsis* showed strong sequence similarity to GluRS in other species (Day et al., 1998). GluRS from different species recognizes $tRNA^{Glu}$ from various sources. The plastidic GluRS is synthesized in the cytoplasm and transferred to chloroplasts. Unlike GluRS, the $tRNA^{Glu}$, involved in ALA synthesis, is encoded by the chloroplast DNA in higher plants (Ratinaud et al., 1983; Andersen and Burbidge, 1992; Masuda et al., 1995; Rogers and Söll, 1995).

1.1.1.2 GluTR encoding genes and protein structure

In *Arabidopsis*, three genes are found encoding GluTR, namely, *HEMA1* (At1g58290), *HEMA2* (At1g09940), and *HEMA3* (At2g31250) (Ilag et al., 1994; Kumar and Söll, 2000). The *HEMA1* and *HEMA2* homologous genes have been found in all reported angiosperms plants; for example, *barley* (Bougri and Grimm, 1996; Vothknecht et al., 1996) and *cucumber* (Tanaka et al., 1996). Some species contained more than 2 copies; for example, six were identified in *Glycine max* (Sangwan and O'Brian, 1999). However, *cyanobacteria* and most of the algae, such as *C. reinhardtii* have only one GluTR encoding gene (Vasileuskaya et al., 2005). The duplication of *HEMA* genes might be taking place during evolution. In *Arabidopsis*, the homozygous *HEMA1* mutant can only grow when supplied with sugar, but showed severe growth retardation, with pale-green leaves, Whereas the knock-out mutant of *HEMA2* does not show any visible mutant phenotype (Apitz et al., 2014). *HEMA1* takes the major responsibility for ALA synthesis activities. The role of *HEMA2* is likely assigned to

provide the substrate for heme biosynthesis and can also affect Chl synthesis, especially under certain stress conditions. *HEMA3* is proposed to be a pseudogene.

The crystal structure of bacterial GluTR from *Thermus thermophiles* was first unveiled by Moser et al., 2001. Each monomer consists of three domains, which are the catalytic domain, NADPH-binding domain, and the dimerization domain, in the order from the N-terminal to C-terminal end. A GluTR dimer forms a V-shaped structure which is the functional unit for ALA synthesis. The V-shaped GluTR dimer provides enough space for interaction with the GSAT dimer or regulating proteins. The crystal structure of GluTR from *Arabidopsis thaliana* was recently reported. The V-shaped dimer structure from *Arabidopsis* is similar to GluTR from *Methanopyrus kandleri* (Zhao et al., 2014). The mutation of cysteine114 of GluTR abolishes its enzyme activity. It was suggested that this cysteine allows the transfer of hydride from NADPH to the thioester-bound glutamate (Moser et al., 2001; Zhao and Han, 2018).

GluTR has a strong preference for the substrate. Stange-Thomann et al., 1994 found a point mutation of plastid $tRNA^{Glu}$ which leads to the inhibition of ALA synthesis, but not of protein synthesis. Another study revealed that chloroplast GluRS from barley accepts $tRNA^{Glu}$ from *Chlamydomonas reinhardtii*, *tobacco*, *cucumber*, *yeast* as well as *Escherichia coli,* but GluTR from barley does not recognize glutamyl-$tRNA^{Glu}$ from *E.coli* or yeast effectively (Willows et al., 1995). GluTR seems to have more rigorous requirements for the substrates than GluRS. However, high ALA synthesis activity was recently detected by using tRNA from bacteria (Zhao et al., 2014). This observation seems to contradict the previous findings. It could be that *Arabidopsis* GluTR can still utilize tRNA from *E.coli* but is less efficient than tRNA source from *Arabidopsis*.

1.1.1.3 GSAT

The conversion of GSA to ALA conducted by GSAT. The reaction requires pyridoxamine phosphate (PMP) as a cofactor. The catalyzing reaction starts from an amino group being transferred from PMP to the substrate GSA when a diamino intermediate and pyridoxal phosphate (PLP) is formed. In a second step, the original amino group of GSA is transferred to PLP, resulting in the regeneration of PMP and the formation of ALA (Song et al., 2016). In *Arabidopsis*, there are two genes encoding GSAT, *GSAT1*(AT5G63570), and *GSAT2* (AT3G48730). They share 90% of sequence identity. Both *GSAT1* and *GSAT2* are highly expressed in leaves. The Chl content is reduced to less than 10% of wild type (WT) in GSAT-antisense tobacco lines (Hartel et al., 1997). Deficiency of *GSAT1* or *GSAT2* alone does not cause a substantial Chl reduction but only leads to a pale-green phenotype (Toyokura et al., 2015). The crystal structure of GSAT1 from *Synechococcus sp. PCC 6301* revealed that GSAT1 forms an asymmetric homodimer with the cofactor (Hennig et al., 1997; Song et al., 2016). From the proposed structure of GluTR-GSAT tetramer, an intermolecular channel for direct transfer of GSA to the active site of GSAT is formed to avoid the release of the highly reactive aldehyde group of GSA (Moser et al., 2001).

1.1.2 From ALA synthesis to the formation of Uro III and siroheme

Two ALA molecules are condensed to porphobilinogen (PBG), the first pyrrole molecule in TBS pathway, by ALA dehydratase (ALAD). Subsequently, a linear tetrapyrrole, 1-hydroxymethylbilane is formed by four molecules of PBG catalyzed by the PBG deaminase (PBGD). This linear molecule is cyclized to form Uro III, the first macrocycle in the pathway by Uro III synthase. This reaction is catalyzed by Uro III synthase (UROS). In *Arabidopsis*, siroheme is formed by 3 enzymatic reactions by utilizing Uro III as the substrate. The first step is catalyzed by S-adenosyl-L-methionine (SAM) dependent methyltransferase (UPM1) to methylate Uro III. The product is then oxidized by an oxidase. Finally, Fe^{2+} is inserted into the macrocycle to form siroheme. This step is catalyzed by sirohydrochlorin ferrochelatase. The enzymes and their coding genes for Uro III or siroheme biosynthesis in *Arabidopsis* are listed in Table 1.1.

Table 1.1: List of enzymes and their coding genes for the synthesis of Uro III or siroheme in *Arabidopsis*.

Enzymes	Number of coding genes	Gene/enzyme names	AGI code
ALA dehydratase	2	*ALAD1*/ALAD1	At1g69740
		ALAD2/ALAD2	At1g44318
Porphobilinogen diaminase	1	*PBGD*/PBGD	At5g08280
Uroporphyrinogen III synthase	1	UROS/UROS	AT2G26540
SAM uroporphyrinogen III methyltransferase	1	UPM1	At5g40850

1.1.3 From Uro III to the synthesis of Proto IX

Uro III decarboxylase (UROD) catalyzes the decarboxylation reaction of Uro III to form coproporphyrinogen III (Copro III). The remaining two propionate side groups of Copro III are decarboxylated again by oxygen-dependent Copro III oxidase (CPOX), which leads to the formation of protoporphyrinogen IX. Subsequently, protoporphyrinogen IX is converted to Proto IX by protoporphyrinogen IX oxidase (PPOX). PPOX uses flavin adenine dinucleotide (FAD) as a cofactor and catalyzes six-electron oxidation of protoporphyrinogen IX (Lermontova et al., 1997). Proto IX is generally known as a potent photosensitizer and can cause lipid peroxidation and cell death. Mutants accumulating Proto IX are highly sensitive to light (von Gromoff et al., 2008; Brzezowski et al., 2014). The enzymes and their coding genes for Proto IX synthesis are listed in Table 1.2.

Table 1.2: List of enzymes and their coding genes for Proto IX in *Arabidopsis*.

Enzymes	Number of coding genes	Gene/enzyme names	AGI code
Uroporphyrinogen III decarboxylase	2	*UROD1*/ UROD1	At2g40490
		UROD2/ UROD2	At3g14930
Coproporphyrinogen III oxidase	2	*CPOX1*/CPOX1	At1g03475
		CPOX2/CPOX2	At4g03205
Protoporphyrinogen IX oxidase	2	*PPOX1*/PPOX1	At5g14220
		PPOX2/PPOX2	At4g01690

1.1.4 Enzymes committed to Chl biosynthesis

Proto IX is the branch point for Chl and heme biosynthesis. Proto IX is directed into the Chl biosynthesis branch when inserted with Mg^{2+} ion, and Mg protoporphyrin IX (MgP) is formed. This step is catalyzed by magnesium chelatase, which consists of 3 subunits, CHLH, CHLI, and CHLD. The reaction needs ATP to provide energy. The CHLI and CHLD form an initial complex which is confirmed to possess ATPase activity (Gibson et al., 1995; Willows et al., 1996; Hansson and Kannangara, 1997). The CHLH subunit can bind Proto IX. The Mg ion is inserted into Proto IX once the proto IX-binding CHLH interacts with the CHLI/D complex (Gorchein, 1972; Hinchigeri et al., 1997; Papenbrock et al., 2000). CHLH has previously been reported to be an abscisic acid (ABA) receptor, which enables the cooperation of Chl biosynthesis with seed germination, post-germination growth, stomatal movement, and other ABA-mediated physiological processes (Shen et al., 2006). The Genomes Uncoupled 4 (GUN4) stimulates the activity of Mg-chelatase, probably by facilitating the binding of porphyrins to CHLH. Furthermore, the binding of porphyrins to GUN4 was suggested to shield porphyrins from collisions with O_2, and thereby attenuate the production of reactive oxygen species (ROS) (Larkin et al., 2003; Adhikari et al., 2011). Although none of the three subunits are predicted to contain a transmembrane (TM) domain, this reaction is generally accepted as happening in the thylakoid membrane. It is speculated that some scaffolding protein (s) are involved in anchoring all the subunits in the membrane.

Subsequently, a methyl group from S-adenosyl-L-methionine is transferred to the carboxyl group of 13-propionate of MgP by MgP methyltransferase (CHLM), which leads to the formation of MgP monomethylester (MME). In the following step, MME cyclase catalyzes the integration of atomic oxygen into MME to form 3,8-divinyl protochlorophyllide (Pchlide). Pchlide is then reduced by protochlorophyllide oxidoreductase (POR) to form chlorophyllide (Chlide). Three POR isoforms are found in *Arabidopsis*, designated PORA, PORB, and PORC. Angiosperms only have light-dependent POR and some lower plants such as algae and cyanobacteria possess

both light-dependent and light-independent POR. The last step for Chl biosynthesis is conducted by Chl synthase using Chlide as the substrate to synthesize Chl a. The enzymes and their coding genes of Chl branch in *Arabidopsis* are listed in Table 1.3.

Table 1.3: List of enzymes and their coding genes of Chl branch in *Arabidopsis*.

Enzymes	Number of coding genes	Gene/enzyme names	AGI code
Mg-chelatase subunit I	2	*CHLI1*/ CHLI1	At4g18490
		CHLI2/ CHLI2	At5g45930
Mg-chelatase subunit H	1	*CHLH*/CHLH	At5g13630
Mg-chelatase subunit D	1	*CHLD*/CHLD	At1g08520
SAM Mg-protoporphyrin IX methyltransferase	1	CHLM/CHLM	At4g25080
Mg-protoporphyrin IX monomethylester cyclase	1	CHL27/CHL27	At3g56940
Protochlorophyllide oxidoreductase	3	PORA/PORA	At5g54190
		PORB/PORB	At4g27440
		PORC/PORBC	At1g03630
Chl synthetase	1	CHLG/CHLG	At3g51820

1.1.5 Enzymes for heme metabolism

Ferrochelatase (FeCh) catalyzes the insertion of a ferrous ion into Proto IX to form protoheme. This reaction does not require additional energy. Two isoforms of FeCh exist in *Arabidopsis* (FeCh1 and FeCh2). They have 83% similar amino acids and share a highly conserved structure except that FeCh2 has a unique putative Chl a/b binding domain (CAB domain) at the C-terminus (Chow et al., 1998; Suzuki et al., 2004; Sobotka et al., 2011; Pazderník et al., 2019). The CAB domain might serve as a regulatory domain to balance Chl biosynthesis with the synthesis of Chl-binding apoproteins (Sobotka et al., 2011; Woodson et al., 2011). The breakdown of heme is conducted by heme oxygenase (HO) to form biliverdin IXα, which can be used to synthesize phytochromobilin (Davis et al., 1999; Muramoto et al., 2002). The enzymes and their coding genes of heme branch in *Arabidopsis* are listed in Table 1.4.

Table 1.4: List of enzymes and their coding genes of heme branch in *Arabidopsis*.

Enzymes	Number of coding genes	Gene/enzyme names	AGI code
Ferrochelatase	2	*FeCh1*/ FeCh1	At5g26030
		FeCh2/ FeCh2	At2g30390
Heme oxygenase	4	*HO1*/HO1	At2g26670
		HO2/HO2	At2g26550
		HO3/HO3	At1g69720
		HO4/HO4	At1g58300

1.1.6 The localization of enzymes involved in TBS

Most of the enzymes involved in the TBS pathway in plants are localized in chloroplasts. The entire pathways for Chl and siroheme are exclusively in the chloroplast, where most of the end products fulfill their function. Although phytochrome is functioning in the cytosol, the synthesis of phytochromobilin is localized within the chloroplast (Kohchi et al., 2001). Whereas, the localization of enzymes involved in heme biosynthesis is less clear. Two isoforms of CPOX exist in *Zea mays* and *Arabidopsis*. One of the CPOX isoforms in *Zea mays* was found in mitochondria, and the other in chloroplasts, whereas in *Arabidopsis*, one CPOX isoform is proposed to be a pseudogene, and the other is exclusively localized in the chloroplast (Smith et al., 1993; Santana et al., 2002; Williams et al., 2006). CPOX of soybean (*Glycine max L.,*) is exclusively in chloroplast and not in mitochondria (Santana et al., 2002). PPOX was found localized in both mitochondria and chloroplast in numerous plant species, including *Arabidopsis* (Jacobs and Jacobs, 1987; Narita et al., 1996; Lermontova et al., 1997). However, PPOX was also reported to be exclusively in the chloroplast in *Chlamydomonas reinhardtii* (Van Lis et al., 2005). Regarding the localization of FeCh, most reports support the conclusion that FeCh exists exclusively in chloroplasts (Chow et al., 1998; Lister et al., 2001; Suzuki et al., 2002; Masuda et al., 2003a; Van Lis et al., 2005). However, the presence of PPOX or CPOX in mitochondria indicates also the possibility of heme synthesis in this organelle. It is not entirely excluded that trace amounts of FeCh are present in mitochondria, which are not detectable by current methods.

The initial steps of TBS, until the synthesis of Copro III, were previously thought to be taken place in the stroma (Pontoppidan and Kannangara, 1994; Eckhardt et al., 2004). Since the products of the following steps are phototoxic, enzymes for the following steps are believed to be localized at the thylakoid membrane, which helps to reduce the probability of the metabolic products reacting with O_2 and also to facilitate the delivery of products to the next enzymes (Eckhardt et al., 2004). The oxidation of

protoporphyrinogen by PPOX and most of the following steps are mainly localized at the thylakoid membrane.

ALA synthesis activity is present in the stroma fraction (Kannangara and Gough, 1977). Czarnecki and Grimm, 2012 recently found a small portion of GluTR in the membrane also. Wang et al., 2016 reported that the dominant amount of GluTR and GSAT, as well as most of the enzymes involved in TBS pathway, are presented in the margin area of the grana stacks of the thylakoid membranes. The inconsistent observations as to the ratio of the membrane-bound to the soluble GluTR might be explained by different procedures adopted for chloroplast isolation, the plant growth conditions, or various development stages. The detailed profile of GluTR localization under various growth conditions or development stages remains unclear.

1.2 The transcriptional regulation of TBS

By performing a mini-array system, Matsumoto et al., 2004 analyzed the expression profiles of genes involved in TBS at the onset of greening. Genes encoding enzymes for TBS pathway can be categorized into different type of classes . The first class includes *HEMA1, CHLH,* and *CHL27*. These are known as the most tightly regulated genes. They are rapidly induced by light and oscillate with diurnal rhythm (Bang et al., 2008; Legnaioli et al., 2009; Gendron et al., 2012; Kobayashi and Masuda, 2016). The second class widely includes genes coding for the enzymes from the early to end steps of TBS; some genes in the early steps, such as *GSAT*, *ALAD*, *PBGD*, *URO*, *CPO3*, and *PPO2*; some genes in the Chl branch, such as *CHLI*, *CHLD, CHLG* and some genes among the heme branch, such as *FeCh2*, *HO2*. The expression of genes of this class is primary controlled by light and oscillates with diurnal rhythm but with a smaller amplitude than of the first class. The third class includes genes relevant for heme metabolism such as *FeCh1*, *HEMA2, HO1.* Genes in this class are not responsive to light and circadian rhythms (Matsumoto et al., 2004).

PORA and *PORB* are expressed during skotomorphogenesis, germination, and greening. After illumination, *PORA* remains shortly expressed and is then negatively regulated while *PORB* and *PORC* are consistently expressed throughout leaf development (Lebedev et al., 1995). In green leaves, the expression of *PORB* is seven-folds higher than of *PORA* in the light and oscillates under control of the endogenous clock with circadian rhythm, but not of *PORC* (Frick et al., 2003). The expression of PORC is induced by high light (HL) and down-regulated in the dark, whereas *PORB* expression is not affected by light-dark shifts (Su et al., 2001; Masuda et al., 2003b; Paddock et al., 2012).

Most of the genes involved in Chl biosynthesis are induced by light and inactivated in the dark. In light, *Hy5* is one of the most important transcriptional factors, which activates many genes involved in Chl biosynthesis and also other light-associated physiologic processes. In the dark, constitutive photomorphogenic 1 (COP1) catalyzes the ubiquitination of Hy5, which leads to destabilization of Hy5, while in the light COP1 is inactivated. Phytochrome-interacting factors (PIFs) execute negative regulation in the dark to repress photomorphogenic responses, including

gene expression for Chl biosynthesis, whereas PIFs are phosphorylated and destabilized by the ubiquitin-proteasome system in the light (Leivar and Quail, 2011).

Key genes involved in TBS are also the targets of golden2-like (GLK) transcription factors which are required for chloroplast biogenesis (Waters et al., 2009; Leister and Kleine, 2016). Furthermore, many genes in TBS are also directly or indirectly controlled by the transcription factors involved in circadian regulation, such as the morning phase transcription factor circadian clock-associated1 (CCA1). CCA1 interacts with Hy5, regulating the expression of photosynthesis associated nuclear genes (PhANGs), including the genes in TBS (Salome et al., 2013; Wind et al., 2013). However, whether common cis-elements exist in the promoters of TBS genes for various transcription regulators are less studied.

1.3 Transcriptional regulation of ALA synthesis

In *Arabidopsis, HEMA1* is expressed in all organs but is dominantly expressed in photosynthetic tissue. The expression of *HEMA1* is light-induced and tightly regulated by a wide range of signals. It has been shown that the phytochrome photoreceptor family can mediate the light-dependent expression of *HEMA1* (Kasemir, 1983; Huang et al., 1989; McCormac et al., 2001). Plant hormones also affect the expression of *HEMA1*. Cytokinin induces the expression of *HEMA1* in the cotyledons of *C. sativus* and barley in light (Yaronskaya et al., 2006). *HEMA2* is weakly expressed in all tissue except in mature pollen according to the expression data from AtGenExpress Visualization Tool (AVT) (Everingham et al., 2005; Kilian et al., 2007). The expression of *HEMA2* can be induced under certain stress treatments, such as wounding (Nagai et al., 2007). Sucrose and glucose repress the gene expression of *HEMA1* and *HEMA2* in *Arabidopsis* (Ujwal et al., 2002). *HEMA3* is hardly expressed in most tissues.

Furthermore, the expression of *HEMA1* correlates with that of the *LHCb1* gene, which encodes a protein of LHC in photosystem II (McCormac and Terry, 2002; Matsumoto et al., 2004). Chl synthesis needs to be coordinated with the synthesis of Chl-binding apoproteins.

GSAT1 and *GSAT2* in *Arabidopsis* are expressed in all organs (Ilag et al., 1994; Muramoto et al., 2002). Expression of *GSAT1* and *GSAT2* is moderately light-induced and oscillates slightly by the endogenous clocks (Czarnecki et al., 2011). Induced gene expression of *GSAT* by light was also found in *C. reinhardtii* (Herman et al., 1999). On the other hand, light does not show any effect on the expression of *GSAT* in *C. sativus*, while in barley even a negative influence of light on *GSAT* expression was observed (Kumar et al., 1996). The expression of *GluRS* is not specifically controlled for TBS, as GluRS is also involved in plastid protein synthesis (Freist et al., 1997).

1.4 Post-translational regulation on ALA synthesis

Post-translational regulation is a fast, precise, and economical way to adjust ALA synthesis according to the requirements of TBS. Multiple post-translational controls

on ALA synthesis have been reported to be essential for fine-tuning ALA synthesis (Figure 1.2)(Richter and Grimm, 2019): Heme exerts a negative effect on ALA synthesis (Pontoppidan and Kannangara, 1994; Terry and Kendrick, 1999); Fluorescent in blue light (FLU) contributes to the feedback repression on ALA synthesis of Chl biosynthesis (Meskauskiene et al., 2001); Caseinolytic peptidase (Clp) is involved in the degradation of GluTR (Nishimura et al., 2013); GluTR binding protein (GBP) competes with the Clp protease for binding to the N-terminus of GluTR and prevents GluTR from degradation (Apitz et al., 2016); The chaperone chloroplast signal recognition particle (cpSRP) can prevent GluTR from aggregation (Wang et al., 2018). Moreover, some other mechanisms are predicted to be potentially involved in ALA synthesis regulation, such as the redox modifications of enzymes of ALA synthesis (Figure 1.2; Richter and Grimm, 2013). The detailed mechanisms are presented in the following chapters.

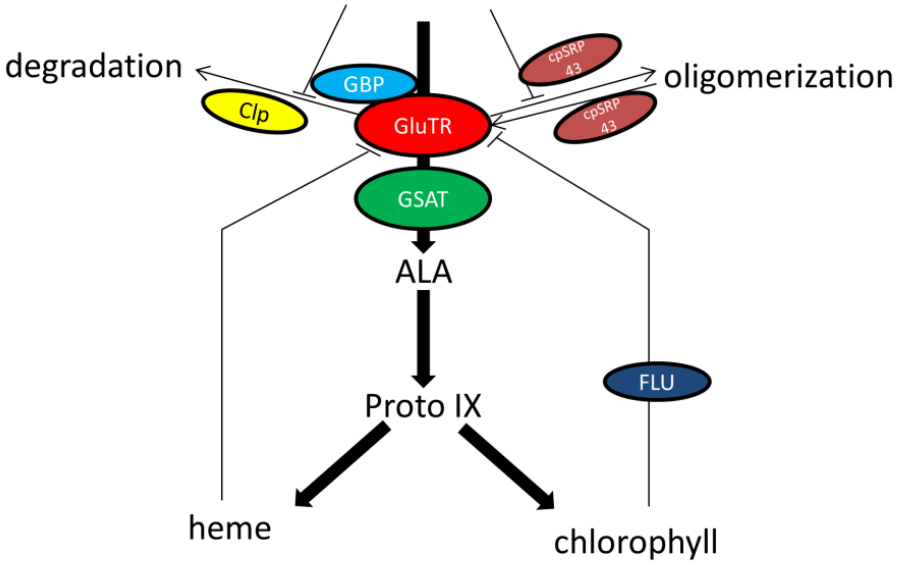

Figure 1.2 Multiple post-translational control mechanisms of ALA synthesis. A detailed description of the regulatory mechanisms is presented in the text. ALA, 5-aminolevulinic acid; Clp, Caseinolytic peptidase; cpSRP43, chloroplast signal recognition particle 43; FLU, Fluorescent in blue light; GBP, GluTR binding protein; GluTR, glutamyl-tRNA reductase; GSAT, glutamate-1-semialdehyde aminotransferase; Proto IX, Protoporphyrin IX.

1.4.1 The feedback repression of ALA synthesis mediated by heme

Evidence has been shown both in vitro and in vivo that heme inhibits ALA synthesis. In an in vitro assay, the enzyme activity of GluTR purified from barley chloroplasts or from *Synechocystis* sp. PCC 6803 cells are substantially repressed by adding heme

(Rieble and Beale, 1991; Pontoppidan and Kannangara, 1994). The conclusion that heme mediates inactivation on ALA synthesis is also supported by in vivo experiments. ALA synthesis rate is increased in etiolated seedlings of *Phaseolus vulgaris L. var.* when infiltrated with some iron chelators, such as α, α'-dipyridyl which is the inhibitor for heme biosynthesis (Duggan and Gassman, 1974). The reaction of heme degradation is catalyzed by HO. Knockout of *HO1* might cause the accumulation of heme. Matthew J. Terry et al. 1999 reported that a mutant of tomato lacking *HO1* showed repressed ALA synthesis rate (Terry and Kendrick, 1996). The accumulation of unbound free heme is proposed to act as an inhibitor of ALA synthesis. Several efforts were made to evaluate the content of free heme in plants. As against acetic acetone solution for the total heme extraction, neutral acetone is more specific for free heme extraction (Thomas and Weinstein, 1990; Espinas et al., 2012).

The N-terminus of GluTR was found to be essential for the feedback regulation by heme. The truncated GluTR with a deletion of the 30 amino acids at the N-terminus has the same activity as the intact GluTR but is highly resistant to the repression by heme (Vothknecht et al., 1998). Thus, the N-terminus of GluTR was previously designated as the heme-binding domain (HBD; Vothknecht et al., 1998; Goslings et al.,2004). It was speculated that heme binds directly to HBD and affects the enzyme activity of GluTR. However, it was recently shown that HBD was not involved in heme-binding. The accumulation of heme, induced by feeding with ALA, reduces the stability of GluTR (Richter et al., 2019).

Moreover, it has been shown that the enzyme activity of GluRS can be inhibited in vitro by heme, revealing that GluRS is also the target for heme-mediated feedback repression of ALA synthesis (Levicán et al., 2007).

Heme-dependent inhibition on ALA synthesis was not only found in organisms which synthesize ALA through C4 pathway but also in organisms, producing ALA by the C5 pathway (Ponka, 1997). Several mechanisms are involved in the downregulation of ALA synthesis by heme in organisms that synthesize ALA through the C4 pathway. Firstly, the half-life of *ALAS* mRNA is decreased when heme is accumulated in chicken embryo hepatocytes (Hamilton et al., 1991). Secondly, the association of heme to the heme-binding motif on ALAS enhances the formation of complexes between ALAS and ATP-dependent proteases, thereby accelerating the degradation of ALAS protein (Kubota et al., 2016). Moreover, heme blocks the translocation of ALAS precursor protein into mitochondria in the liver (Kikuchi and Hayashi, 1981).

1.4.2 FLU contribution to repression of ALA synthesis in the dark

Chl biosynthesis of higher plants is stopped at the formation of Pchlide in the dark. Pchlide is a highly photosensitive molecule. It is generally believed that to avoid the accumulation of Pchlide, plants need to inhibit Chl biosynthesis at the step of ALA synthesis in the dark. Feeding the etiolated seedlings with ALA, Pchlide is accumulated at a high level, indicating that dark-dependent rate of ALA synthesis limits Pchlide accumulation (Granick, 1959).

Several tigrina mutants of barley accumulate a high level of Pchlide in the dark (Nielsen, 1974; Von Wettstein et al., 1974). ALA synthesis rate is increased in the *tig* mutants (Gough and Kannangara, 1979). Subsequently, *Arabidopsis flu* was found to accumulate a high level of Pchlide in the dark (Meskauskiene et al., 2001). The etiolated seedlings of *flu* cannot green after exposure to light and do not survive light-dark conditions, whereas *flu* grows wild-type like under CL condition. The ALA synthesis rate in the *flu* mutant increases by four-fold in comparison with WT. Pchlide content in *flu* is nine times higher than WT in the dark. However, heme content in *flu* remained unchanged (Meskauskiene et al., 2001). The *tigrina d* of barley is an ortholog of the *FLU* gene of *Arabidopsis* (Lee et al., 2003). These data demonstrated that FLU is an essential negative regulator of ALA synthesis in the dark.

1.4.2.1 Interaction of FLU with GluTR isoforms

GluTR is encoded by three genes in *Arabidopsis* as mentioned before (Chapter 1.1.1.2). FLU interacts only with GlulTR1 but not with GluTR2 in a yeast two-hybrid assay, although the similarity of the two GluTR isoforms is over 80% (Goslings et al., 2004). Evidence in vivo also supports the observation. A *pHEMA1::HEMA2* complemented *hema1* mutant showed elevated accumulation of Pchlide after an extended period of darkness (*pHEMA1* indicates *HEMA1* promoter). The over-accumulated Pchlide in the dark results in a necrotic phenotype after the transition to light (Apitz et al., 2014). This data demonstrates that FLU does not inactivate GluTR2 in the dark, which supports the idea that GluTR1 is dedicated to the Chl biosynthesis which is switched off in the dark by FLU, but GluTR2 facilitating the heme biosynthesis can avoid the inactivation by FLU in the dark (Apitz et al., 2014). However, the Chl and heme content in *pHEMA1::HEMA2* complemented *hema1* lines remains wild-type like level, which indicates that GluTR2 has an equal contribution to Chl and heme biosynthesis as GluTR1 under normal growth conditions. It was suggested that GluTR2 has only a preference to support the heme biosynthesis under limited ALA production conditions, such as extended dark incubation (Apitz et al., 2014).

1.4.2.2 The crystal structure of FLU in *Arabidopsis*

A hydrophobic region from amino acid position 125 to 146 was predicted to be a TM domain (Meskauskiene et al., 2001). The C-terminus of FLU is a hydrophilic region. Database search has predicted two different domains in this region, a non-canonical tetratricopeptide repeat domain, TPR(FLU), and a coiled-coil domain (Figure 1.3)(Meskauskiene et al., 2001). The TPR motif typically mediates protein-protein interaction (Das et al., 1998). Yeast two-hybrid assay and isothermal titration calorimetry (ITC) experiments demonstrated that the TPR(FLU) domain is involved in the interaction with GluTR (Meskauskiene and Apel, 2002; Zhang et al., 2015). The region between the TM and TPR(FLU) was predicted to be a coiled-coil domain, here designated as the linker domain. The function of the linker domain remains unknown (Meskauskiene et al., 2001; Lee et al., 2003; Falciatore et al., 2005; Zhang et al., 2015).

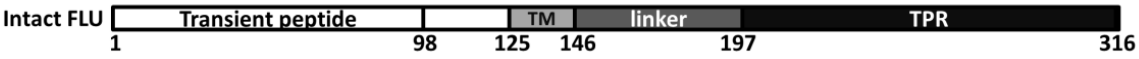

Figure 1.3 The schematic presentation shows the structure of WT FLU protein with four domains. From N-terminal to C-terminal end: transit peptide; TM, transmembrane domain; linker, the coiled-coil domain; TPR, the tetratricopeptide repeat domain. The numbers below indicate the positions of amino acid in the FLU sequence.

The crystal structure of TPR(FLU) with the dimerization domain of GluTR from *Arabidopsis* was published (Zhang et al., 2015). *Arabidopsis* FLU contains 3 TPR motifs. From N-terminus to C-terminus, they are designated as TPR1, TPR2, and TPR3. Each TPR motif contains 40 amino acids. That differs from the prototype of TPRs which typically contain 34 amino acids (Das et al., 1998). TPR(FLU) can itself form a homodimer through its TPR3 region or interacts with GluTR through TPR1 and TPR3. The binding of TPR(FLU) to GluTR does not change its conformation (Figure 1.4, cited from Zhang et al., 2015). In an in vitro assay, TPR(FLU) directly represses the enzyme activity of GluTR by around 3.5 folds (Zhang et al., 2015). The detailed crystal structure of TPR(FLU) and the dimerization domain of GluTR revealed that the FLU-GluTR interaction relies on the positively charged residues on TPR(FLU). As tRNA is negatively charged, the FLU-GluTR interaction might prevent GluTR from binding to its substrate, glutamyl-tRNA (Zhang et al., 2015).

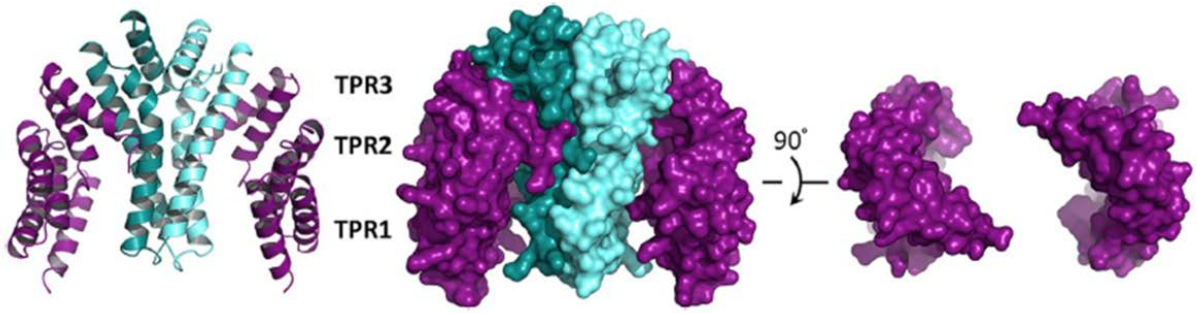

Figure 1.4 The structure of TPR(FLU) with the dimerization domain of GluTR. Left, overall structure in ribbon representation; Middle, overall structure in surface representation. Right, TPR structure in surface representation without GluTR. FLU (TPR domain) molecules are colored purple; one GluTR is colored teal, the other is colored cyan. Figures are cited from Zhang et al., 2015.

1.4.2.3 *Chlamydomonas* contains a FLU like gene

The homologs of FLU can be found in all angiosperms which lack the light-independent POR and show very high similarities in all angiosperms, but not in cyanobacteria, which contains a dark-dependent Pchlide reductase (DPOR). It is hypothesized that FLU might co-evolve with the loss of DPOR. However, Chlamydomonas, which uses a DPOR, contains a FLU-like gene, which could be an evolutionary "intermediate state" of the ALA synthesis regulatory system (Falciatore et al., 2005). This FLU-like gene can form two transcripts through alternative splicing leading to the production of two FLU-like proteins (FLP), a short and a long form, which differ by 12 amino acid residues in length. The *flu* mutant of *Arabidopsis* can be rescued by expressing both FLP forms from *Chlamydomonas*, indicating that FLP

functions similarly as the *Arabidopsis* FLU. An in vitro assay showed that both long and short FLP forms could interact with GluTR of *Arabidopsis* (Falciatore et al., 2005). The sequence alignment revealed that *Chlamydomonas* FLP has a similar protein structure to the *Arabidopsis* FLU: a putative transit peptide at the N-terminus, a hydrophobic region, a coiled-coil domain and a TPR domain at the C-terminus. *Chlamydomonas* FLP consists of two TPR motifs while *barley* and *Arabidopsis* FLU consists of three TPR motifs (Zhang et al., 2015).

1.4.2.4 Rescue of *flu* phenotype by second-site mutations

One possible way to rescue the *flu* phenotype is to suppress the TBS pathway. By screening for a *flu*-rescue mutation, a second-site mutant gene (*ulf3*) positioned in the *HO* gene was found. This phenotype was ascribed to the inhibitory effect of accumulating heme on ALA synthesis, which has been mentioned in chapter 1.4.1 (Goslings et al., 2004).

Pchlide is capable of generating singlet oxygen ($^1O_2$) in light (Wagner et al., 2004). $^1O_2$ was found to be generated within the first minute in *flu* transferred from dark to light (op den Camp et al., 2003). Subsequently, the high level of $^1O_2$ in *flu* acts as a signal that activates the gene expression involved in programmed cell death (PCD) and consequently causes cell death (Danon et al., 2005; Ledford and Niyogi, 2005; Laloi and Havaux, 2015). Another approach to rescuing *flu* is to block the $^1O_2$ dependent PCD signal pathway. A second mutation of the *Executer 1* (EX1) in the *flu* mutant rescues the *flu* phenotype. EX1 is speculated to be one of the key players of the $^1O_2$-dependent PCD signal pathway (Wagner et al., 2004). The chloroplast FtsH2 metalloprotease was also suggested to be involved in this pathway (Wang et al., 2016; Dogra et al., 2017). FtsH2 is co-localized with EX1 in the grana margins. The mutation of *ftsH2* in *flu* partially rescues the *flu* phenotype (Wang et al., 2016; Dogra et al., 2017). It was proposed that FtsH2 promotes the degradation of EX1, a process which is induced by the accumulation of $^1O_2$ and thereby releases an active peptide of EX1, which triggers PCD (Wang et al., 2016). $^1O_2$ has recently been found to be able to oxidize the Trp643 residue in DUF3506 of EX1 and the oxidation of Trp643 of EX1 is essential for initiating $^1O_2$-derived signaling (Dogra et al., 2019).

1.4.2.5 FLU is a negative regulator on ALA synthesis of Chl synthesis

ALA synthesis rate and Pchlide levels have been shown to be inversely proportional to each other (Richter et al., 2010). Pchlide accumulation is accompanied by a decrease of the ALA synthesis rate in the dark. The decrease of ALA synthesis rate is not detectable in the dark when plants are treated with Pchlide synthesis inhibitor (Stobart and Ameen-Bukhari, 1986; Richter et al., 2010). Pchlide might act as a signal molecule to mediate the repression strength on ALA synthesis. FLU was found co-migrating with several enzymes of the Chl biosynthesis pathway on a Blue-Native polyacrylamide gel electrophoresis (BN-PAGE), such as PORB, CHL27 and geranylgeranyl reductase (Kauss et al., 2012a). Based on these observations, a model was previously proposed to explain the feedback repression of ALA synthesis mediated by FLU-GluTR interaction that is dependent on Pchlide levels: FLU is a part

of the inactivation complex containing POR and CHL27; In light, Pchlide are converting to Chlide. This protein complex does not bind excessive amounts of Pchlide. FLU does not interact GluTR; In the dark, Pchlide cannot convert to Chlide and is bound to POR. FLU in the "Pchlide containing" protein complex would interact with GluTR and inhibit its activity (Figure 1.5).

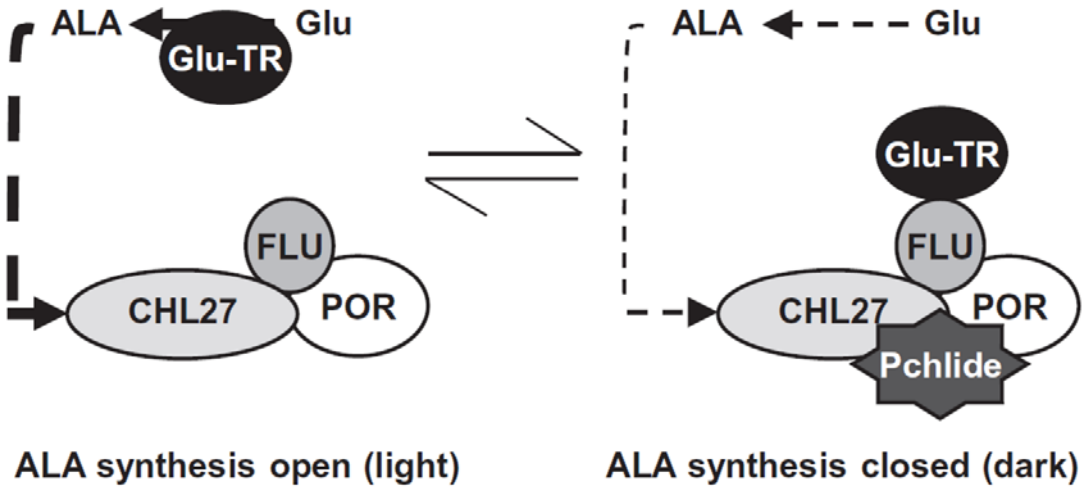

Figure 1.5 A hypothetical mechanism of FLU-mediated regulation of ALA synthesis in light or dark. The detailed mechanisms are explained in the main text. The figure is cited from Kauss et al., 2012.

1.4.3 GBP and Clp protease

More than 20 chloroplast proteases have been reported in recent decades (Nishimura et al., 2016, 2017). The plastid stroma-localized Clp system plays an essential role in the plastid protein homeostasis. Clp protease is an ATP-dependent multimeric complex, which comprises of a proteolytic core complex and a chaperone sub-complex. *Arabidopsis thaliana* chloroplast consists of five ClpP subunits and four ClpR subunits in the core complex. The chaperone sub-complex consists of ClpC1, ClpC2 or ClpD, all of which show ATPase activity (Olinares et al., 2011). ClpC1 and ClpC2 share greater similarity than ClpD and show higher ATPase activity than ClpD (Rosano et al., 2011). ClpC1 supports also the functioning of TOC (translocon at the outer envelope membrane of chloroplasts) and TIC (translocon at the inner envelope membrane of chloroplasts) complexes, mediating the translocation of pre-proteins across the envelope membrane (Kovacheva et al., 2005; Rosano et al., 2011; Bruch et al., 2012). The chaperone complex recognizes the substrates of Clp protease. The recognition of these proteins is mediated by adaptor proteins, such as ClpS1 and ClpF. Through affinity chromatography, GluTR was found to be interact with ClpS. It was shown that ClpS1, as well as ClpC1, interact with the HBD of GluTR. GluTR content is more stable in *clp* mutants than in WT. Furthermore, this truncated GluTR without the HBD domain becomes less accessible for proteolytic degradation (Apitz et al., 2016). These data provide evidence that the Clp protease is involved in the regulation of ALA synthesis through interaction with the HBD domain of GluTR (Nishimura et al., 2013; Apitz et al., 2016).

GBP in *Arabidopsis thaliana* (Col-0) was initially named proton gradient regulation 7 (PGR 7) in the *Arabidopsis* ecotype, *Ler*. PGR7 is localized in the chloroplast, which has been demonstrated by an analysis of the localization of a GFP fused with the transit peptide of PGR7 and also by immunoblot analysis of chloroplast proteins. although GBP does not contain a TM domain, GBP is dominantly presented in the stromal (Jung et al., 2010). However, by performing an in situ immune-gold labeling experiment, GBP is also found in the grana stacks (Czarnecki et al., 2011).

Loss of PGR7 caused slightly retarded growth and reduced Chl content. *pgr7* also showed lower non-photochemical quenching (NPQ), which was initially explained by the deficient photosynthetic electron transport, as the N terminal domain of PGR7 was previously predicted to be a flavin mononucleotide (FMN) binding protein (Jung et al., 2010). However, a subsequent experiment showed that GBP could not bind FMN. The reduced NPQ is likely due to heme deficiency (Czarnecki et al., 2011; Zhao et al., 2014).

GBP is introduced to be a post-translational regulator for ALA synthesis by Czarnecki et al., 2011. By screening an *Arabidopsis* cDNA library for proteins interacting with GluTR through the yeast two-hybrid method, GBP was found to be one of the interacting partners of GluTR (Czarnecki et al., 2011). Additionally, this interaction is confirmed by bimolecular fluorescence complementation (BiFC) assay and pull-down experiments. Binding of GBP to GluTR stimulates the enzymatic activity of GluTR by threefold in an in vitro experiment (Zhao et al., 2014), and therefore, GBP was suggested to be a stimulator of ALA synthesis. However, it still remains to be confirmed whether GBP can stimulate ALA synthesis in vivo. Subsequently, the binding site of GluTR for GBP was identified as the HBD domain that is also the binding site of Clp protease (Apitz et al., 2016). The *gbp* mutant showed a reduced amount of GluTR and the degradation rate of GluTR becomes fast in the dark. GBP, therefore, is suggested to be acting as a protective protein for GluTR to prevent GluTR from degradation by competing with Clp protease for the GluTR binding (Apitz et al., 2016).

The homologous genes of *GBP* are found in all chloroplast-containing organisms, such as algae, mosses, and agiospermswhich synthesize ALA by the C5 pathway, whereas eukaryotes or bacteria that synthesize ALA via C4 pathway do not contain a *GBP*-like gene (Czarnecki et al., 2011). Both the transcript and protein amount of *GBP*/GBP during the onset of greening or in the day/light cycle remains nearly constant (Czarnecki et al., 2011). The expression pattern resembles gene cluster 3, which contains most genes involved in heme metabolisms (Matsumoto et al., 2004). Therefore, GBP was suggested as belonging to the ALA synthesis regulator supporting heme synthesis (Czarnecki et al., 2011; Czarnecki and Grimm, 2012).

The crystal structure reveals that GBP forms a hetero-tetramer with GluTR. GBP can interact with HBD of GluTR via its C-terminus. The binding of GSAT-GluTR was proposed as being similar to the GBP-GluTR binding (Moser et al., 2001; Zhao et al., 2014). Therefore, simultaneous binding of GBP and GSAT to GluTR is unlikely. However, the binding of GBP to GluTR stimulates the enzyme activity by threefold. It is proposed that GBP facilitates the hydrogen transfer from NADPH to the substrate

(Zhao et al., 2014). Furthermore, size-exclusion chromatography (SEC) and ITC experiments have demonstrated that GBP could bind heme (Zhao et al., 2014). It has been recently found that binding of heme to the GBP inhibits the GBP-GluTR interaction, thereby making GluTR more accessible to the Clp protease. Thus, heme can promote the degradation of GluTR through binding with GBP (Richter et al., 2019).

As FLU interacts with the C-terminal end of the dimerization domain of GluTR and GBP interacts with the HBD of GluTR at the N-terminus, one report proposed a ternary formed by FLU, GBP and GluTR (Fang et al., 2016). However, whether a ternary structure exists in plants and if so, the functional role of this ternary structure remains to be explained.

1.4.4 Aggregation of GluTR and cpSRP43 chaperone

Aggregation of GluTR might be an essential mechanism to inactivate excessive amounts of GluTR. *HEMA1* overexpression in *tobacco* plants caused the accumulation of GluTR, but the excessive accumulation of GluTR does not correlate with the ALA formation rate. A portion of GluTR is migrating at the high molecular weight part in the GluTR overexpression lines even after the protein samples were treated with denaturing buffer (Schmied et al., 2011). This portion of GluTR could be the oligomeric form of GluTR.

In higher plants, the synchronized synthesis of LHC proteins and Chl is essential for the homeostasis of chloroplasts (Plumley and Schmidt, 1995). The dedicated chaperones of the LHC protein family, cpSRP43 and cpSRP54, interact with the LHC proteins and deliver the mature proteins to the thylakoid membrane. cpSRP43 was suggested to be involved in the control of ALA synthesis, and therefore providing a link between Chl biosynthesis and LHC protein biogenesis (Wang et al., 2018). BiFC and pull-down assays demonstrated that cpSRP43 binds to the N-terminal end of GluTR. Loss of cpSRP43 causes a lower GluTR protein accumulation in plants. Concurrent knockout of cpSPR43 and GBP causes a drastic reduction of GluTR and results in a severe pale-green phenotype. Both GBP and SRP43 stabilize GluTR but might have distinct roles in the stability of GluTR (Wang et al., 2018). At the N-terminal end of GluTR, two highly conserved aggregation-prone regions (APRs) were predicted. Deletion of the APR domain in GluTR primarily reduces the aggregation of GluTR. The binding of cpSRP43 to GluTR reduces the aggregation tendency of GluTR. These results strongly suggest that SRP43 can also chaperone GluTR to prevent GluTR from aggregation (Wang et al., 2018).

1.4.5 Potential thiol-based redox control of ALA synthesis

Thiol-redox regulation plays a vital role in the catalytic activity, dimerization, folding, and turnover of proteins in plants (Baier and Dietz, 2005; Buchanan and Balmer, 2005). Three systems have been reported to control the redox state of targets in chloroplasts, including the ferredoxin-thioredoxin system, the NADPH-dependent TRX-reductase (NTR) system, and the glutathione/glutaredoxin (GRX) system

(Pfannschmidt, 2003; Balsera et al., 2014). Five classes of the thioredoxin family have been identified to be localized in chloroplasts, namely f (f1 and f2), m (m1-4),x, y (y1 and y2), and z (Da et al., 2017). Three Isoforms of NTRs can be found in *Arabidopsis*, namely NTRA, NTRB, and NTRC. NTRC functions in the chloroplast (Pérez-Ruiz et al., 2006; Michalska et al., 2009; Richter et al., 2013). The enzyme activity or stability of several key enzymes involved in TBS has been recently reported as being controlled by thioredoxins (Luo et al., 2012; Da et al., 2017). ChlI has been found to be the target of TRX f and m. ChlI is more oxidized, and the MgCh activity is reduced in the m, and f knockout mutant relative to WT (Luo et al., 2012). Besides, the redox state of CHLM is regulated by both TRX and the NTRC systems (Richter et al., 2013; Da et al., 2017). Change of the redox state in CHLM affects both the activity and the stability of CHLM.

Most of the redox modifications in proteins happen on cysteine residues. The redox state of enzymes can be modified through the formation of inner- or inter- molecule disulfide bonds. Substitution of cysteine144 of GluTR with serine can almost abolish its ALA synthesis activity (Zhao and Han, 2018). The protein amount of GluTR is significantly reduced in the *ntrc* mutant, but the transcript of *HEMA1* is not alerted. Correspondingly, the ALA synthesis rate is also reduced in the *ntrc* mutant. These facts indicate an NTRC-dependent post-translational control on the stability of GluTR (Richter et al., 2013; Richter et al., 2018).

1.5 Aims of the project

FLU is a negative regulator for ALA synthesis. As the knock-out mutant of FLU only showed a necrotic phenotype in light after exposure to a period of darkness but not under CL, the FLU function to repress ALA synthesis was mainly addressed in the dark. However, *flu* also showed elevated ALA synthesis in CL, indicating that FLU might also exert negative repression of ALA synthesis during light exposure. The first aim of this project is to elucidate the physiological role of FLU in light. The metabolic flow in *flu* will first be analyzed. Secondly, FLU overexpression (FLUOE) lines will be generated to exaggerate the FLU-dependent effects on ALA synthesis. The ALA synthesis rate and the contents of tetrapyrroles in FLUOE lines will be examined under medium light (ML), low light (LL) growth conditions. Thirdly, *flu* or FLUOE lines will be grown under HL or fluctuating light to reveal the function of FLU under complex light conditions.

FLU inactivates ALA synthesis by interaction with GluTR. ALA synthesis activity was previously found in the stroma fraction. FLU is a membrane located protein. The binding of GluTR to FLU might remove GluTR from the stroma, which might decrease the possibility for binding with glutamyl-tRNA. On the other hand, in vitro experiments have shown that TPR(FLU) interacts with the dimerization domain of GluTR and might prevent GluTR from binding with the substrate, $tRNA^{Glu}$, thereby inactivating ALA synthesis. Besides, FLU was found in a complex with PORB, CHL27, indicating that POR might be involved in the FLU-dependent inactivation of ALA synthesis. However, the detailed mechanisms of how FLU-GluTR interaction leads to inactivation of ALA synthesis are not entirely clear. The second aim of the project is to elucidate the inhibitory mechanisms of FLU on ALA synthesis. Firstly, the sub-organelle localization of GluTR will be analyzed in WT, *flu,* and FLUOE lines to find out whether FLU affects the localization of GluTR. Secondly, several *flu* complementation lines with truncated FLU peptides will be generated to investigate the functional domains of FLU involved in the inactivation of ALA synthesis. Thirdly, the interactions of FLU or GluTR with several enzymes of the Chl biosynthesis branch will be examined. Last but not least, cysteine substitution lines of FLU will be generated to explore the potential redox control on FLU-GluTR interaction.

2 Methods

2.1 Plants and growth conditions

Arabidopsis Thaliana (L.) Heynh. Col (Col-0) was taken as the WT for comparison with mutants in this thesis. *Nicotiana benthamiana* (*N.benthamiana*) plants were used for transient transformation. *Arabidopsis Thaliana* T-DNA insertion lines were purchased from Arabidopsis Biological Resource Center (ABRC) or the Nottingham Arabidopsis Stock Centre (NASC). Those lines were generated either by Salk Institute for biological studies (La Jolla, USA; Salk-lines, (Alonso et al., 2003) or by Syngenta Agro (Maintal, Deutschland; Sail-lines). The table below (Table 2.1) shows the description of lines used in this study.

Table 2.1: Transgenic lines used in this study

Name	Source	Description
flu	Obtained from Kauss Apel; Meskauskine et al., 2001;	A knockout mutant of *FLU* (At3g14110). *Arabidopsis Thaliana* Col-0 background; point mutation line; Screened by EMS in *Arabidopsis* Ler and back cross to Col-0
gbp	SALK line; SALK_200203	The *GBP*(At3g21200) knockout mutant; Homozygote line identified by Judith Schmit.
clpc1	SALK line; SALK_014058	A knockout mutant of *CLPC1* (At5g50920)
HEMA1/WT	Generated by Janina Apitz, Apitz et al., 2016	*HEMA1* overexpression lines driven by *HEMA1 promoter*
A1ΔHBD	Generated by Janina Apitz, Apitz et al., 2016	A *hema1* complementation line with HEMA1 cDNA sequence deletion of 87bp (HBD motif) under the control of *HEMA1* promoter.
FLUOE	Generated by Hedtke, Boris, Dr. rer. nat. and Träder, Kersten	Overexpression of *FLU* (At3g14110)in WT *Arabidopsis* driven by the CaMV-35S promoter.
FLUC119S	In this study	The *flu* complementation line, expressing a point-mutated FLU with the substitution of cysteine 119 into a serine in *flu* controlled by the *FLU* promoter.
FLUC292S	In this study	The *flu* complementation line, expressing a point-mutated FLU

		with the substitution of cysteine 292 into a serine in flu controlled by the FLU promoter.
FLUWT	In this study	The *flu* complementation line, expressing an intact FLU in *flu* controlled by the *FLU* promoter.
TPR/flu	In this study	The *flu* complementation line, expressing a truncated FLU, TPR(FLU) in *flu* controlled by the CaMV-35S promoter.
TPR/WT	In this study	The *flu* complementation line, expressing a truncated FLU, TPR(FLU), in WT controlled by the CaMV-35S promoter.
pAlc_FLUΔlink/*flu*	In this study	The *flu* complementation line, expressing a truncated FLU, FLUΔlink, in *flu* controlled by an ethanol-induced promoter.
FLUΔTM/*flu*	In this study	The *flu* complementation line, expressing a truncated FLU, FLUΔTM, in *flu* controlled by the CaMV-35S promoter.

Arabidopsis thaliana plants were grown on GS90 soil or on 1/2 Murashige & Skoog Medium (MS) medium plates with or without sucrose under different light regimes according to experimental requirements (Table 2.2). The growth temperature is around 22°C in the photo chamber (PGV 36, Conviron). Seeds were first vernalized at 4°C for 2 days and then transferred to growth conditions.

Table 2.2: 1/2 MS medium

Compositions	**Concentrition**
Murashige & Skoog Medium with Vitamins	1.1g l^{-1}
MES	0.5g l^{-1}
Adjust pH to 5.7 with KOH	

To obtain etiolated seedlings, seeds were first surface sterilized in meliseptol (B. Braun, Germany) for 3min and then washed with sterilized ddH2O for five times. Subsequently, seeds were plated on agar plates containing 1/2 MS, vernalized at 4°C for two days. Before 4~6 days incubation in the dark, seeds were exposed to light for 3 hours. Seedlings were harvested in the green safe light for measurements.

2.2 DNA techniques

2.2.1 Plasmid DNA extraction

4mL Lysogeny broth (LB) medium (Table 2.3) with relevant antibiotics (Table 2.4) was inoculated with a single colony and was incubated overnight at 37°C with shaking. The cell culture was then pelleted by centrifugation at 5,000rpm for 2min and was re-suspended in a 300µl solution I buffer (10mM Tris-HCl, 1mM EDTA pH 8.0) to lyse cells. Subsequently, 300µl freshly prepared solution II (0.2M NaOH, 1% SDS) was added into the cell lysis and was mixed by inverting. Followed by adding 300µl ice-cold solution III (3M potassium acetate, 5M acetic acid), precipitated proteins were pelleted by centrifugation at 4°C 12,000rpm for 10min. Subsequently, the supernatant was transferred to a new Eppendorf tube and was mixed with the same volume of isopropanol. The plasmid was then pelleted by centrifugation at 4°C 12,000 rpm for 10min. After washed with 500µl 75% ethanol for two times, the pellet containing plasmid DNA was re-suspended in 30µl ddH2O and stored at -20°C.

Table 2.3: LB medium

Compositions	Concentrition
Bacto Tryptone	10g/l
Yeast extract	5g/l
Adjust pH to 5.7 with KOH. For sodium, 1.5g/l agar was added	

Table 2.4: List of antibiotics used for selection

Name	Stock concentration	Work concentration	Solvent
Ampicilin	100mg·ml^{-1}	100µg·ml^{-1}	ddH_2O
Gentamycin	15mg·ml^{-1}	15µg·ml^{-1}	ddH_2O
Kanamycin	50mg·ml^{-1}	50µg·ml^{-1}	ddH_2O
Rifampilin	25mg·ml^{-1}	100µg·ml^{-1}	DMSO

2.2.2 DNA fragments manipulation

The plasmid DNA or DNA fragments were digested by restriction enzymes produced by NEB Biolabs or Fermentas according to the instruction from the manufacturers. The products of digestion were separated by gel electrophoresis running in the TAE buffer (Table 2.5), and then the target DNA fragments were recycled by using a gel

recycle kit (GeneJET Gel Extraction Kit, Thermo Fischer Scientific). Subsequently, DNA fragments were jointed together by T4 DNA ligase produced by NEB Biolabs.

Table 2.5: TAE buffer

Compositions	Concentrition
Tris-Acetate	40mM
EDTA	1mM
Adjust pH to 8.0 with HCl	

2.2.3 Chemically competent *Escherichia coli* cells preparation and transformation

4ml LB medium was inoculated with a single colony and incubated overnight at 37°C with shaking. 1ml cell culture was subsequently inoculated into a 500ml LB medium with 5ml sterilized 1M MgCl2 solution. The culture was then incubated at 28°C, with shaking, for around 4h until OD600 reached 0.5~0.7. The cell culture was then cooled down on the ice for 10min. The cells were then harvested by centrifugation at 4,500rpm for 10min at 4°C and were then dissolved in the 80ml pre-cooled TB buffer (10mM Pipes, 15mM CaCl2, 250mM KCl, pH6.7 with KOH and 55mM MnCl2). Finally, aliquots of 50µl competent cells were frozen in liquid nitrogen and stored at -80°C.

For transformation, around 100ng DNA was added into 50µl aliquot of competent cells. The aliquot was then incubated on ice for 30min. After a heat-shock treatment at 42°C for 90s, the aliquot was quickly cooled down on ice for 5min, and 500µl LB medium was added. Subsequently, the cells were incubated at 37°C for 45min and were plated on selection media and were grown overnight at 37°C.

2.2.4 DNA extraction from plants

Two methods were used to extract genomic DNA of *Arabidopsis* according to the requirements on the DNA quality in different experiments. A protocol was used to isolate a small amount of unpurified DNA. 4-10mm^2 leaf disk was harvested and homogenized by a pestle in 100µl rough DNA extraction buffer (Table 2.6). After centrifugation at 14,000rpm for 4min, 80µl supernatant was transferred to a new tube and was mixed with 80µl isopropanol. DNA was pelleted by centrifugation at 13.000rpm for 5min. The pellet was washed by 500µl 75% ethanol for two times and was finally dissolved in 20µl ddH_2O. DNA samples were stored at -20 °C.

Table 2.6: Rough DNA extraction buffer

Compositions	Concentration

Tris	200mM
NaCl	150mM
EDTA	25mM
SDS	0.5%

Another method was used to isolate a large amount of purified and clean DNA. Around 20mg leaf material was harvested and frozen in liquid nitrogen. Samples were homogenized at 25Hz for 1.5min by a Retsch cyro grinding mill (MM301, Retsch). 500µl clean DNA extraction buffer (Table 2.7) and 66µl 10% SDS were added into the samples and incubated at room temperature (RT) for 10min. After centrifugation at 13,000rpm for 15min, the supernatant was transferred into a new tube and mixed with 166µl KOAc solution (Table 2.8). The same volume of isopropanol was then added into the mixture and was incubated on ice for 20min. After centrifugation at 16,000rpm for 20min, the supernatant was removed, and the pellet was washed with 500µl 70% ethanol for two times. Finally, pellets were dissolved in 100µl TE buffer containing 1µg/ µl RNase A.

Table 2.7: Clean DNA extraction buffer

Compositions	**Concentrition**
Tris	0.1M
NaCl	0.5M
EDTA	0.05M
Polyvinylpyrrolidone PVP-40	1%

Table 2.8: KOAc solution

Compositions	**Concentrition**
Potassium acetate	3M
acetic acid	2M

2.2.5 Polymerase chain reaction and DNA sequencing

Primers for polymerase chain reaction (PCR) were designed by the software, PrimePrimer. The components and thermos-cycling conditions for standard PCR reaction were listed in Table 2.9 and Table 2.10. The annealing temperatures of primers were designed around 58°C. Sequences of PCR products were verified by the

second generation DNA sequencing technology by LGC Genomics (Berlin, Germany). Samples were provided according to the requirements of the company.

Table 2.9: Standard PCR reaction

Compositions	Volume
DNA polymerase (Taq or Phusion)	0.2µl
10x Buffer	2µl
10mM dNTPs	0.5µl
10µM forward primer	1µl
10µM reverse primer	1µl
DNA template	1µl
ddH2O	14.3µl

Table 2.10: Program for the standard PCR reaction

Steps	Temperature (°C)	Time (s)
Pre-denaturing	95	120
Denaturing	95	15
Annealing	58	15
Extending	72; go back to denaturing 29 cycle	60 per 1kb
Additional extending	72	120

2.2.6 The overlap extension PCR

For the linkage of two or three PCR fragments, the overlap extension PCR was applied, which generally includes three round PCR reactions. The first-round PCR was performed as the standard PCR reaction as described in 2.2.5 to amplify the single fragments from *Arabidopsis* genomic DNA or from cDNA. PCR products were then purified by a gel recycle kit after electrophoresis. The fragments were jointed together to form the full-length fusion product in the second-round PCR. No primers were added in this round, the linkage of the single fragments took place, relying on the complementary sequences within the fragments. The reaction mixtures

contained PCR products from the first round, 5xHF-buffer, dNTP mix (10mM each) and Phusion® (2U/µl). The thermos-cycling conditions for the second round were similar to the standard PCR, except that the annealing temperature was reduced to 50~55°C and the cycle number was reduced to 10. The last reaction was a standard PCR reaction to amplify the full length of target DNA by using the PCR products of the second round as the template. The PCR products from the last-round PCR was then separated by electrophoresis and recycled by a DNA gel recycle kit.

2.3 RNA techniques

2.3.1 RNA extraction from plants and reverse transcription

Around 20~30mg leaf material was harvested and frozen in liquid nitrogen. Samples were either stored in -80°C or directly homogenized for RNA extraction by a Retsch cyro grinding mill. RNA was extracted according to Oñate-Sánchez and Vicente-Carbajosa, 2008. After homogenization, 300µl solution I (Table 2.11) was added and incubated at RT for 5min until the mixture became clear. Then 100µl solution II (Table 2.11) was added to the mixture and mixed by inverting. After incubation at 4°C for 10min, the samples were then centrifuged at 14.000rpm for 10min. RNA was in the soluble fraction. The supernatant was transferred to a new tube and mixed with the same volume of isopropanol to precipitate RNA. After centrifugation at 14.000rpm for 10min, the supernatant was removed. The pellet which containing the RNA was washed for two times by 500µl 75% ethanol. Samples were air-dried at RT to get rid of ethanol and finally dissolved in 30µl ddH_2O. The RNA concentration was analyzed by NanoDrop®2000 Spectrophotometer produced by Thermo Fischer Scientific. 1µg RNA sample was loaded on a 1% agarose gel running in 0.5×TBE buffer to check the quality of RNA samples (Table 2.12). 1µg RNA was diluted to a final volume of 4µl with ddH_2O. 0.5µl DNase I buffer and 0.5µl DNase I was added for DNA digestion. Reactions were incubated at 37°C for 30min. DNase I was then inactivated by adding 0.5µl EDTA and incubated at 70°C for 10min. A solution containing 0.5µl Oligo-dT primer, 2µl RT buffer (5x), 1 µl dNTPs (10mM each), 0.25µl ribolock rnase inhibitor (=10units) and 0.25µl RevertAid Reverse Transcriptase (=50units) were mixed with RNA samples and was incubated at 42°C for 60min for reverse transcription. After the RNA was reverse transcribed into cDNA, the reaction was stopped by incubation at 72°C for 10min.

Table 2.11: RNA extraction solutions

Solution I	Solution II
68mM Na-citrate	4M NaCl
132mM Citric acid	16mM Na-citrate
1mM EDTA	32mM Citric acid

2% SDS

Table 2.12: 0.5×TBE buffer

Components	**Concentrition**
Tris-Cl	40mM
boric acid	45mM
EDTA	1mM
Adjust pH to 8.3	

2.3.2 Quantitative Real-time PCR

Primers used for quantitative real-time PCR (qRT-PCR) were designed by Perlprimer (download site: http://perlprimer.sourceforge.net/download.html). The reactions were performed on a Bio-rad CFX96. cDNA was amplified with a SensiMix SYBR kit (Bioline) using reaction mixtures as described in Table 2.13. The thermos-cycling condition was similar to the standard PCR except that the cycle number was 40 for qRT-PCR. Relative gene expression was calculated according to $2^{-\Delta\Delta Ct}$ method. RNA amounts were normalized to the expression of the housekeeping gene *SAND*(AT2G28390) in WT.

Table 2.13: qPCR reaction mixture for SensiMix SYBR kit

Components	**Volume (µl)**
SYBR Green mixture	3
forward primers	0.15
reverse primers	0.15
cDNA template	1
ddH2O	1.7

2.4 Protein techniques

2.4.1 Protein extraction and western blot analysis

Around 30mg leaf sample was harvested and homogenized in liquid nitrogen. Samples were then dissolved in 2×laemmli buffer (Table 2.14) with the ratio 1:10mg/µl. Pellet was removed by centrifugation at 13,000×g for 5min at RT. 10µl

protein extract was loaded on a sodium dodecyl sulphate-polyacrylamide (SDS-PA) gel for separation. The compositions of the SDS-PA gel were listed in Table 2.15. Subsequently, a semi-dry method was used to transfer the proteins from the SDS-PA gel to a nitrocellulose membrane by a blotting device produced by Bio-rad (Trans-Blot® SD Semi-Dry Transfer Cell) (Lauriére, 1993). The transformation architecture is organized the way from the bottom to the top: three pieces of filter papers, nitrocellulose membrane, the SDS-PA gel, and three pieces of filter papers. All the filter papers and nitrocellulose membrane were pre-incubated with the western transfer buffer containing 25mM Tris, 200mM glycine, 20% methanol (v/v) for 5min. The transfer was performed at a currency of 1.2mA/cm^2 for 1h. After the transfer, proteins on the nitrocellulose membrane were stained with Ponceau solution (5% (v/v) acetic acid, 0.1% Ponceau S). The membrane was then blocked by 5% low-fat milk in TBST buffer (50 mM Tris, 150mM NaCl, 0.1% (v/v) Tween-20) for 1h. After blocking, the membrane was washed with TBST for 5min and then with TBS (50mM Tris, 150mM NaCl) twice for 5min each time. The first antibody against the target protein was incubated with the membrane for 2h at RT or 4°C overnight. After three washing steps, the secondary antibody against rabbit IgG carries with a label, horseradish peroxidase (HRP) which catalyzes the oxidation of luminol to 3-aminophthalate. This reaction accompanied with a LL emission that can be enhanced in the presence of enhanced chemiluminescence (ECL) solution, therefore the signal was then detected and imaged by a CCD-camera.

Table 2. 14: Gradients of 2× laemmli buffer

Compositions	Concentrition
Tris-HCl	100mM
SDS	4% (w/v)
glycerol	20% (v/v)
DTT	200mM
Bromphenol blue	0.15% (w/v)

Table 2.15: Gradients of SDS-PAGE gel

Solutions	Stacking gel	Separating gel (12%)
30% Acrylamide (29:1) [ml]	0.3	1.6
1.5M Tris/HCl pH 8.8 [ml]	-	1
0.5M Tris/HCl pH 6.8	0.25	-

[ml]		
10% SDS [µL]	20	40
10% APS [µL]	20	40
TEMED [µL]	2	1.6
total volume ddH2O [ml]	2	4

The Tricine SDS-PA gel was applied to separate proteins smaller than 20kDa according to (Hermann, 2006). Gels were prepared as in Table 2.16. Protein samples were extracted by the 2×laemmli buffer. The electrophoresis started with a voltage of 30V. The voltage was increased to 190V until the protein samples fully entered the stacking gel. Then, the voltage was gradually increased to 270V until the end of the run. To maintain the temperature of the gel at around 30°C to 40°C, the gel has to be running in a cold room (4°C).

Table 2.16: Gradients for a tricine-SDS-PAGE gel. AB3, acrylamide-bisacrylamide (AB)-3 stock solution (49.5% T, 3% C mixture) produced by Sigma-Aldrich; gel buffer (3×), 3M Tris, 1M HCl, 0.3% SDS, adjust pH to 8.45; APS, Ammonium persulfate; TEMED, Tetramethylenediamine.

	10% separating gel	**4% stacking gel**
AB3 [ml]	0.2	0.083
Gel buffer (3x) [ml]	0.33	0.25
Glycerol [ml]	0.1	0
Water [ml]	0.37	0.67
10% APS [µl]	5	7.5
TEMED [µl]	0.5	0.75

2.4.2 Analysis of the amounts of membrane-bound and soluble proteins in the chloroplasts

20mg leaf material was harvested and frozen immediately in liquid nitrogen. 200µl phosphate buffer (20mM sodium phosphate buffer and 150mM NaCl, pH 7.4; PBS) was added into the samples after homogenization. Samples were then mixed thoroughly by the vortex. 50µl suspension was taken as a total extraction mixed with the same volume of 5×laemmli buffer. 120µl suspension was separated into membrane and soluble fractions by centrifugation at 4°C, 16,000×g for 10min. 100µl soluble fraction was mixed with the same volume of 5×laemmli buffer as a soluble fraction. Pellet was washed for two times by 500µl PBS buffer and dissolved in 120µl

PBS buffer with 120µl 5×laemmli buffer as a membrane fraction. An equal volume of total extracts, membrane fraction, and the soluble fraction was separated by sodium dodecyl sulfate-polyacrylamide gel electrophoresis (SDS-PAGE), followed by a western blot analysis to determine the protein amounts in each fraction.

2.4.3 Recombinant protein expression and purification

To express a desired protein in *E.coli*, the coding gene of *Arabidopsis* was sub-cloned into the expression vectors, such as pET-28a (+) (His-tag) and pGEX-6P-1 (GST-tag). Consequently, the expression of the desired gene was controlled by an isopropyl-β-d-thiogalactoside (IPTG) induced promoter in *Ecoli.* cells. The vectors were then transferred into the *E.coli* bl21 competent cells. 5ml LB medium was inoculated with a single colony and incubated overnight at 37°C. The culture was inoculated into 500ml fresh LB medium containing the relevant resistance and was incubated at 37°C until the cell intensity increased to around 0.5 at OD_{600}. Subsequently, IPTG (a final concentration of 0.5 to 1.0mM) was added to into the cell culture to induce the expression of the desired protein. The induction was conducted at 37°C/30°C for 4h or at 4°C overnight. The cells were then harvested after centrifugation at 5500×g for 5min.

The Ni-NTA affinity column (Qiagen) was used to purify the His-tagged protein from *E.coli* cells. After cell-harvesting, the cell pellet was dissolved in a lysis buffer (50mM Tris-HCl, pH8.0 300mM NaCl 10mM Imidazole). The suspension was then mixed with lysozyme (final concentration 1mg/ml) on ice for 30min. Cells were then broken by ultrasonic wave for 2min. The supernatant was separated by centrifugation at 14,000×g for 10min and then was filtered through a 45µm bacterial filter. 100µl Ni-NTA agarose was added into the supernatant and was transferred to 10ml filter column with a cap at the bottom. Until the agarose beads fall down at the bottom of the column by gravity, the cap was removed. Then the suspension flew through the column while the beads left in the column. 10ml wash buffer (50mM Tris-HCl, pH8.0; 300mM NaCl; 40mM Imidazole) was carefully added into the column to wash the beads without breaking the stack of beads. The wash step was repeated for five times. Subsequently, the elution step was performed with an elution buffer containing 50mM Tris-HCl, 300mM NaCl, and 250mM imidazole. After washing, 500µl elution buffer was added into the column with the cap at the bottom, and the column was incubated at 4°C for 5min. The elution buffer containing the target protein was recycled in a 1.5ml tube as the first aliquot. Another two aliquots were obtained by repeat the elution step twice.

General strategies and procedures for the purification of GST-tagged proteins were similar to the His-tagged recombinant protein purification, except that buffers and agarose beads were different. A phosphate buffer containing 140mM NaCl, 2.7mM KCl, 10mM Na_2HPO_4, and 1.8mM KH_2PO_4 was used as the binding buffer and also for the washing step. The elute buffer containing 50mM Tris-HCl, pH8.0, and 10mM reduced glutathione was prepared freshly before use. Glutathione sepharose 4B resin produced by GE healthcare was used for purification of GST tagged protein.

2.4.4 Protein concentration determination

Two methods were applied for determining the concentration of protein samples, the bicinchoninic acid (BCA) and Bradford measurements. For Bradford measurement, 5µl protein samples were added into 1ml 1× Bradford solution produced by Bio-Rad and were incubated at RT for 5min. The absorption at OD_{595} was measured after centrifugation at 12,000×g for 1min. Protein concentration was calculated by a standard curve with a BSA standard. There are certain limitations to this method. For example, an alkaline substance or carbohydrates like sucrose in the protein samples can interference the measurement. The BCA protein determination method is based on the absorption shift when reaction with the protein samples. This method functions under alkaline conditions and does not affect by SDS. This method was performed with a Pierce BCA Protein Assay Kit provided by Thermo Fisher Scientific.

In addition, a coomassie brilliant blue stain was used to reconfirm the protein concentration determined by BCA or Bradford methods. 1µg protein samples and bovine serum albumin (BSA) standards were mixed the same volume of 2×laemmli buffer and loaded onto a SDS-PA gel, followed by staining with the coomassie brilliant blue solution for 1h. The protein bands were then visualized by a de-stain solution (Table 2.17 and Table 2.18). The signal intensities of the protein bands were then semi-quantitatively determined by a gel analyzer.

Table 2.17: Gradients of coomassie brilliant blue solution

Components	Concentration
Coomassie brilliant blue R-250	0.1% (w/v)
methanol	40%
acetic acid	10%
filter through paper	

Table 2.18: Gradients of coomassie brilliant blue destain solution

Components	Concentration
methanol	45%
acetic acid	10%

2.4.5 Dialysis

After determination of the concentration of the desired protein, two methods were applied for dialysis to remove the imidazole or glutathione in the elution buffer. Depending on concentrations of the purified recombinant proteins, for samples with low concentrations, Amicon® Ultra centrifugal filters were used to dialysis the purified protein at the same time to concentrate the protein elution. Ten volumes of PBS buffer were combined with the elution and flow through a specific filter depending on the molecular weight of the target protein by centrifugation at 4°C, 5,000×g. This step was repeated for 3 times. Another method is to use a special tube for dialysis (SnakeSkinTM Pleated Dialysis Tubing, Thermo Fischer Scientific). This tube contains a semi-permeable membrane allowing the tiny molecular to pass through but not the desired protein and therefore to remove imidazole or glutathione from the protein samples.

2.4.6 Pull-down assay with recombinant protein

10µl Ni-NTA agarose beads were washed with 500µl PBS buffer to get rid of ethanol. 30µg His-tagged recombinant protein as bait in 500µl PBS was incubated with 10µl Ni-NTA agarose beads at 4°C for 1h. Beads were precipitated by centrifugation at 4°C, 1500×g for 2min and the buffer was then removed by careful pipetting. The pellet was washed twice by 500µl PBS. Subsequently, the beads were re-suspended in 500µl PBS buffer containing 30µg GST-tagged prey protein and were incubated at 4°C for 1h. After centrifugation at 1500×g for 2min, the beads were pelleted and washed by 1ml PBS buffer for five times. Finally, the beads were incubated with 30µl 2×laemmli buffer at 100°C to elute the proteins associated with beads. 10µl elution was loaded on a SDS-PA gel for protein separation and followed by a coomassie brilliant blue stain.

2.5 ALA synthesis rate measurement

Around 30mg leaf material was harvested and incubated in 40mM levulinic acid buffer (Tris2,1 ml 98% levulinic acid HCl up to pH 7,2) under growth light condition for 3h. Samples were then dried and frozen in liquid nitrogen. After homogenization, 500µl 20mM tripotassium phosphate buffer was added into the samples for ALA extraction. 400µl supernatant was transferred to a new Eppendorf tube after centrifugation at 4°C, 16,000×g for 10min. 100µl acetoacetic acid ethyl ester (EAA) were then mixed with the 400µl supernatant and boiled at 100°C for 10min. Samples were immediately cooled down on ice for 5min, and then 500µl modified Ehrlich-Reagenz solution (373ml acetic acid, 90ml 70% perchloric acid, 1,55g $HgCl_2$ (mercuric chloride) ddH_2O) and 18mg Dimethylaminobenzaldehyd were freshly added and mixed by inverting. After centrifugation at 14,000rpm for 10min, the absorption at 553nm, 525nm, and 600nm were measured by a photometer. OD_{600} measured as a basic absorption from the sample, which was expected to be nearly 0. The ratio between OD_{553}/OD_{525} of an ALA standard is around 1.5. An ALA standard curve was generated with a standard ALA produced by Sigma-Aldrich, which was used to calculate the concentration of ALA in samples.

2.6 Thylakoids extraction and chloroplast isolation

Thylakoids were extracted according to (Järvi et al., 2011). Around 50mg leaves were harvested and homogenized by a mortar and a pestle on ice in 5ml homogenization buffer. The extract was filtered through a Miracloth into a 15ml Falcon tube. After centrifugation at 4°C, 2000×g for 5min, the supernatant was discarded, and the pellet was re-suspended in 300µl homogenization buffer. Chl concentration was determined according to (Porra et al., 1989). 5µl thylakoids extract were dissolved in 1ml 80% acetone and incubated on ice under LL for 10min and the absorption at 663nm, 645nm, 720nm was determined by a spectrophotometer. The Chl amount can be then calculated (Total Chl=$17.95A_{645}$+$7.90A_{663}$). Subsequently, the rest of the thylakoids extract was centrifuged at 4°C, 5000×g for 5min. After removal of the supernatant, the pellet was dissolved in 25BTH20G buffer (25mM BisTris-HCl, pH7.0, 20% (w/v) glycerol and 0.25mg ml^{-1} Pefabloc) to a final Chl concentration of 0.5µg ml^{-1}. Thylakoid sample was stored at -80°C for further experiments.

To obtain the intact chloroplasts, around 2g plants were harvested. The whole extraction process was performed at a 4°C cold room. Plants were homogenized in a Waring® blender in 200ml chloroplast homogenization buffer (CHB, 0.45M sorbitol, 20mM Tricin-KOH pH8.4, 10mM EDTA, 10mM $NaHCO_3$ and 0.1% BSA). The total extracts were filtered through 2 layers Mira cloth into a 25ml centrifuge beaker. Chloroplasts were pelleted by centrifuge at 4°C, 500×g for 20min. The supernatant was removed completely and 500µl chloroplast washing buffer (CWB) containing 0.3M sorbitol, 20mM Tricin-KOH, 2.5mM EDTA and 5mM $MgCl_2$ was then added to re-suspend the pellet by shaking the centrifuge tube. The chloroplasts were then loaded onto a percoll gradient. The gradient contains two-layer percoll solutions with different percentages. The up layer containing 14ml 40% percoll (Percoll: 5×CGB=2:1) was first filled in an ultracentrifuge tube. The bottom layer containing 5ml 80% percoll (Percoll: 5×CGB:H2O=2:1:2) was added underlay carefully and slowly. The gradient with chloroplasts was then centrifuged at 4°C, 6,500×g for 30min in a swing-out rotor. After the centrifugation, the intact chloroplasts were presented in the interlayer of the gradient. Subsequently, the first layer until 1cm above the chloroplasts was discarded and the layer with chloroplasts was taken out with a truncated 1ml tip into 20ml CWB buffer. Finally, chloroplasts were collected by centrifugation at 4°C, 500×g for 5min and were stored at -80°C.

2.7 BN-PAGE analysis

The BN-PAGE was performed according to Järvi et al., 2011. For the preparation of the gradient for the separating gel, the recipe for 4% and 12.5% separating gel was shown in Table 2.19. A gradient mixer with two chambers was used to produce a gradient gel. 2ml 12.5%-gel-solution were added into the chamber near the outfall and a magnetic stirrer kept stirring inside during the gel preparation to avoid the fast solidification. 1.9ml 4%-gel-solution was added into the chamber away from the outfall and then the pump was started to mix the gel in the two chambers gradually. Finally, the gel mixture was loaded into a protein gel system. The stacking gel was prepared according to the recipe shown in Table 2.19. A total of 8µg Chl in 1×

loading buffer (100mM BisTris-HCl, pH7.0, 0.5M ACA, 30% (w/v) sucrose and 50mg/ml Serva Blue G) was loaded on a BN-PA gel. Anode buffer (50mM BisTris-HCl, pH 7.0) and the cathode buffer contained Serva Blue G dye (50mM Tricine, 15mM BisTris-HCl, pH7.0, 0.01% (w/v) Serva Blue G) were used for electrophoresis. The voltage for electrophoresis was started at 75V on ice with 25V increasing every 30min until max 200V was reached. After electrophoresis, the first dimensional gel was incubated with the SDS sample buffer (50mM Tris-HCl [pH6.8], 10% [v/v] glycerol, 2% [w/v SDS, 0.002% [w/v] bromophenol blue, and 50mM DTT) at RT for 30min and was then sliced into strips. The strips were transferred onto the top of the SDS-PA gel and proteins in the strips were separated again by SDS-PAGE.

Table 2.19: Ingredients of the Blue-native gel

	Stacking	**4%**	**12.5**
40% Acrylamide [ml]	0.3	0.25	0.781
3×Gel buffer [ml]	1	0.0833	0.0833
75% Glycerol [ml]	0	0.15	0.75
H_2O [ml]	1.72	1.257	0.125
TEMED [µL]	6	3	3
10%APS [µL]	16	7.5	7.5

2.8 Measurements of intermediates and end products of TBS pathway

Around 30mg (fresh weight) leaves were harvested for measurements of the contents tetrapyrrole end-products or intermediates. Samples were harvested under the growth conditions and were immediately frozen in liquid nitrogen. For measurements of the contents of MgP, MME, Pchlide and Chlide, 300µl acetone extraction buffer (Table 2.20) was added into the samples and mixed by vortexes. The extracts were then incubated at -20°C for 1h in the dark with occasional inverting the tubes. Pellets were removed after centrifugation at -4°C for 15min. 20µl extracts were loaded for HPLC analysis. For calculations, a standard of MgP, MME were purchased from Sigma-Aldrich. A Pchlide standard sample was extracted from 7-day old etiolated barley leaves, according to (Koski and Smith, 1948). Dark samples and etiolated seedlings for Pchlide content measurements were collected in a dark room with a green safelight. Before re-exposed to light for balancing, the samples were boiled for 2min to inactivate POR. For Chl measurements, 30mg leaf samples were finally dissolved in 1.2ml acetone extraction buffer, and 20µl extracts were loaded for an HPLC analysis.

Table 2.20: Aceton extraction buffer

Compositions	Percentage(V:V)
Acetone	90%
0.2N NH_4OH	10%

For a heme measurement, after Chl was removed by acetone extraction buffer, pellets were dissolved in 300µl acidic extraction buffer (Table 2.21) and incubated at RT for 30min with inverting the tube every 5min. After centrifugation at 14,000rpm for 20min, pellets were removed. 20µl supernatant was loaded for HPLC measurement.

Table 2.21: Acidic extraction buffer

Compositions	Percentage(V:V)
acetone	80%
DMSO	16%
HCl	4%

2.9 Transit transformation and stable transformation of plants by Agrobacterium infection

Constructs for transit or stable transformation were transferred to electrocompetent *A.tumefacien* cells. 2ml overnight culture of *A.tumefacien* was inoculated into 200ml YEP medium (Table 2.22) with relevant antibiotics (GV3101 strains, Rif/Gen; GV2260 strains, Rif/Amp). Cell culture was incubated at 30°C with shaking for around 4h until OD600 reached 1.5~2.0. Cells were harvested at 4,000×g, and 4°C for 10min and the cell pellet was washed by 200ml ddH_2O for 4 times and 20ml ice-cold 10%- glycerol once. Finally, cells were re-suspended in 20ml ice-cold 10%-glycerol and frozen in 40µl aliquots by liquid nitrogen. For transformation, 20µl electro-competent cells were mixed with 50-100ng purified plasmids and electroporated at 2,200V with a pulse of 5~8ms. After recovery at 30°C for 2h, cells were then plated onto a YEP plate containing appropriate antibiotics. Transformants appeared after two days grown at 30°C.

Table 2.22: YEP medium

Compositions	concentrition
Bacto Tryptone	$5gl^{-1}$

Yeast extract	$1gl^{-1}$
Adjust pH to 7.2 with NaOH, Autoclaved	
Sucrose (filter sterilized)	$5gl^{-1}$
MgSO4 • 7H2O	0.5g

Two weeks old *N. benthamiana* plants were used for transient transformation. A single *Agrobacterium tumefaciens* colony from a freshly transformed plate was inoculated into a 3ml YEB medium containing relevant antibiotics. The culture was incubated overnight at 28°C with shaking at 250rpm. Cells were then harvested by centrifugation at 5.500×g for 20min at RT. The cell pellet was re-suspended in the infiltration buffer (10mM MgCl, 10mM MES, pH5.7 and 100µM acetosyringone) to a cell density of OD_{600}=0.6. The cell suspension was incubated at RT for 2-3 hours and then infiltrated into *N. benthamiana* leaves with a 1ml syringe.

For a stable transformation of *Arabidopsis* WT plants, a modified Floral Dip method was used according to (Clough and Bent, 1998). A single *Agrobacterium* colony was inoculated into 4ml YEB medium containing relevant antibiotics. The culture was then overnight incubated at 28°C with shaking. Subsequently, cells were harvested by centrifugation at 5,500×g for 10min and re-suspended in an inoculation medium containing 0.5×MS salts, 0.05% MES buffer, 5% sucrose, 0.05% Silwet L-77 pH5.7 to a final cell density of OD_{600}=0.8. The cell suspension was then dropped onto the green inflorescences of *Arabidopsis* plants. This treatment was repeated for 3 times. Seeds of the plants were collected. Positive transgenic plants were selected by a BASTA or kanamycin selection. For a BASTA selection, around 500µl seeds were germinated on the soil. 0.05% BASTA solution was sprayed on the 2 weeks old plants. The treatment was repeated for 2 times with an interval of 4 days until the transformants appeared.

2.10 Antibody production of FLU

For the production of FLU antibody, the recombinant protein containing TPR(FLU) (from amino acids 199 to 317) and a GST tag (at the N terminus) was purified as the antigen. 1mg antigen with the concentration of 1.5µg/µl was sent to BioGenes GmbH for immunization of a rabbit.

In addition, another purified antibody recognizing the intact *Arabidopsis* FLU was kindly provided by Klaus Apel (Meskauskiene et al., 2001). Western blots using this antibody was designate FLU(AB).

2.11 BiFC assay

BiFC assay was taken to analyze protein-protein interaction according to (Walter et al., 2004). Desired genes were amplified from *Arabidopsis* cDNA with primer pairs containing attB sequence at the 5' and 3' terminus of the genes. The PCR fragments were cloned into pDoner 207 vector by gateway method with a BP reaction kit

produced by Thermo Fisher Scientific. Sequences of positive clones were determined by the second generation of sequencing by LGC and aligned to *Arabidopsis* Col-0 cDNA sequence. Genes for interaction partners were finally sub-cloned into pDEST-GW-VYNE (G1) / pDEST-GW –VYCE (G3) by an LR reaction (a recombination reaction between attL and attR sites) with a kit produced by Thermo Fisher Scientific. The G1 and G3 vector contain N-terminus or C-terminus of a venus YFP sequence, respectively. The constructs were then transformed into *Agrobacterium* (GV2260) cells. *Agrobacterium* (GV2260) cells expressing the interaction partners with YFP halves were co-transferred into three weeks old *N. benthamiana* leaves with a transit transformation protocol as described in 2.9. After three days in darkness, fluorescence from YFP or Chl (excitation at 488nm, emission at 530-555nm for YFP- and 600-700nm for Chl autofluorescence) were imaged by a confocal laser-scanning microscope (CLSM TCS SP2 AOBS, Leica). A western blot analysis was performed to analyze the expression of desired proteins in *N. benthamiana* leaves.

2.12 Yeast two-hybrid assay

2.12.1 Constructs generation

A pDHB1MCS2 vector, modified from pCub, was used to express the bait proteins. The pNub vector was used for expression of the prey proteins. Fragments of genes for interaction partners were amplified from Arabidopsis cDNA were first sub-cloned into an intermediate vector pJET 2.1 by restriction-site cloning or into pDoner 207 by the gateway cloning method. The sequence was then determined by sequencing and aligned to Arabidopsis Col-0 cDNA sequence. Gene fragments were finally inserted into pDHB1MCS2 or pNub by restriction-site cloning or the gateway cloning method and verified by a PCR reaction with gene-specific primers.

2.12.2 Yeast competent cells preparation

A single yeast colony of L40 ccuA or L40 ccuα cells grown on a Yeast Extract-Peptone-Adenine-Dextrose (YPAD) (Table 2.23) agar plate was inoculated into 10ml YEP medium and was incubated overnight at 30°C with shaking. 40ml YEP medium was added and incubated at 30°C for another 3-4h until OD_{600} reached 1.0. Cells were then harvested by centrifugation at 30°C for 10min and washed with sterilized ddH_2O for two times and re-suspended in 100mM LiAc to OD_{600}=1. The cell resuspension was aliquoted into 100µl for each transformation.

Table 2.23: YPAD medium

Compositions	concentrition
yeast extract	1%(w/v)
peptone	2%(w/v)

glucose (filter sterilized)	2%(w/v)
adenine sulfate (filter sterilized)	20mg/l

2.12.3 Transformation of constructs into yeast cells YPAD medium

100µl yeast competent cells were mixed with 200µg carrier DNA (Salon sperm) and less than 5µg transforming DNA. 600µl PEG solution was added into 100µl resuspension of competent yeast cells and mixed by inverting the tubes. The mixture was incubated at 42°C for 30min. Cells were then harvested and re-suspended in sterilized TE buffer and poured onto SD plates (pDHB1 = -leu, pNUB = -trp). Transformants appeared after three days of incubation at 30°C.

2.12.4 Mating and Split Ubi assay

A single colony of cells expressing the bait protein and a single colony of cells expressing the prey protein were inoculated into 500µl YEP medium and incubated at 30°C overnight in a shaker. Subsequently, the overnight cell culture was adjusted to OD_{600}=1 with YEP medium and dropped 10µl cell culture on an SD plate lacking Leu and Trp. Colonies grown on SD plates lacking leu and trp were inoculated into 4ml YPAD. The culture was overnight incubated at 30°C. Cells were then harvested by centrifugation at 3,000×g and washed by sterilized ddH_2O for two times. The cells were re-suspended in YPAD medium and cell intensity was adjusted to OD_{600}=1.0. Finally, 10µl cell culture was dropped onto an SD plate (-his - ura -leu –trp) or an SD plate (-leu –trp). The plates were incubated at 30°C for 3-5 days.

3 Results

3.1 FLU exerts a regulatory impact on ALA synthesis during light exposure

3.1.1 The steady-state levels of intermediates of TBS in *flu*

The knockout of FLU was previously reported to result not only in elevated ALA synthesis in the dark but also in the light (Goslings et al., 2004). The increased ALA synthesis is expected to cause an elevated metabolic flow. Here, the ALA synthesis rate in the leaves of flu seedlings grown under CL for two weeks was elevated by 44% compared to WT. The different value of ALA synthesis found in a previous publication is probably due to the different age of seedlings and different growth conditions. The contents of intermediates of Chl biosynthesis were analyzed to substantiate the molecular differences in the TBS when FLU is absent. The steady-state levels of porphyrins (MgP, MME) and Pchlide were elevated in flu, whereas the Chl content in flu did not change compared to WT (Figure 3.1). These data demonstrate that FLU deficiency causes an elevated ALA synthesis and consequently higher levels of TBS intermediates in plants under CL growth condition.

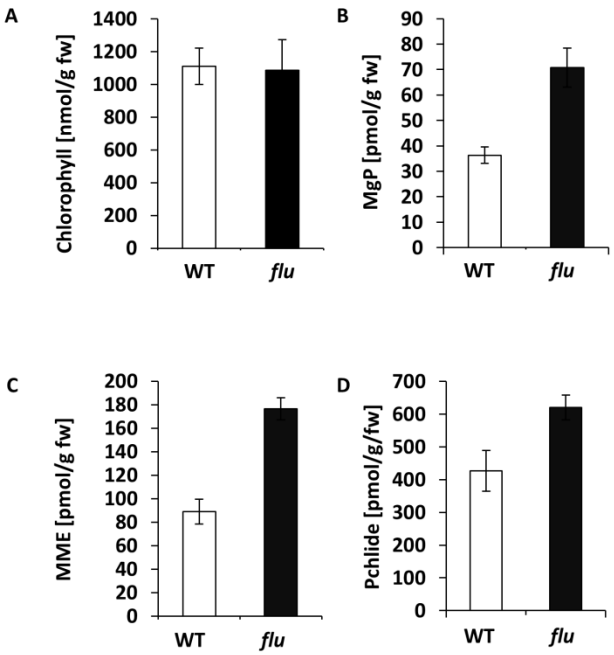

Figure 3.1 The steady-state levels of intermediates of TBS in *flu* under CL. (A) Chl content; (B) MgP content; (C) MME content; (D) Pchlide content. Plants were grown under CL for two weeks. The light intensity was 90 µmol photons $s^{-1}m^{-2}$.

3.1.2 Analysis of FLU overexpressor lines under various light conditions

To analyze the effects of FLU on Chl biosynthesis during light exposure, FLU overexpression lines were generated by expressing the WT genomic *FLU* sequence under the control of the CaMV-35S promoter in WT *Arabidopsis* plants. Fourteen T1 transgenic lines, which resistant to Basta were obtained. This experiment was done

by Dr rer. nat. Hedtke, Boris, and Kersten Träder. Pale-green T2 seedlings were obtained for 11 transgenic lines. Protein samples harvested from green or pale-green progenies were analyzed by western blot analysis with the FLU antibody. The progenies, which contained WT-like amounts of FLU or only slightly elevated amounts of FLU, did not show a pale-green phenotype. The pale-progenies normally contained a high content of FLU (around 30-times more than WT). The pale-green corresponded with a strong overexpression of *FLU*. Individual plants from three independent T2 transgenic lines, FLUOE (#7, #8, #12), which contained the highest amount of FLU, were selected for seeds collection (T3). In the T3 generation, all progenies showed a pale-green phenotype and were taken for further experiments.

3.1.2.1 FLUOE lines under different light intensities

WT and FLUOE plants grown under ML or LL conditions were used to investigate the FLU-mediated regulations on ALA synthesis under different light intensities. FLUOE lines showed a pale-green phenotype and retarded growth compared to WT. The phenotype of FLUOE lines was more severe under LL than ML (Figure 3.2A). The steady-state levels of tetrapyrrole end-products or its biosynthetic intermediates were examined in FLUOE lines. To harvest leaf samples of similar developmental stage, the plants grew two weeks longer under LL than under ML. Consistent with the pale-green phenotype of FLUOE lines, the Chl content in FLUOE lines was 68% of the WT-level in ML while only 24% of the WT level in LL (Figure 3.2B). The different impacts on Chl contents in FLUOE lines under different light intensities were not due to various FLU amounts. Western blot analysis showed that the protein amount of FLU in FLUOE lines under LL was similar to under ML (Figure 3.2C). Interestingly, GluTR content was found to be significantly increased in FLUOE lines compared to WT under both ML and LL conditions (Figure 3.2C). Additionally, the GBP amounts in FLUOE lines also showed increased levels relative to WT (Figure 3.2C). The increased ratio of Chl a/b in FLUOE lines in comparison with WT was detected, indicating likely impaired antenna complexes of both photosystems in FLUOE plants (Figure 3.2D).

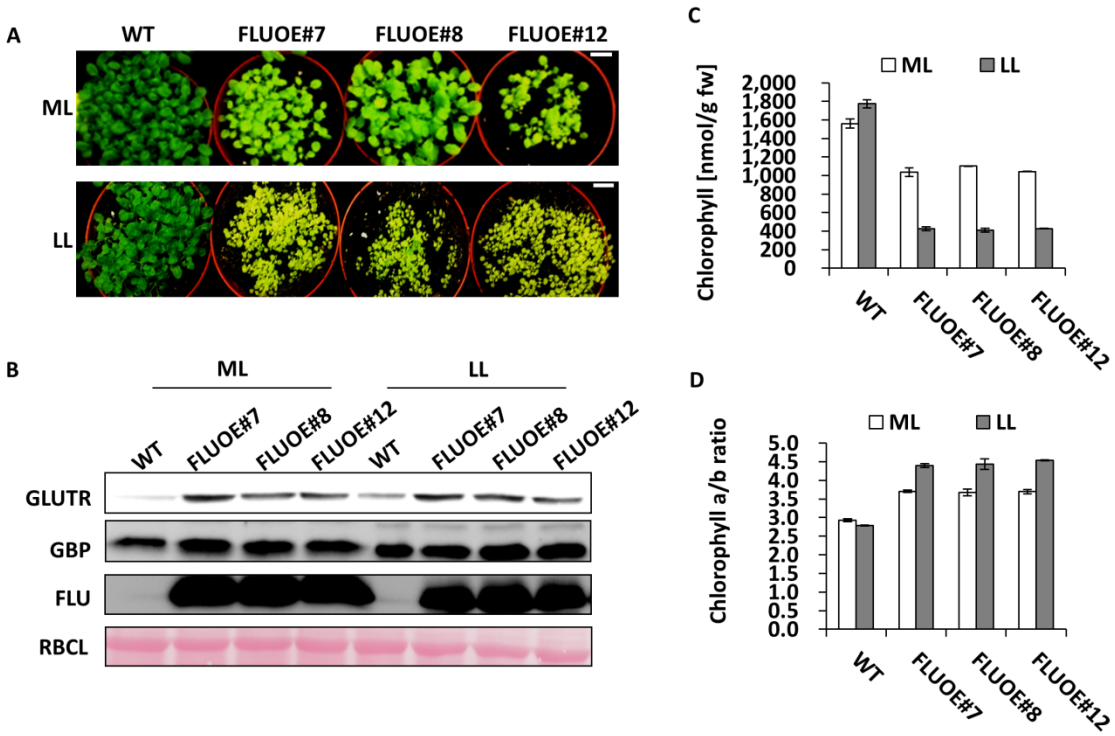

Figure 3.2 Phenotypes of FLUOE lines under ML and LL. (A) FLUOE lines showed a pale-green phenotype, which is more severe under LL than under ML. (B) Western blot analysis of the protein amounts of GluTR, GBP, and FLU in FLUOE lines under LL and ML. The Chl content (C) and Chl a/b ratio (D) in FLUOE lines were measured in seedlings grown under ML (120 µmol photons $s^{-1}m^{-2}$) for 3 weeks or under LL (20 µmol photons $s^{-1}m^{-2}$) for 5 weeks.

Heme contents in FLUOE lines showed reduced levels compared to WT (Figure 3.3). Both WT and FLUOE lines showed decreased levels of heme contents in LL grown leaves compared to ML. Heme content was reduced by 35% in LL-exposed WT leaves compared to ML, while heme content was reduced by 60% in LL-exposed FLUOE leaves relative to ML (Figure 3.3). The LL-dependent decline of heme levels was more pronounced in FLUOE plants in comparison with WT. Chl content in LL-exposed WT leaves was similar to that in ML-exposed WT leaves, while Chl contents in FLUOE lines displayed reduced levels under LL relative to ML (Figure 3.2C). These observations indicate that FLUOE has a specific impact on the Chl biosynthesis while the heme content light dependently varied in WT and FLUOE lines.

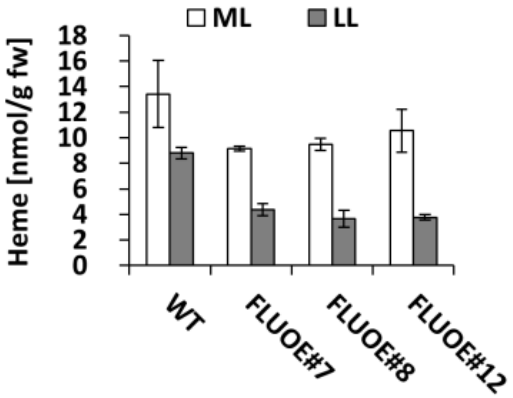

Figure 3.3 Heme contents in FLUOE lines and WT under ML or LL conditions. Plants were grown under the same growth condition as stated in the legend to Figure 3.2.

The overexpression of FLU is expected to cause an over-inactivation of ALA synthesis. Although GluTR content was increased in FLUOE lines compared to WT under both growth conditions (Figure. 3.2), the ALA synthesis rate in FLUOE lines was 29% of the WT level under ML and was only 17% of the WT level under LL (Figure 3.4A). The decline of ALA synthesis rate was more pronounced under LL than ML. Consequently, the steady-state levels of intermediates for Chl biosynthesis, including MgP (Figure 3.4B), MME (Figure 3.4C), and Pchlide (Figure 3.4D), were reduced in FLUOE lines compared to WT, and the reduction was greater under LL than ML conditions.

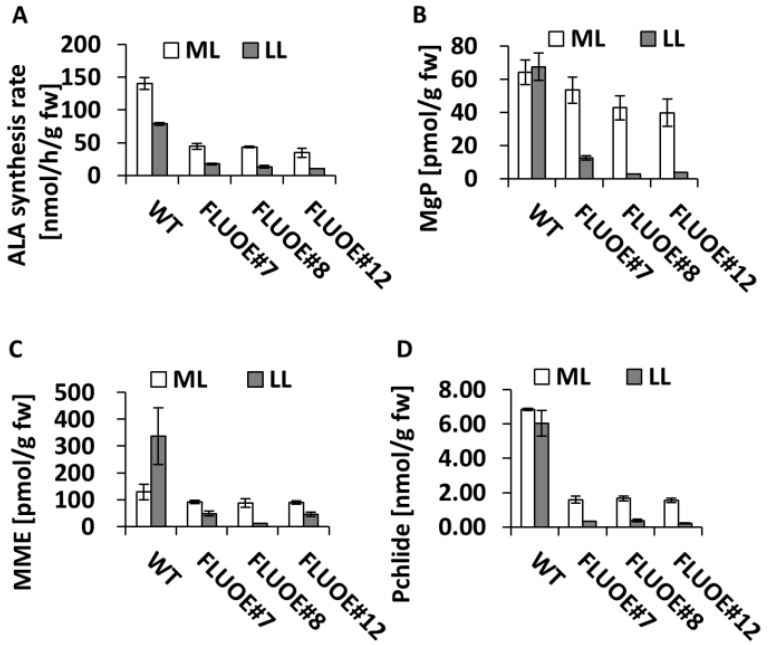

Figure 3.4.The steady-state levels of intermediates of TBS in WT and FLUOE lines under ML or LL conditions. Plants were grown under the same growth condition as stated in the legend to Figure 3.2. (A) ALA synthesis rate; (B) MgP content; (C) MME content; (D) Pchlide content.

Although Pchlide contents in FLUOE lines showed reduced levels compared to WT during day-time, they reached a similar level to WT after a 14h darkness treatment (Figure 3.5). It is assumed that a WT-like amount of FLU is already able to inactivate

most of the GluTR that is allocated for Chl synthesis in a typical dark period during periodic growth. Thus, an excess amount of FLU did not result in a greater inactivation of ALA synthesis in the dark.

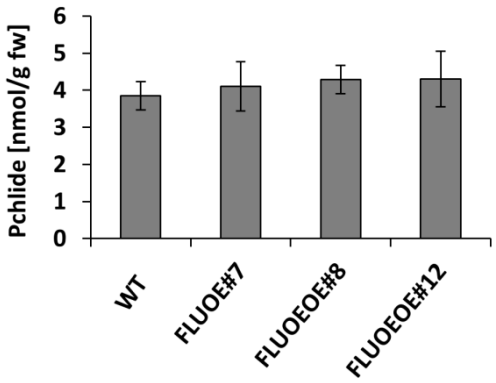

Figure 3.5. Pchlide levels in WT and FLUOE lines in the dark. Plants were grown under light-dark conditions (10h light/14h dark) for three weeks and then transferred to darkness for 14 h.

To exclude an effect of dark growth, FLUOE and WT plants were grown under continuous LL or ML for two weeks. The mutant phenotype of FLUOE lines was more pronounced under continuous LL than ML, while the protein contents of FLU were similar in FLUOE lines under the two different growth conditions (Figure 3.6A). GluTR accumulated in FLUOE lines compared to WT also under CL (Figure 3.6B).

Overall, FLUOE plants showed a less severe pale-green phenotype under CL than under light-dark conditions with the same light intensity. Under ML, Chl contents in FLUOE lines were decreased to 68% of the WT level under light-dark conditions, while CL gave rise to 85% of the WT level. Similarly, under LL, Chl contents in FLUOE lines were reduced to only 24% of the WT level under light-dark conditions while they were still 63% of the WT level under CL (Figure 3.7A and Figure 3.2B). Besides, the steady-state levels of covalent binding heme in FLUOE lines were also reduced compared to WT under CL. The heme contents in FLUOE lines yielded 85% of the WT level under continuous ML, compared to 78% of the WT level under continuous LL (Figure 3.7B).

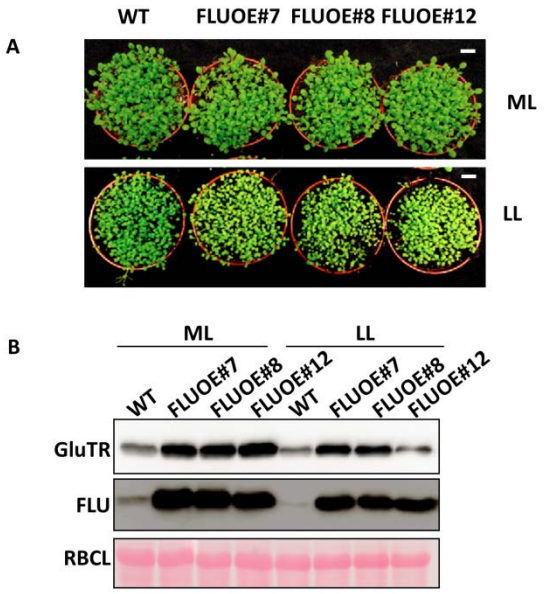

Figure 3.6 Phenotypes of FLUOE lines under continuous ML or LL. (A) FLUOE lines showed a pale-green phenotype, which is more severe under LL than under ML. (B) Western blot analysis of the protein amounts of GluTR and FLU under ML or LL. Plants were grown under light-dark conditions for two weeks. The light intensity was around 90 µmol photons $s^{-1}m^{-2}$ for ML and 20 photons $s^{-1}m^{-2}$ for LL.

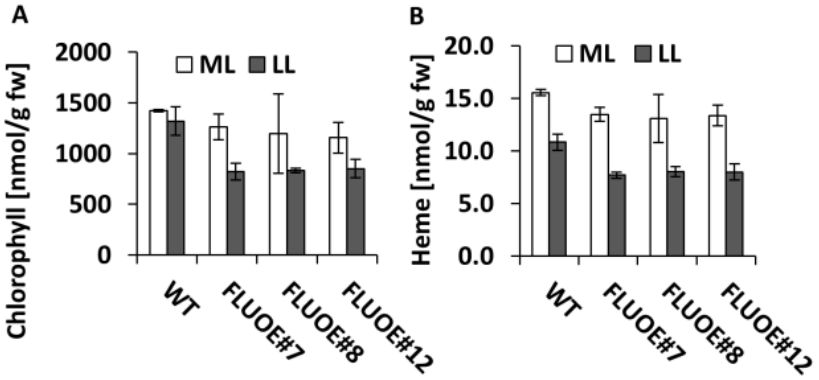

Figure 3.7 The Chl and heme contents in FLUOE lines under continuous ML or LL conditions. (A) Chl contents. (B) Heme contents. Plants were grown under the same growth condition as stated in the legend to Figure 3.6.

The metabolic flow of Chl biosynthesis was analyzed in FLUOE lines grown under CL. The steady-state levels of intermediates of Chl biosynthesis, such as Mg Proto, Chlide and Pchlide were decreased in FLUOE lines compared to WT and were decreased even more under LL than ML, except for MME, which has a high turnover rate. These data indicate that the metabolic flow of Chl biosynthesis was suppressed in FLUOE lines under CL.

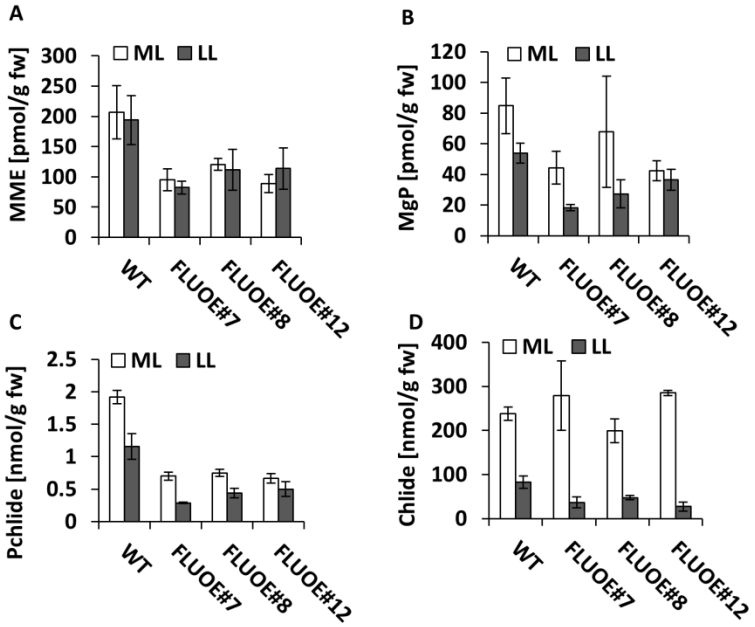

Figure 3.8 The steady-state levels of intermediates of Chl biosynthesis in FLUOE lines under continuous ML or LL conditions. (A) MME content; (B) MgP content; (C) Pchlide content; (D) Chlide content. Plants were grown under the same growth condition as stated in the legend to Figure 3.6.

3.1.2.2 The gene expression and protein levels of enzymes/genes involved in TBS

The protein amounts and transcripts of key genes involved in Chl biosynthesis were examined in FLUOE lines. The amount of GluTR in FLUOE lines increased dramatically compared to WT, while the transcript of *HemA1* did not significantly change (Figures 3.9 and Figure 3.10). Thus, the increased amount of GluTR was not due to an increased expression of *HemA1*, but likely a result of the post-translational control. The GBP also accumulated in FLUOE lines compared to WT (Figure 3.9). A direct interaction between FLU and GBP could not be found by BiFC assays (data is not shown). Therefore, the increased GBP amount in FLUOE lines is unlikely the result of a stabilizing effect through direct interaction with FLU. The contents of GSAT in FLUOE lines showed a similar level to WT (Figure 3.9).

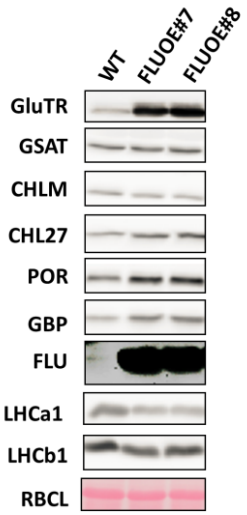

Figure 3.9 The levels of proteins involved in TBS or photosynthesis in FLUOE lines and WT. Plants were grown under light-dark conditions for three weeks. The total proteins of plant extracts were separated by SDS-PAGE and then transferred to a membrane. Specific antibodies were incubated with the membrane. Signals were finally probed by the enhanced chemiluminescence detection. LHCa1 and LHCb1 are the major light-harvesting proteins of PSI and PSII. RBCL indicates the Ponceau S-stained protein band of the large subunit of RuBisCo and is used for equal loading. Abbreviations for enzymes involved in TBS are explained in the legend to Figure 1.1.

FLU was found in a complex with the enzymes catalyzing the last steps of Chl biosynthesis (Kauss et al., 2012b). It was observed that the protein amounts of PORB and CHL27 were increased while the content of CHLM remained unchanged in FLUOE lines. The protein amounts of the light-harvesting proteins LHCa1 and LHCb1, which are present in PSI and PSII respectively, were decreased in FLUOE lines, indicating that the stability of the antenna complexes of the photosystems are compromised when Chl biosynthesis is impaired in FLUOE lines (Figure 3.9). The expression of most of the genes involved in TBS was not significantly changed in FLUOE lines compared to WT (Figure 3.10).

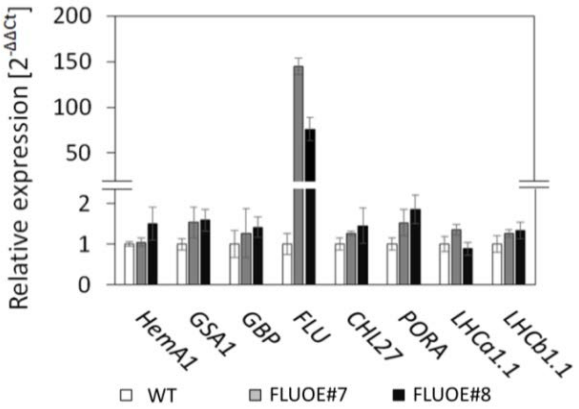

Figure 3.10 The transcript level of genes involved in TBS or photosynthesis in FLUOE lines and WT. Plants were grown under light-dark conditions for three weeks. Gene expression was normalized to SAND transcript content, and the relative expressions were calculated by $2^{-\Delta\Delta Ct}$. *LHCa1.1* and *LHCb1.1* encode the light-harvesting proteins. Abbreviations are explained in the legend to Figure 1.1.

3.1.2.3 FLUOE plants under high light stress

Under HL stress condition, plants tend to reduce the antenna for light-harvesting to avoid the absorption of excess light energy, which may result in the generation of excessive ROS in plants. It was hypothesized that plants grown under HL stress also need a negative regulator of ALA synthesis to reduce the Chl synthesis and thereby to reduce the Chl supply for the light-harvesting antenna. FLUOE plants were first grown under continuous ML for three weeks. Consistent with the previous data, a minor reduction of Chl content in FLUOE lines could be observed under continuous ML condition (Figure 3.7 and Figure 3.11A). After a short period (5h) of HL stress, the Chl contents in WT and FLUOE lines did not change significantly; however, after an extended period of HL stress (3 days), both the Chl contents in FLUOE lines and WT decreased significantly. FLUOE lines showed a greater reduction in Chl content than WT, especially in the newly grown leaves (Figure 3.11A). However, heme levels in WT and FLUOE lines were not altered by HL stress (Figure 3.11B). The expression of two of the marker genes responsive to the ROS accumulation was examined in WT and FLUOE lines under ML or HL. *CYP81D8*(AT4G37370) encodes a protein that belongs to the cytochrome P450 family. *CYP81D8* is a general oxidative stress-responsive marker gene (Baruah et al., 2009b). The expression of the AAA-ATPase gene (*AAA1*, At3g28580) is specifically activated by $^1O_2$, but not by superoxide or hydrogen peroxide (Danon et al., 2005; Baruah et al., 2009a). Under HL stress, the WT expression of both *CYP81D8* and *AAA1* was induced compared to ML condition. However, an induced *CYP81D8* expression was observed to a low extent in one FLUOE line compared to WT. But the expression of *AAA1* was drastically declined in the FLUOE lines relative to WT under HL (Figure 3.11C and D). This indicates a low level of $^1O_2$ content in the FLUOE lines relative to WT.

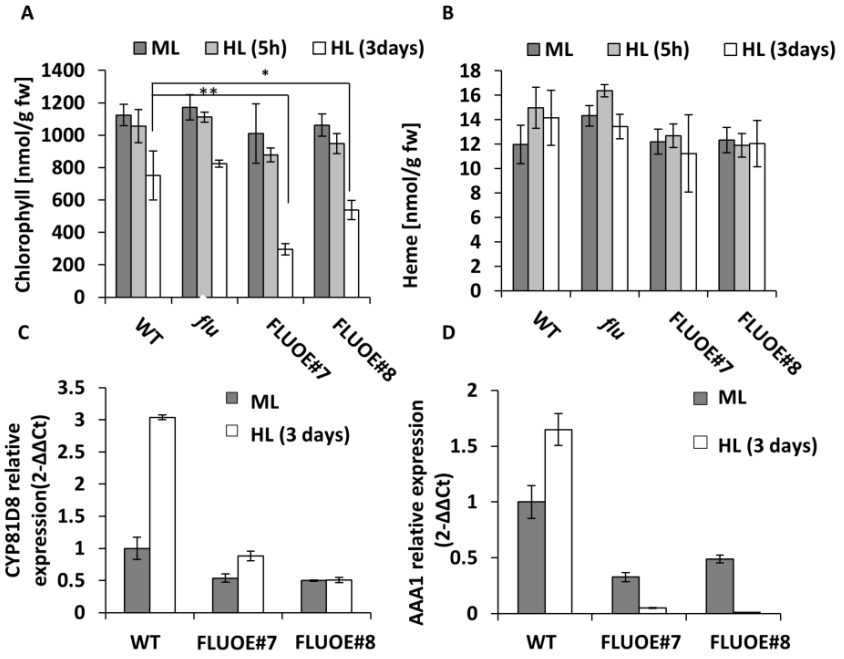

Figure 3.11 *flu* and FLUOE lines under HL stress. Plants were grown under continuous ML (90 photons $s^{-1}m^{-2}$) for three weeks and then transferred to HL (900 photons $s^{-1}m^{-2}$) for 5 hours (HL, 5h) or 3 days (HL, 3 days). The steady-state levels of Chl contents (A) and heme contents (B) in WT, *flu* and FLUOE lines. *, P<0.05 **, P<0.01. (C) and (D), the expressions of ROS marker genes in WT and FLUOE lines under ML or 3 days HL. *AAA1* is a $^1O_2$ induced gene; The expression of *CYP81D8* is induced by general ROS accumulation. The relative gene expressions were normalized to the expression of the housekeeping gene, *SAND*.

3.1.2.4 Sub-compartmental localization of GluTR in plants

GluTR and GSAT do not contain a TM domain. Recently, several reports suggested that a portion of GluTR was associated with the thylakoid membrane (Czarnecki et al., 2011; Wang et al., 2016). It was proposed that some of the interaction partners on the membrane are responsible for anchoring GluTR in the membrane. FLU is a membrane protein. It is speculated that GluTR-FLU interaction affects the localization of GluTR, and consequently affects its enzyme activity. This could be a novel mechanism for controlling ALA synthesis by changing the sub-compartmental localization of GluTR. Therefore, the ratio between the membrane-associated and soluble GluTR amounts was investigated under various growth conditions in WT and transgenic lines, which have a modified ALA synthesis.

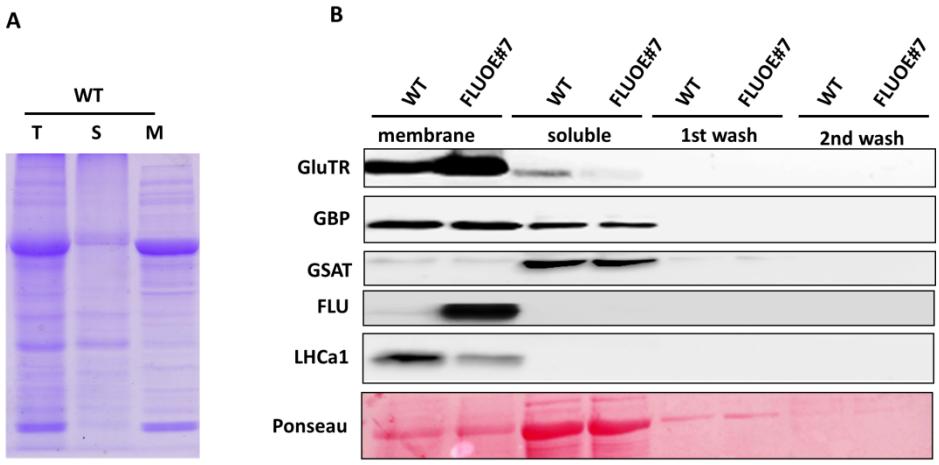

Figure 3.12 Analysis of the amounts of the membrane-associated and soluble proteins involved in ALA synthesis and light-harvesting. (A) A coomassie stain of proteins of the total extract (T), soluble fraction (S) and the pellet fractions separated by SDS-PAGE. WT plants were grown under light-dark conditions for three weeks. Fractions were obtained as described in 2.4.2 (B) Western blot analysis of the protein amounts of GluTR, GBP, GSAT, FLU and LHCa1 in the membrane and soluble fractions. In order to test whether most of the soluble proteins were extracted in the initial PBS buffer, two additional washing steps were performed on the membrane fraction.

Initially, the traditional chloroplast isolation method was performed to obtain intact chloroplasts. However, this method needs a huge amount of plant material. Moreover, during the lengthy procedure of chloroplast isolation, damage to chloroplasts is inevitable due to the removal of chloroplasts from the cytoplasm environment. A fast and crude method was applied to separate whole plant tissue into soluble and membrane fractions in a fast and material-saving way (Chapter 2.4.2). Since most of the enzymes of the Chl biosynthesis pathway are exclusively localized in chloroplasts, fractions separated by this rough method can also reflect the distributions in the chloroplasts.

The membrane and soluble fractions of total leaf extracts were separated on a 12% SDS-PA gel and stained with a coomassie brilliant blue. It was found that the most abundant protein, the large subunit of Rubisco (RBCL), was present in the soluble fraction (Figure 3.12A). Subsequently, the amounts of the membrane-associated and soluble proteins of GluTR, GSAT, GBP, FLU, and LHCa1 were analyzed in WT and one of the FLUOE lines by western blot analysis. It was shown that the thylakoid-localized proteins FLU and LHCa1 were exclusively present in the membrane fraction and that the vast majority of GSAT was in the soluble part. This fits very well with previous observations (Pontoppidan and Kannangara, 1994; Meskauskiene et al., 2001; Wientjes et al., 2009). GluTR and GBP were found in both membrane and soluble fractions. In the FLUOE line, most of the GluTR was found in the membrane fraction and only a small amount remained in the soluble part. These findings support the idea that FLU-GluTR interaction anchors GluTR to the thylakoid membrane. Furthermore, to determine whether all of the soluble proteins were dissolved in the initial PBS buffer, two additional wash steps were performed with the pellet fraction. As result, hardly any signal was found in western blot analysis of the eluate of the 2nd

and 3rd wash steps, which means that most of the soluble proteins were already dissolved in the initial PBS buffer.

In addition, the thylakoid membrane complexes of WT and FLUOE lines were separated on a two-dimensional blue-native PA gel. The distributions of GluTR and FLU in different complexes were analyzed. According to the first-dimensional gel, the amount of LHCII timers in FLUOE lines decreased relative to WT, which was consistent with the previous finding that LHC protein amounts decreased in FLUOE lines (Figures 3.13A and Figure 3.9). Due to the lack of antenna complexes, the LHCI core complex showed a relatively increased content in FLUOE lines in comparison to WT (Figures 3.13A). By western blot analysis, the distribution pattern of GluTR in the second-dimensional gel resembles that of FLU in WT and FLUOE lines. The majority of FLU migrated to the low molecular weight part of the gel (Figure 3.13B). This result indicates that GluTR is associated with FLU on the thylakoid membrane.

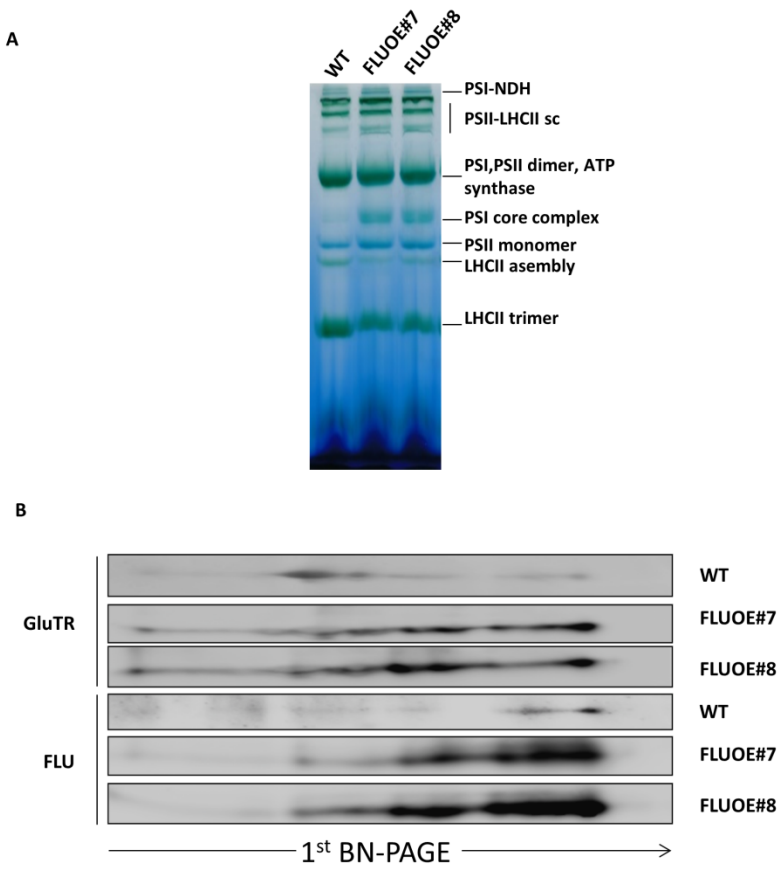

Figure 3.13 BN-PAGE analysis of the distribution of GluTR and FLU on the thylakoid membranes of *Arabidopsis* WT and FLUOE lines. (A) The first-dimensional BN-PAGE of thylakoid membrane protein complexes from 3-week-old WT and two FLUOE lines. (B) Immunoblot analysis of GluTR and FLU of the second-dimensional BN-PAGE. Plants were grown under light-dark conditions (120 µmol photons $m^{-2}s^{-1}$, 14h light/ 10h dark).

Judith Schmied analyzed the amounts of membrane-associated and soluble GluTR under various light conditions and in leaves of different age (Schmied et al., 2018). My data confirmed her results that ALA synthesis in plants correlates with the amount of soluble GluTR. ALA synthesis oscillates with a diurnal rhythm and reaches a peak in the middle of the day (Kruse et al., 1997). GluTR amounts in the membrane and soluble fractions were analyzed over the course of a day. WT plants grown under light-dark conditions for 2.5 weeks were harvested in the morning (1 hour after the onset of light exposure), in the middle of the day, in the afternoon, or in the dark (1 hour after the beginning of darkness). Higher levels of soluble GluTR were found in the middle of the day, while levels of membrane-associated GluTR remained similar (Figure 3.14).

Chl biosynthesis activity was thought to vary in different leaf positions. ALA synthesis is expected to be more active in the newly developed leaves than in the older leaves. To analyze GluTR localization in leaves of different ages in mature WT plants, newly grown leaves (indicated in the red frame) and old leaves (indicated in the yellow frame) were harvested. In the old leaves, the majority of GluTR was found in the membrane fraction, while newly developed leaves, which are expected to have a

higher ALA synthesis, contained more soluble GluTR (Figure 3.15). Taken together, plant material harvested from tissues, which are expected to have a higher ALA synthesis rate, relatively showed a higher soluble GluTR content.

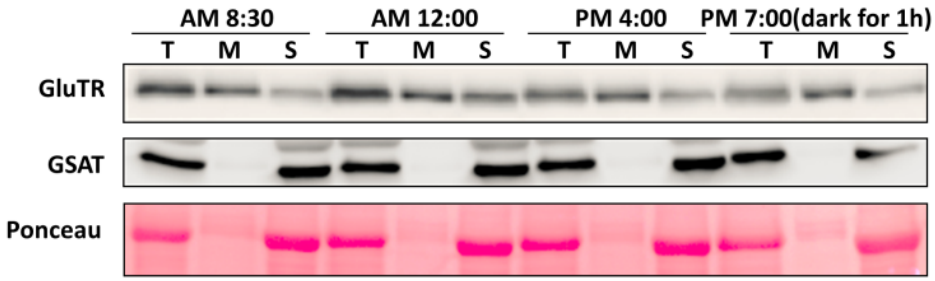

Figure 3.14 Western blot analysis of the contents of GluTR and GSAT in total protein extract (T), membrane fraction (M) or the soluble fraction (S) at several time points during a day in WT plants under periodic growth. WT plants were grown under the 10h light/14h dark condition for three weeks. Ponceau indicates the Ponceau S-stained protein band of the large subunit of RuBisCo, and is used for equal loading.

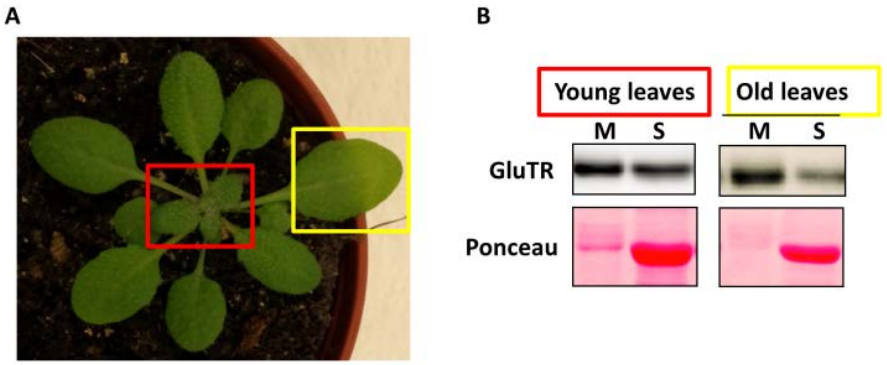

Figure 3.15 The contents of the membrane-associated and soluble GluTR in leaves of different developmental stage of 4-week-old seedlings. (A) An image of a four-week-old plant. Young leaves were marked red and old leaves were marked yellow. (B) The contents of soluble (S) and membrane (M) GluTR in young and old leaves.

In addition, GluTR localization in mutants missing GluTR interaction partners was determined. Plants were grown under CL for two weeks. The first and second true leaves were harvested for the separation of the membrane and soluble fractions. Under these conditions, the majority of GluTR in WT was found in the membrane fraction. Most of the mutants have a similar GluTR localization as WT, such as HEMA1/WT (*HEMA1*-overexpressor lines) and GluTRΔHBD (*HEMA1* complementation line with truncated GluTR lacking the HBD domain, Apitz et al. 2016) and *gbp*. The *clpc1* mutant showed elevated levels of soluble GluTR compared to WT, which could be explained by a reduced degradation rate of soluble GluTR in the *clpc1* mutant (Apitz et al., 2016). The FLUOE line contained a higher total GluTR amount than HEMA1/WT and the majority of GluTR of the FLUOE line was found in the membrane fraction. Conversely, the *flu* mutant contained higher amounts of

GluTR in the soluble fraction than in the membrane fraction (Figure 3.16). However, a small portion of GluTR can still be found in the membrane fraction in the *flu* mutant (Figure 3.16).

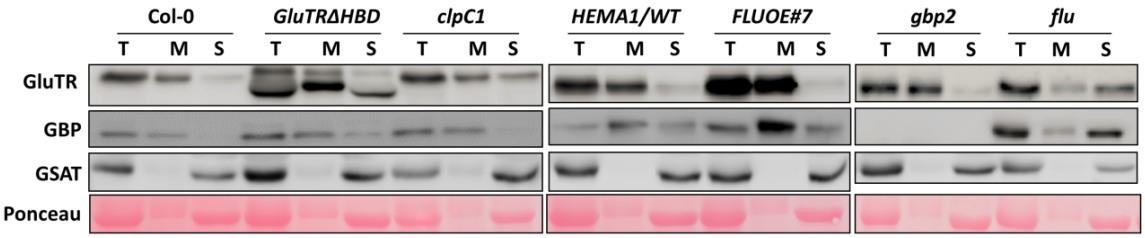

Figure 3.16 Western blot analysis of the contents of GluTR, GBP and GSAT in the total protein extract (T), membrane fraction (M) or the soluble fraction (S) of WT and mutants grown under CL for two weeks. Ponceau indicates the Ponceau S-stained protein band of the large subunit of RuBisCo and is used for equal loading. GluTRΔHBD is a *hema1* complementation line with a GluTR variant with deleted HBD. HEMA1/WT is a *HEMA1* overexpression line with slightly increased levels of GluTR. FLUOE#7 is a FLU overexpression line.

It was proposed that the FLU-GluTR interaction is driven by the Pchlide accumulation in the dark (Kauss et al., 2012b). More GluTR is expected to be associated with the thylakoid membrane by FLU in the dark than in light. GluTR localization in the light or dark was analyzed in WT, *flu,* and FLUOE lines. The ratio of soluble/membrane amounts of GluTR shown in Figure 3.16 was different from that shown in Figure 3.17. The difference was explained by the different harvesting strategies. Plant material for analysis depicted in Figure 3.16 was harvested from the first and second true leaf of 2-week-old plants and that in Figure 3.17 was from the newly developed young leaves of 3-week-old plants. In the newly developed leaves, the amount of soluble GluTR was found to be similar as the amount of membrane GluTR (Figure 3.17). When WT plants were transferred to darkness for 5h, the amount of soluble GluTR was significantly reduced, while the amount of membrane-associated GluTR increased (Figure 3.17). However, the majority of GluTR remained in the soluble or membrane fractions in the *flu* or FLUOE, respectively, before or after a 5h dark period. The relative amounts of GluTR in membrane and soluble fractions in WT, *flu* and FLUOE seedlings were quantified and displayed in Figure 3.18. The quantifications were based on two biological repeats.

ALA synthesis rate was increased in *flu* and decreased in the FLUOE line (Figure 3.19). This indicates that ALA synthesis negatively correlates with the amount of FLU protein, but positively with the amount of soluble GluTR (Figure 3.17 and Figure 3.19). The GBP amount was equal in the soluble and membrane fractions in WT while in *flu* and FLUOE, the dominant content of GBP was found in the soluble and membrane fraction, respectively. GBP appears to co-fractionate always with GluTR. As a negative control, GSAT was exclusively found in the soluble fraction, and FLU was exclusively found in the membrane fraction (Figure 3.17).

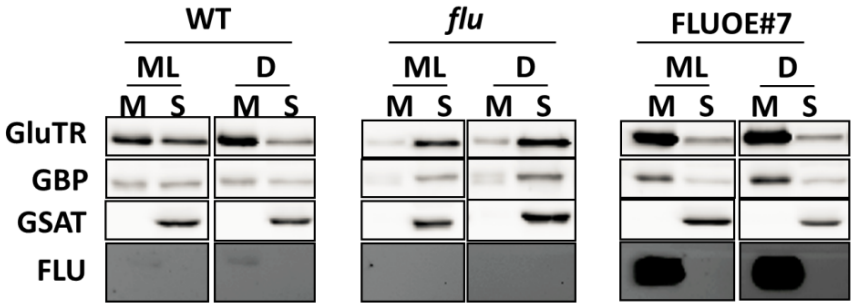

Figure 3.17 Western blot analysis of the amounts of membrane-associated (M) and soluble (S) proteins involved in ALA synthesis under ML or after 5h darkness (D). Plants were grown under CL for three weeks and transferred to the dark for 5h. The young leaves were harvested for separation of the membrane, and soluble fractions. Proteins extracts were separated on a SDS-PA gel, then transferred to a membrane, and subsequently probed by specific antibodies.

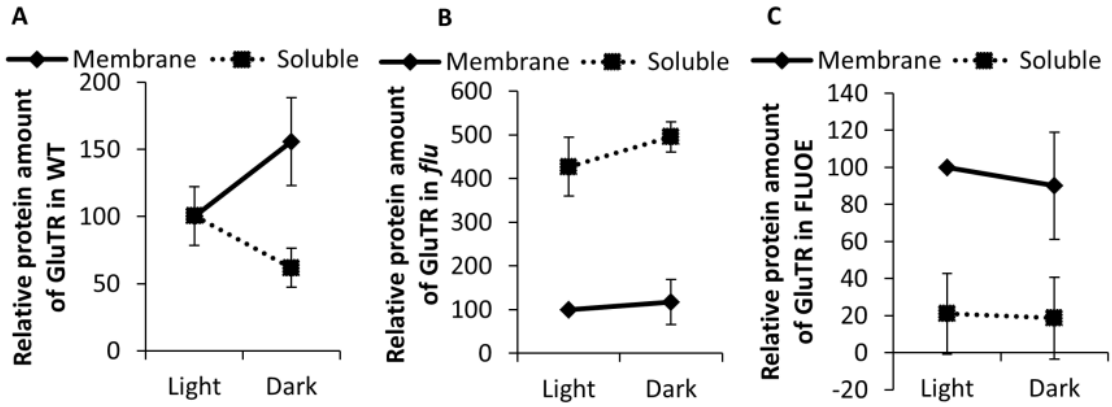

Figure 3.18 Relative quantifications of the immune signal of GluTR in Figure 3.17. The signal intensities of the membrane-associated GluTR in the light-exposed samples of WT, *flu,* or FLUOE were defined as 100, and the relative signal intensities in other fractions were then determined. (A) WT, (B) *flu*, (C) FLUOE#7. The quantifications are based on two biological repeats.

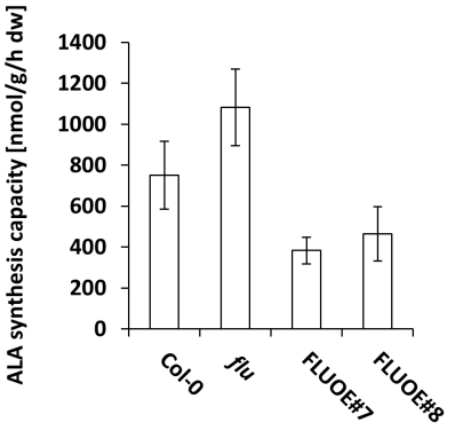

Figure 3.19.ALA synthesis rate in WT, *flu* and FLUOE plants. Plants were grown under CL for two weeks. The light intensity was around 90 µmol photons $m^{-2}s^{-1}$. Leaves were harvested for ALA measurement. Values were normalized to the dry weight of plant samples.

ALA synthesis is expected to be highly stimulated during the de-etiolation of plants, as there is a huge demand for Chl to drive the assembly of the photosynthetic apparatus (Stephenson and Terry, 2008). The amounts of membrane and soluble GluTR in plants during this physiological process were analyzed. Before being exposed to light, GluTR was mainly found in the membrane fraction of WT and FLUOE seedlings, while GluTR was predominantly found in the soluble part in *flu*. In WT, the content of soluble GluTR increased gradually 30 min after exposure to light, while membrane-bound GluTR remained almost the same (Figure 3.20A). In *flu*, programmed cell death was triggered when the etiolated seedlings were exposed to light (Meskauskiene et al., 2001). The transcript of *HEMA1* was dramatically decreased in *flu* after 30 min of light exposure (Figure 3.20B). The soluble part of GluTR in *flu* was rapidly degraded 10 min after exposure to light, while a similar amount of GluTR remained in the insoluble fraction (Figure 3.20A). In FLUOE seedlings, the dominance of GluTR was exclusively found in the membrane of the etiolated seedlings or de-etiolated seedlings. The amount of soluble GluTR was also slightly increased in FLUOE line during de-etiolation (Figure 3.20A). The intensities of immune signals of the immune-reacting protein band representing GluTR blot displayed in shown in Figure 3.20A were quantified by GelAnalyzer 2.0; the results were shown in Figure 3.20 C, D, and E, based on two biological repeats.

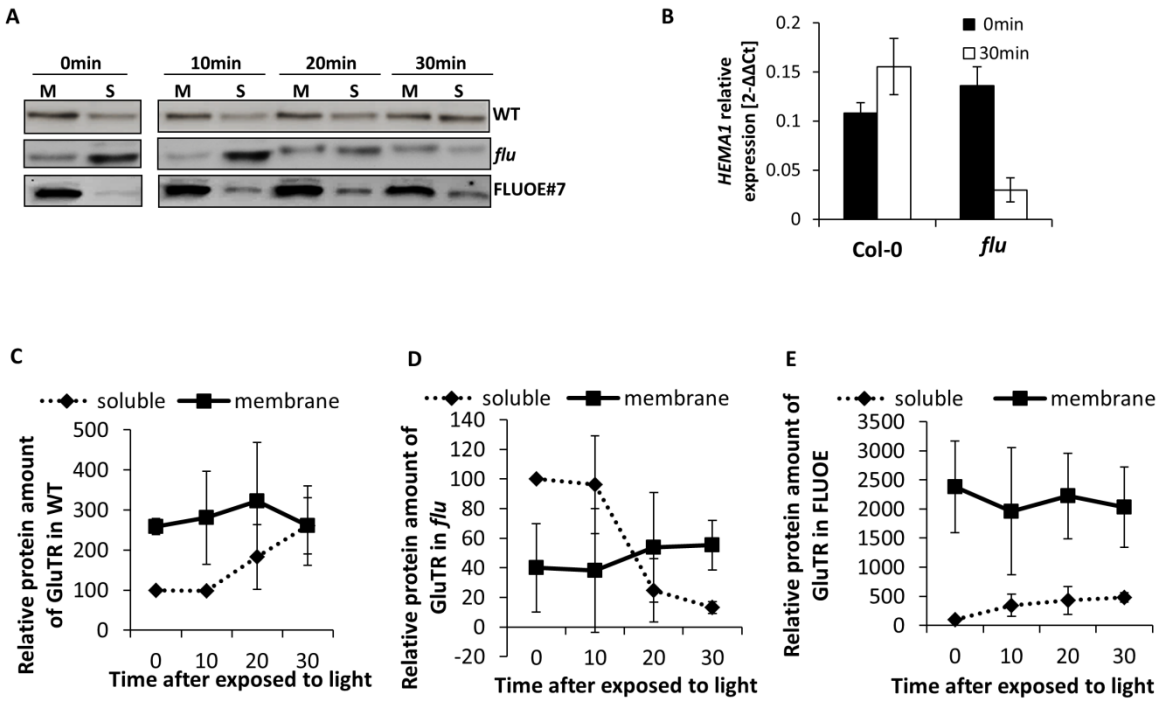

Figure 3.20 The amounts of soluble and membrane-associated GluTR in the etiolated seedlings exposed to light. (A) Western blot analysis of the contents of membrane and soluble GluTR in the etiolated or de-etiolated seedlings exposed to light for 10 min, 20 min and 30 min (light intensity is around 100µmol photons $m^{-2}s^{-1}$). (B) The *HEMA1* transcripts were calculated relative to the expression of *SAND* in etiolated seedlings of WT and *flu* in the dark or after 30 min exposure to light. (C-D) The quantifications of the signal intensities of the immune-reacting protein band representing GluTR blot displayed in Figure A. The signal intensity of the membrane-associated GluTR in the etiolated seedlings (0 min) of WT, *flu,* and FLUOE was defined as 100. The relative signal intensities in

other fractions were then determined. (C) WT, (D) *flu*, (E) FLUOE. The quantifications are based on two biological repeats.

The proteolytic degradation of GluTR was previously shown to be conducted by the stroma-localized Clp protease (Apitz et al., 2016). It was hypothesized that the binding of GluTR to the thylakoid membrane affects the proteolytic degradation of GluTR. To assess this hypothesis, mutants and WT were grown under the light-dark conditions for three weeks and then transferred to dark for 12 h or 72 h. GluTR in WT or HEMA1/WT was dramatically degraded after 72 h of dark treatment. The *gbp* mutant showed an even faster degradation of GluTR in the dark compared to WT. The content of GluTR in the *clpc1* mutant or the truncated GluTR in GluTRΔHBD remained almost unchanged after 72 h incubation in the dark (Figure 3.21).

GluTR were previously shown to be mainly in the membrane fraction in FLUOE lines. The membrane association of GluTR by FLU might prevent the degradation of GluTR. After 72h incubation in the dark, GluTR content in the FLUOE line decreased compared to 0h as like in WT (Figure 3.21A). To compare the degradation rate of GluTR in FLUOE and WT, the relative amount of GluTR were quantified in three biological repeats of WT and FLUOE samples harvested from 0h and 72h and displayed in Figure 3.21B. It was found that the degradation rate of GluTR in the dark was slowed down in the FLUOE line compared to WT. These results indicate that the FLU-GluTR interaction might partially protect GluTR from degradation by Clp protease after an extended period in the dark.

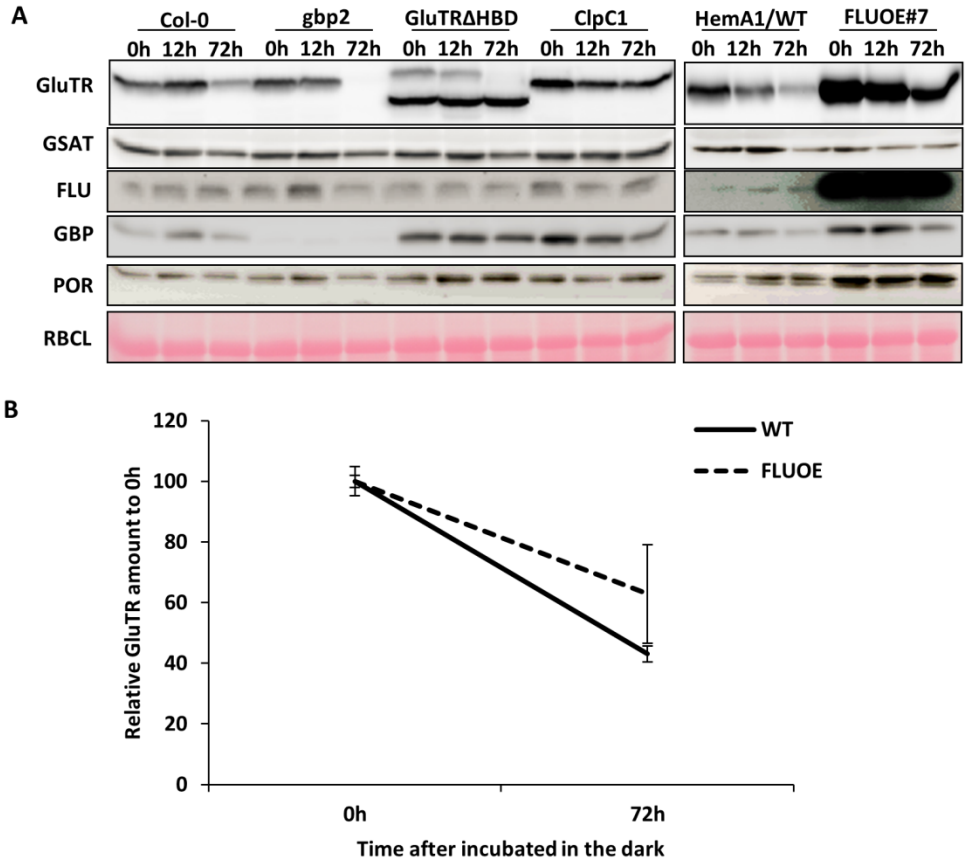

Figure 3.21 GluTR amounts in WT and mutants in the light (0) or after a 12h or 72h dark treatment. (A) Western bot analysis of the contents of proteins involved in ALA synthesis in the light or dark. Plants were grown under light-dark conditions for three weeks and transferred to the dark for 12h or 72h. Protein samples were separated on a SDS-PA gel. After transfer to a membrane, proteins were probed by specific antibodies and visualized by ECL detection. RBCL was used for equal loading (B) Quantification of the immune signal intensities of GluTR at time point 0 h and after the 72 h dark-incubation of WT and FLUOE seedlings. The intensities of the signal corresponding to GluTR content at 0 h of WT and FLUOE seedlings were defined as 100. The relative signal intensity in WT and FLUOE samples after 72h dark incubation were determined, respectively.

3.1.2.5 FLU is required under fluctuating light growth conditions

Although the ALA synthesis rate was increased in *flu,* no obvious phenotype was previously found under CL of 14-day-old seedlings (Figure 3.1; Meskauskine et al., 2001). However, while the light intensities under laboratory conditions can be kept constant, the light conditions are usually more complex in field experiments. The light intensity is continuously changing, often quite rapidly by sudden appearance of sun-flecks or shading through clouds and subsequent removal of the clouds, etc, (Kaiser et al., 2018; Slattery et al., 2018). ALA synthesis requires precise control under rapidly changing light conditions, as the requirements for Chl amounts vary under different light conditions (Zhang et al., 2016). To test how important the role of FLU under the changing light conditions, *flu* was grown under fluctuating light (FL), changing light intensities from ML to LL every 30 min.

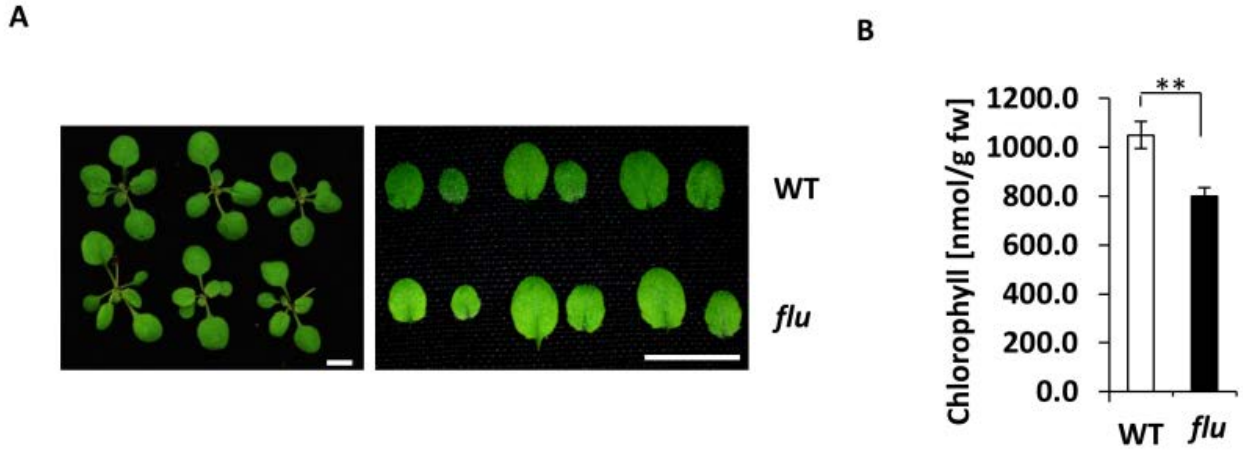

Figure 3.22 The phenotype of *flu* under fluctuating light. WT and *flu* were grown under CL and changing light intensity every 30 min from LL (20 µmol photons $m^{-2}s^{-1}$) to ML (130 µmol photons $m^{-2}s^{-1}$). (A) The left panel shows the phenotype of seedlings, while the right panel shows the third and the fourth true leaves from three individual WT (upper) and *flu* (underneath) plants. (B) The Chl contents in *flu* and WT grown under fluctuating light. The third and fourth true leaves were harvested for the measurements.

Under FL growth condition (30min LL/30 min ML), *flu* showed a pale-green phenotype; the phenotype was more obvious in the newly formed leaves (Figure 3.22A). The Chl contents of 2-week-old of *flu* and WT plants grown under FL were analyzed. *flu* has 20% less Chl content relative to WT under this growth condition (Figure 3.22B). To exclude effect from genetic background, the growth of two *flu* complementation lines FLU(WT) were also tested under FL. The contents of FLU in FLU(WT) lines showed increased levels compared to WT, although the expression of *FLU* was driven by the endogenous *FLU* promoter. GluTR amounts in FLU(WT) were not significantly change compared to WT (Figure 3.23B). WT, *flu* and FLU(WT) lines were first germinated under CL and then transferred to FL for 1 week. The newly formed true leaves of *flu* showed apparently pale-green phenotype but not those of FLU(WT) lines (Figure 3.23A).

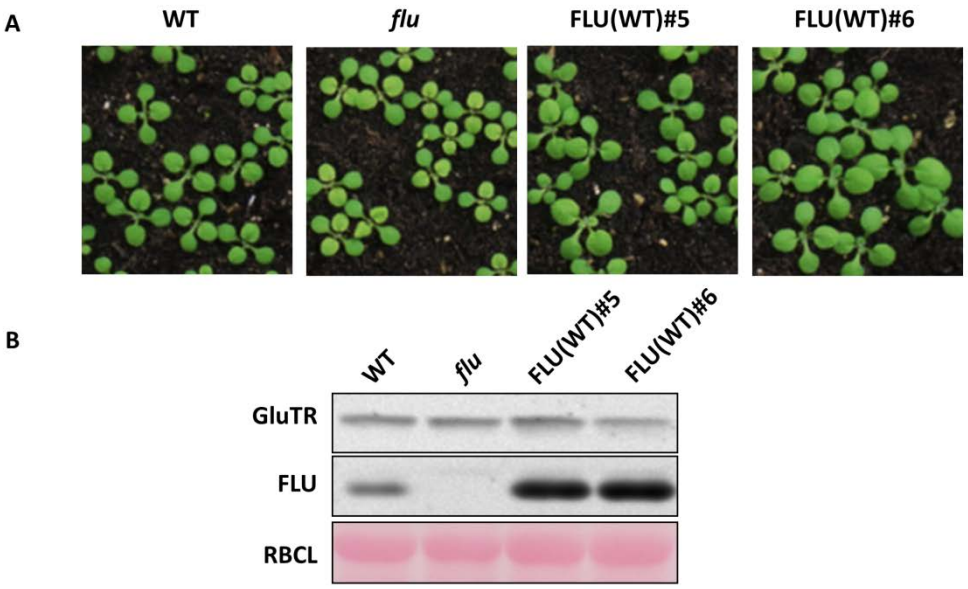

Figure 3.23 *flu* complementation lines under fluctuating light. (A) WT, *flu,* and FLU(WT) lines were grown under continuous fluctuating light with a frequency of changing light intensity every 30 min from LL (20 µmol photons $m^{-2}s^{-1}$) to ML (130 µmol photons $m^{-2}s^{-1}$). (B) Western blot analysis of the contents of GluTR and FLU in WT, *flu*, and FLU(WT) lines. RBCL is used for equal loading.

To determine the reason for the impaired Chl biosynthesis of *flu* under FL, the metabolic flow of Chl biosynthesis was analyzed. Samples were harvested at the end of LL or ML period of FL for tetrapyrrole contents analysis. ALA synthesis rate under LL was lower compared to ML in both WT and *flu*. The *flu* mutant has a higher ALA synthesis rate than WT under CL (Goslings et al., 2004). But this was not observed under FL (Figure 3.24). The amounts of proteins involved in ALA synthesis (GluTR, GSAT, and GBP) were not changed in comparison with WT (Figure 3.25). The contents of porphyrins (MgP and MME) showed increased levels in *flu* under LL, but decreased under ML compared to WT (Figure 3.24B and C). Pchlide contents increased in *flu* and WT under LL compared to ML. Under LL, *flu* accumulated the highest amount of Pchlide, which was three folds higher than the amount of Pchlide in WT under ML. This Pchlide accumulation in *flu* under LL might cause the generation of ROS in plants, which is deleterious for plants upon light exposure (op den Camp et al., 2003; Brzezowski et al., 2014).

The expression of several ROS-responsive marker genes was analyzed under FL growth condition. The expression of *AAA1* and *BON ASSOCIATION PROTEIN 1 (BAP1)* was specifically activated by $^1O_2$ but not by superoxide or hydrogen peroxide (op den Camp et al., 2003; Baruah et al., 2009b). The expressions of *AAA1* and *BAP1* increased under ML and increased even more under LL in *flu. CYP81D8*, a general ROS-responsive gene, showed increased expression in *flu*. Ascorbate peroxidases (APX) and glutathione peroxidases (GPX) catalyze the reduction of H_2O_2 to water (Dietz et al., 2006; Chang et al., 2009; Foyer and Shigeoka, 2011; Juszczak et al., 2012). The expression of *APX1*, *GPX1* and *GPX7* did not show a significant change compared to WT under FL (Figure 3.26). These data indicate that the production of $^1O_2$ increased in *flu* under FL.

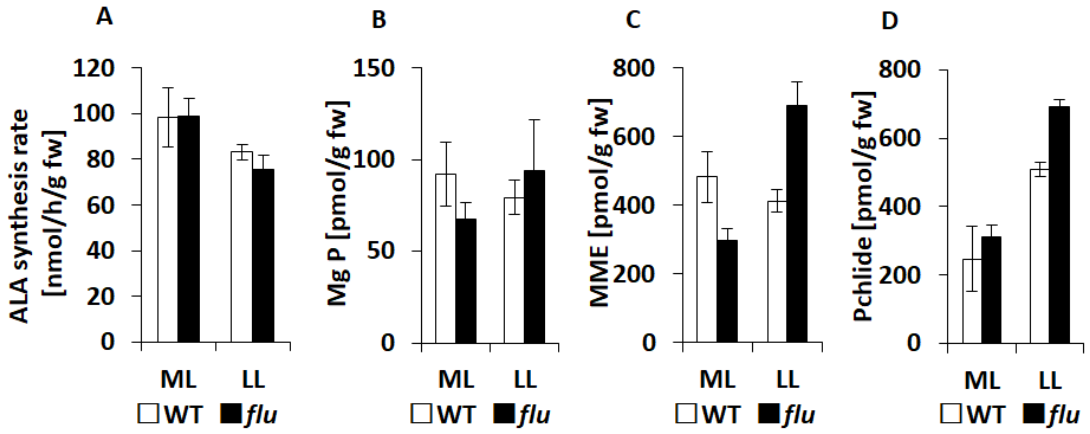

Figure 3.24 Analysis of the metabolic flow of TBS pathway in *flu* and WT grown under fluctuating light. (A) ALA synthesis rate, (B) MgP contents, (C) MME contents, (D) Pchlide contents. Plants were grown under CL fluctuating at LL, 20 µmol photons $m^{-2}s^{-1}$, 30min/ML, 130 µmol photons $m^{-2}s^{-1}$, 30min for two weeks. The third and fourth leaves were harvested at the end of the LL periods or at the end of the ML periods.

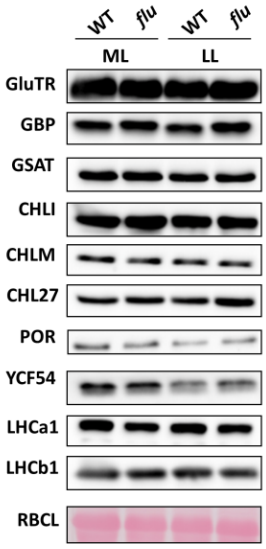

Figure 3.25 Western blot analysis of the contents of proteins involved in the TBS pathway and photosynthesis in WT and *flu* grown under continuous fluctuating light. Plants were grown under fluctuating light with changing light intensity from 20 µmol photons $m^{-2}s^{-1}$ (LL) to 130 µmol photons $m^{-2}s^{-1}$ (ML) every 30 min for 2 weeks. Total protein was extracted at the end of the LL period or at the end of the ML period.

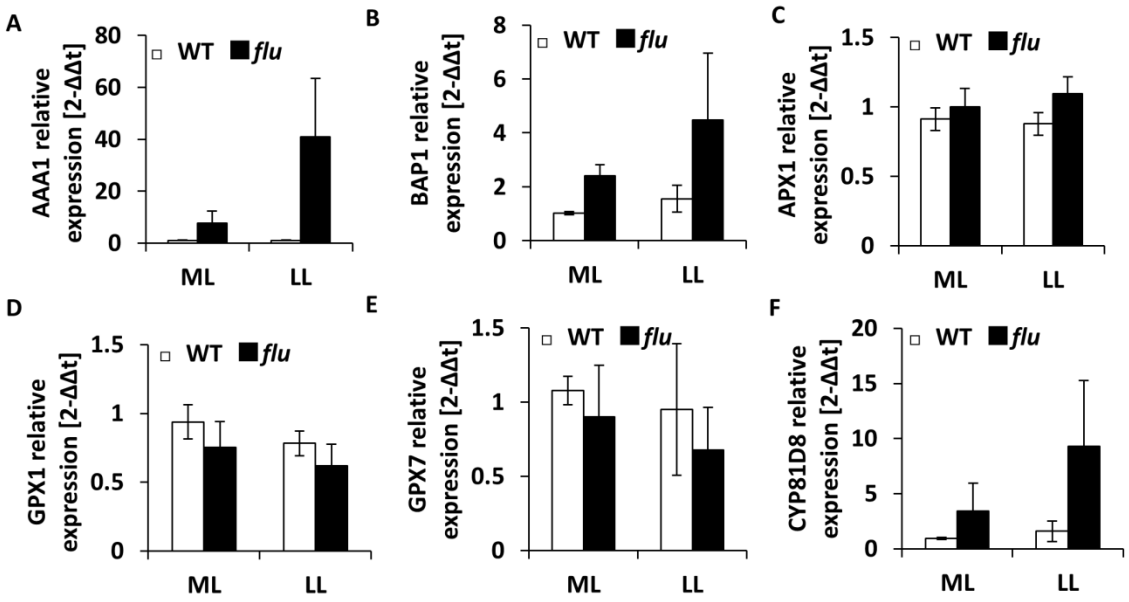

Figure 3.26 Analysis of the expression of ROS responsive marker genes in *flu* and WT plants grown under fluctuating light. Plants were grown under CL fluctuating at LL, 2L0 µmol photons $m^{-2}s^{-1}$, 30min/ ML, 130 µmol photons $m^{-2}s^{-1}$, 30 min for 2 weeks . The third and fourth leaves were harvested at the end of the LL and at the end of the ML period.(A) *AAA1*, encoding an AAA-type ATPase and (B) *BAP1* are $^1O_2$-responsive genes; (C) *ascorbate peroxidase 1, APX1* ; (D) *glutathione peroxidase 1, GPX1* and (E) *glutathione peroxidase 7, GPX7* are H_2O_2-responsive genes; (f) *CYP81D8* is a gene induced by oxidative stress. Data are given as means ± SD (n=3).

The light intensity during an open field trial was recorded seasonally and it was found that the light intensities vary from extreme HL to darkness, while the time scales differ for each season within less than one second (Slattery et al., 2018). The growth of *flu* was tested under FL with different fluctuating schemes. Under FL with 12h LL and 12h ML, *flu* showed a pale-green phenotype. The Pchlide content in *flu* increased substantially at the end of the LL period. More than four times the amount of Pchlide accumulated in *flu* at the end of the LL period compared to the ML period (Figure 3.27). Moreover, the growth of WT and *flu* under FL with 30 min, 50 µmol photons $m^{-2}s^{-1}$/ 30min, 300 µmol photons $m^{-2}s^{-1}$was tested. The newly developed leaves of *flu* also showed an apparent pale-green phenotype. Under this growth condition, Chl content in *flu* was found to be 86%±7.6 of the WT value.

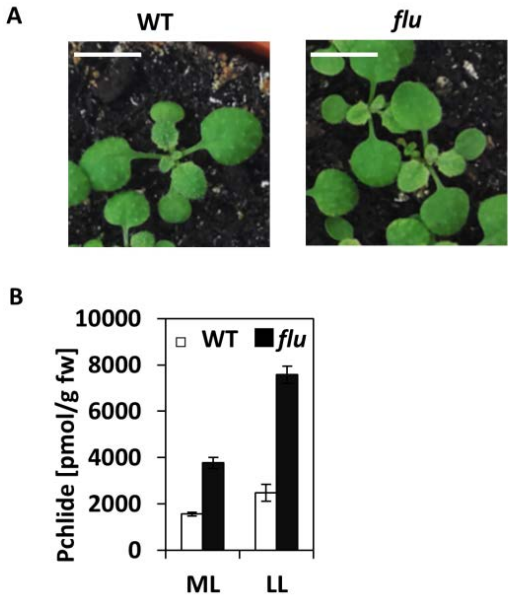

Figure 3.27 The phenotype (A) and the Pchlide contents (B) of *flu* and WT grown under continuous FL with longer intervals of the same light intensities. Plants were grown under continuous FL with changing light intensities from 20 µmol photons $m^{-2}s^{-1}$ (LL) to 130 µmol photons $m^{-2}s^{-1}$ (ML) within 12h intervals. Pchlide samples were harvested at the end of the LL period or at the end of the ML period.

3.2 Redox-dependent cysteine residues of FLU

It was suggested that enzymes of ALA synthesis are controlled by thiol-based regulation (Richter and Grimm, 2013). Dithiothreitol (DTT) is used in a standard SDS-PAGE to reduce disulfide bridges of proteins. To explore the potential of redox-active cysteine residues in FLU/GluTR, a non-reducing SDS-PA gel (without DTT) was applied to separate the total protein extract of WT, and FLUOE lines. Plant materials were harvested in the dark (23:00, 5h transferred to dark) or light (12:00). Proteins were then transferred to a membrane and probed with specific antibodies against GluTR or FLU. Under reducing condition (+DTT), FLU migrated as a 23 kDa protein, which is the predicted size of the monomeric FLU, while under non-reducing condition (-DTT), both in WT and FLUOE lines, FLU migrated as a 45 kDa protein band, which is the size of FLU dimers (Figure 3.28). The majority of GluTR migrated at the 55kDa level, which is related to the predicted size of GluTR monomers (Figure 3.28). This data indicated that FLU in plants forms a homo-dimer, probably through the formation of an intermolecular disulfide bond between two FLU proteins. The FLU homodimer was also analyzed under various growth conditions in WT, such as HL, LL, cold stress, or in etiolated and de-etiolated seedlings. However, no change in dimer formation was found for any of the examined conditions (Figure S1).

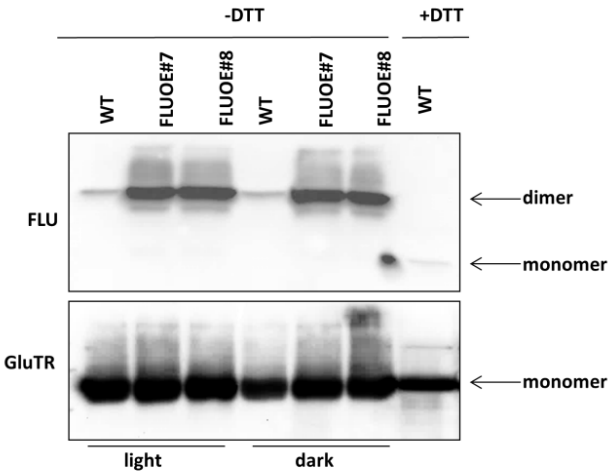

Figure 3.28 Redox-state of FLU and GluTR in WT or FLUOE lines in the dark and in the light. Total protein samples of WT or FLUOE lines were extracted under non-reducing conditions (-DTT) or reducing conditions (+DTT). Plants were grown under light-dark conditions (10h light/14 dark) for two weeks. Samples from light-grown seedlings were harvested in the middle of the day, and dark samples were harvested 5 hours after a transition from light to darkness. Protein samples were separated on a SDS-PA-gel. Subsequently, proteins were transferred to a membrane and probed with specific antibodies reacting with FLU or GluTR. The immune-reacting bands migrate at the predicted size of monomeric or dimeric FLU and GluTR, respectively, as indicated by arrows.

In *Arabidopsis thaliana*, FLU has two conserved cysteines (Cys119 and Cys292) (Figure S2). To determine which cysteine residue is required for the formation of the FLU dimer, two cysteine-substitution mutants (FLUC119S#, FLUC292S#) were generated expressing one of the site-directed *FLU* mutants. As a negative control, FLU(WT)# *flu* complementation lines expressed the WT *FLU* in the *flu* mutant. The expression of these mutant genes was under the control of the *FLU* promoter. Both FLUC119S# and FLUC292S# lines were able to grow under light-dark conditions (14h light/10h dark). A 20% reduced Chl content was determined in the FLUC119S lines compared to WT (Figure 3.29B). The ALA synthesis rate was decreased in the FLUC119S lines, while the other lines showed similar levels to WT (Figure 3.29C). Pchlide substantially accumulated in *flu* in the dark (Meskauskiene et al., 2001). Successful complementation of *flu* is defined when Pchlide accumulation in the dark reaches WT levels. Pchlide levels of the *flu* complementation lines in the dark were measured. Plant material was harvested at several time points in darkness. It was found that the Pchlide accumulation in all cysteine-substitution lines was not higher than the dark-grown WT (Figure S3). The expression of the WT FLU, FLUC119S and FLUC292S proteins in *flu* suppressed the Pchlide accumulation of *flu* in the dark. Pchlide levels of FLUC119S lines in the dark were even lower than in FLU(WT) lines (Figure S3).

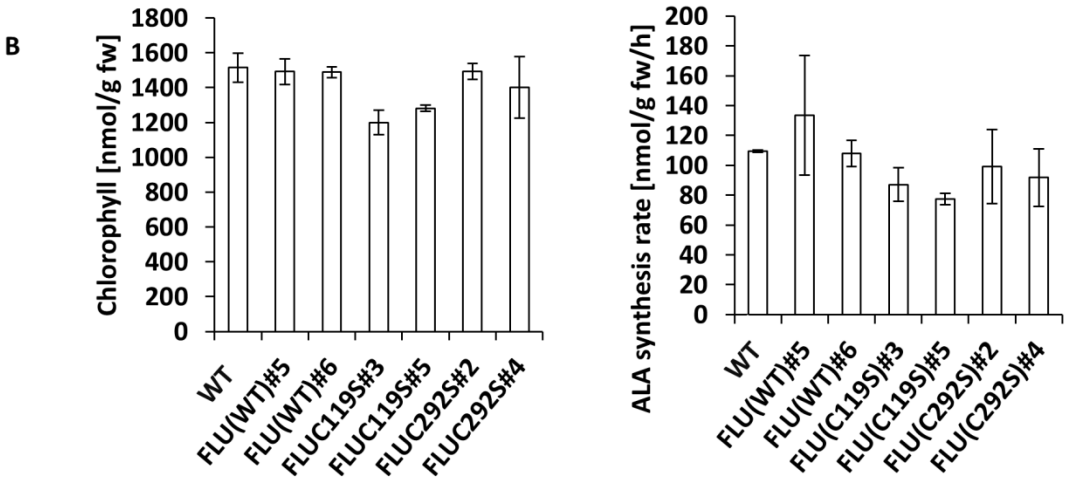

Figure 3.29 The image of single plants, Chl contents and ALA synthesis rate of WT, and FLU cysteine-substitution lines. Plants were grown under light-dark conditions for three weeks. FLU(WT)#5 and FLU(WT)#6 are two lines expressing the WT *FLU* in the *flu* background. FLUC119S#3 and #5 are two individual lines expressing a DNA sequence coding for a serine substitution FLU at the position 119; FLUC119S#2 and #4 are two *flu* complementation lines expressing a DNA sequence coding for a mutant FLU with the cysteine292 substituted by a serine. The expression of all mutant genes is under the control of the *FLU* promoter.

Under the non-reducing condition FLU of WT and FLU(WT), and FLUC292S of FLUC292S lines migrated as a 45kDa protein band in the SDS-PA gel, which is the predicted size of the FLU-dimer, while FLUC119S of FLUC119S lines migrated at a 23kDa protein, which is the predicted size of the FLU monomer (Figure 3.30A). The mutation of cysteine119, rather than cysteine292, on FLU, disrupted the FLU homo-dimer formation in plants. The signal intensity of the FLU monomer in FLUC119S lines was significantly lower than that of the FLU-dimer in WT or other complementation lines (Figure 3.30A). The substantially lower signal intensity of the band representing the monomer of FLU than of the band representing the dimer of FLU is probably due to the antibody recognizing the FLU dimer more efficiently than the monomeric form of FLU. Under reducing condition, the steady-state level of FLU in all the complementation lines was higher than in WT, which was due to the elevated *FLU* transcripts in the complementation lines (Figure 3.30C).

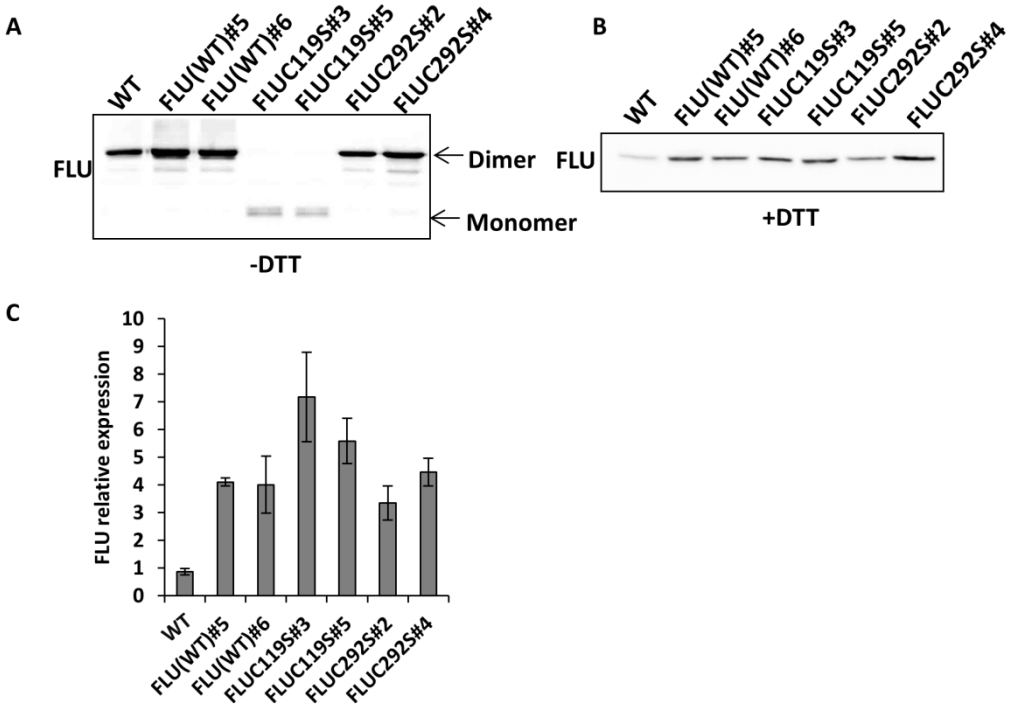

Figure 3.30 Immune-blotting analysis of FLU under non-reducing (A) and reducing conditions (B) and the levels of the *FLU* transcript in WT and *flu* complementation lines (C). Plants were grown under light-dark conditions for three weeks. Protein samples were extracted under non-reducing condition (A) or reducing condition (B) and then separated by SDS-PAGE. Proteins were transferred to a membrane and probed with FLU antibody. FLU(WT)#5 and FLU(WT)#6 are two lines expressing *FLU* in the *flu* mutant background. FLUC119S#3 and #5 are two individual lines expressing a DNA sequence coding for a mutated FLU with cysteine119 substituted with a serine in *flu*. FLUC119S#2 and #4 are two *flu* complementation lines expressing a DNA sequence coding for a mutated FLU with cysteine292 substituted with a serine. The expression of all complementation lines is under the control of the original *FLU* promoter.

3.3 Analysis of functional domains of FLU

Three functional domains were proposed to be in FLU, namely TPR(FLU), TM and the linker domain (Chapter 1.4.2.2). It was previously demonstrated that the direct physical interaction of the TPR(FLU) peptide with GluTR suppresses the enzyme activity of GluTR in an in vitro experiment (Zhang et al., 2015). To determine whether TPR(FLU) suppresses the ALA synthesis in vivo, *flu* complementation lines expressing the TPR(FLU) peptide were generated. In addition, to determine the function of the linker domain and the TM domain of FLU, the respective truncated FLU peptides lacking either the TM domain or the linker domain were also aimed to be expressed in the *flu* mutant (Figure 3.31).

The transit peptide of FLU for chloroplast import had not yet been determined. The alignment of homologs of *FLU* from several species of angiosperms tells that 98 amino acids residues at the N-terminus of the precursor protein of FLU are non-conserved, which is the typical characteristic for a transit peptide (Figure S2). The mature FLU of WT plants was migrated as a 23 kDa protein on a SDS-PA gel. The molecular weight of the intact precursor protein of FLU is predicted to be around

34kDa. Therefore, the transit peptide is speculated to be around 11kDa, which also indicates that the cleavage site for maturing FLU should be at around 98 amino acids. A fusion protein of the predicted FLU transit peptide and GFP was transiently expressed in *N. benthamiana* leaves. The green fluorescence emitted from the GFP fusion protein co-localized with the Chl fluorescence (Figure S4), showing that the fusion protein is targeted to the chloroplasts. This result indicates that the predicted FLU transit peptide contains the transit peptide for chloroplast import. This peptide was fused to TPR(FLU) so that TPR(FLU) could be imported into chloroplast (Figure 3.31). In addition, a HA-tag was added to the N-terminus of TPR(FLU) which enables detecting of the expected protein with the anti-HA antibody by western blot analysis.

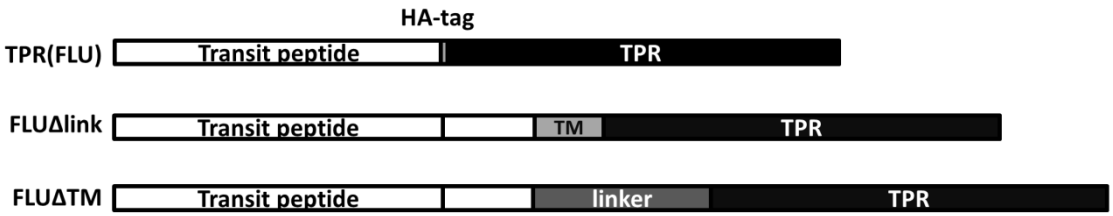

Figure 3.31 The protein constructs of the truncated FLU peptides that were aimed to be expressed in plants. TPR(FLU), the protein construct of TPR(FLU), which consists of 98 amino acid residues (putative transit peptide) of the precursor protein of FLU at the N-terminus and the last 118 amino acids residues (the TPR domain of FLU at the C-terminus. An HA-tag consisting of the amino acid sequence YPYDVPDYA is in between these two domains;

FLUΔlinker, the protein construct of a desired truncated FLU peptide with the deletion of the amino acids residues from 146 to 197 (linker);

FLUΔTM, the protein construct of a desired truncated FLU peptide with the deletion of the amino acids residues from 125 to 146 (TM).

3.3.1 Expressing *TPR(FLU)* in the *flu* mutant

The genomic DNA sequence encoding the transit peptide and TPR(FLU) was amplified and fused together by overlapping PCR. The expression of the target gene was driven by the CaMV-35S promoter (Figure 3.32A). This gene construct is designated TPR(FLU) (Figure 3.32A) and was introduced into the flu mutant. These flu complementation lines are designated TPR/flu#. The genotype of the transgenic plants was determined by PCR reactions using two pairs of primers. One primer pair was specific for the endogenous FLU. This primer pair contained two genome-specific sequences that hybridize to regions flanking the deleted sequences (linker and TM motif). By using this prime pair, a PCR product was amplified both from the genomic DNA of WT and all mutants. As the transgene did not contain the linker and TM motifs, an additional smaller PCR product could be amplified from the genomic DNA of TPR/flu lines (Figure 3.32B). A separate PCR reaction using a CaMV-35S-promoter-specific primer and a FLU-specific primer was applied to test the presence of the transgene. By using this primer pair, a PCR product was only amplified from the genomic DNA of TPR/flu lines which contained the transgene, but

not from WT and flu (Figure 3.32B). This PCR product was purified and was further verified by sequencing.

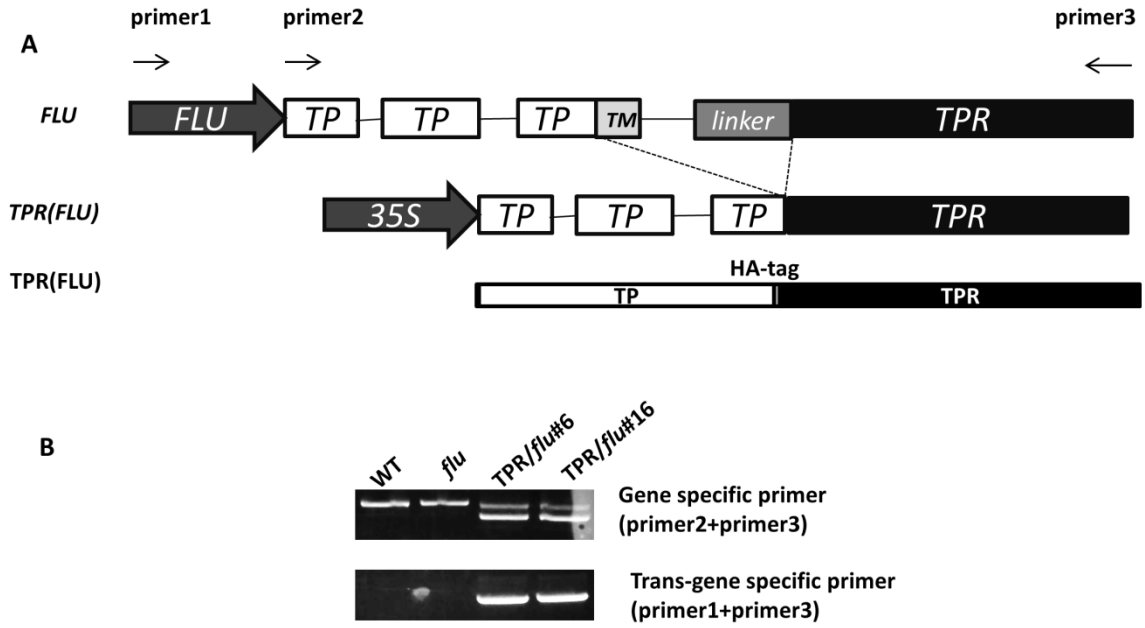

Figure 3.32 The gene construct to express TPR(FLU) in *flu* (A) and genotyping of the transgenic lines (B).(A) From top to bottom: the first two schematic representations show the gene constructs of the endogenous *FLU* and the transgene expressing the genomic DNA sequence encoding the transit peptide and TPR(FLU); the third schematic representation shows the protein domains encoded by the transgene. (B) PCR reactions and gel electrophoresis were used to determine the genotype of the DNA samples of T1 TPR/*flu* plants. In the upper panel, A primer pair specific for *FLU* was used to check for the presence of WT *FLU* in WT or point-mutated *FLU* in *flu* mutant lines, indicated by the higher band and also check for the presence of the transgene in TPR/*flu* lines, indicated by the lower band. In the lower panel, a separate PCR reaction using a CaMV-35S-specific primer and a *FLU*-specific primer was applied to test for the presence of the transgene. Arrows on the top of (A) indicate the location on *FLU* of the primers used for genotyping.

Sixteen individual primary transgenic TPR/*flu* plants of T1 generation were resistant to the herbicide Basta. In the next generation, pale-green progenies could be found in all the TPR/*flu* lines under CL. The molecular weight of transgenic truncated FLU protein, TPR(FLU), was expected to be 15 kDa. Using purified antibodies for FLU (obtained from the group of Prof. Apel) or anti-HA-tag, two specific immune-reacting bands of 15 kDa and 20 kDa could be found in the pale progenies but not in the green progenies of TPR/*flu* lines (Figure 3.33). The truncated FLU was successfully expressed in the pale progenies of TPR/*flu* lines. The presence of TPR(FLU) caused a pale-green phenotype even under CL. Plant materials were harvested from the pale progenies of TPR/*flu* lines for further experiments.

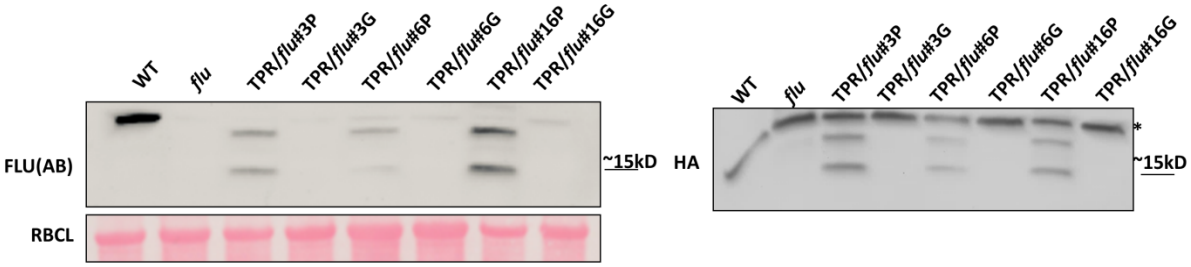

Figure 3.33 Western blot analysis of the T2 progenies of TPR/*flu* lines with purified antibodies specific for the intact FLU or anti-HA-tag. The T2 generation of TPR/*flu* lines comprised pale (sample numbers with P at the end) and green progenies (samples with G at the end). The truncated forms of FLU were found in the pale progenies. * indicates the unspecific band recognizing by the HA antibody. RBCL indicates the Ponceau S-stained protein band of the large subunit of RuBisCo.

Using a primer pair specific for the *TPR(FLU)* motif for qRT-PCR analysis, the transcript level of *TPR(FLU)* motif in the TPR/*flu* lines was around 140 times higher than the level of endogenous *FLU* in the WT (Figure 3.34). To compare the protein amount of TPR(FLU) in TPR/*flu* lines with the amount of intact FLU in WT, the antibody specifically recognized TPR(FLU) was generated (Chapter 2.10). The amount of TPR(FLU) protein in TPR/*flu* lines only reached similar level of FLU in WT (Figure 3.35); this indicates that TPR(FLU) in plants is highly unstable. The transcript levels of other genes involved in ALA synthesis, namely *HEMA1, GBP,* and *GSAT1* did not change (Figure 3.34). However, the protein amounts of GluTR and GBP strongly increased (6 folds higher) in TPR/*flu* lines compared to WT and *flu* (Figure 3.35). The protein amounts of CHLI, GSAT, and the light-harvesting protein LHCa1 did not significantly change in TPR/*flu* lines compared with WT and *flu*.

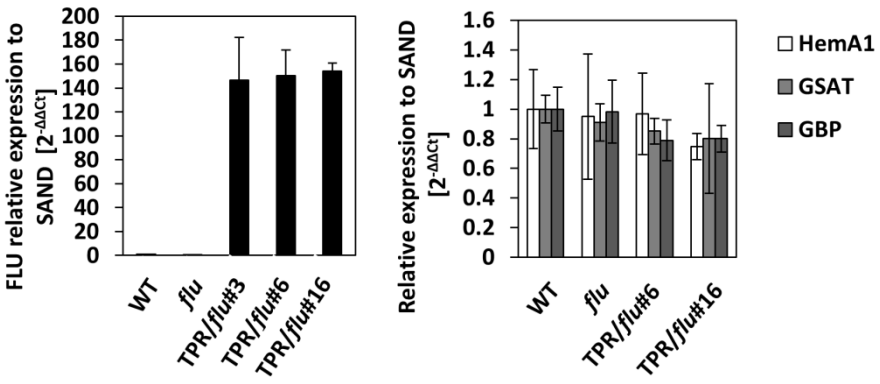

Figure 3.34 qRT-PCR analysis of levels of genes involved in ALA synthesis in TPR/*flu* lines. The expression of genes was normalized to the expression of *SAND* in WT. Primers used for amplification of *FLU* in qRT-PCR are specific for *TPR(FLU)* motif.

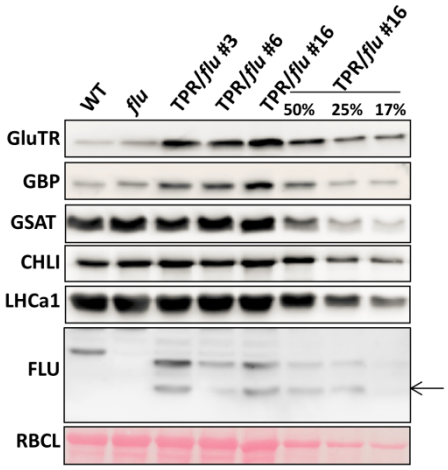

Figure 3.35 Western blot analysis of proteins involved in TBS pathway or photosynthesis. The arrow indicates the 15 kDa TPR(FLU) peptide. TPR/*flu*# indicates the *flu* complementation lines expressing *TPR(FLU)*.

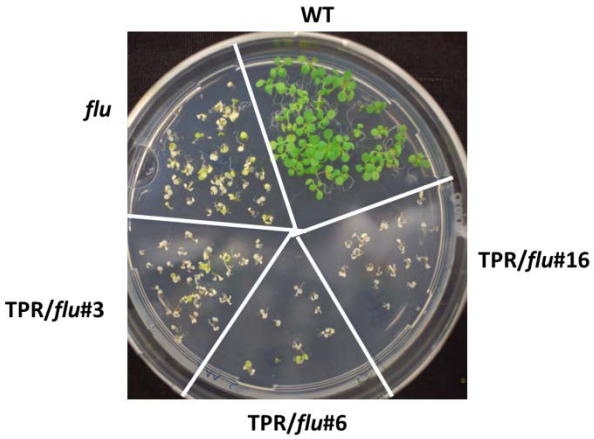

Figure 3.36 The TPR/*flu* lines cannot grow under photoperiodic conditions. Plants were germinated under light-dark conditions with 14 h darkness and 10 h light (120 µmol photons $m^{-2}s^{-1}$) for 1 week. WT grew normally, while all mutant seedlings showed necrosis in the cotyledons before they died.

flu cannot grow under light-dark conditions due to a large amount of Pchlide which accumulates in the dark. It was hypothesized that TPR(FLU) alone interacts with GluTR and inactivates ALA synthesis, thereby prohibiting the accumulation of Pchlide in the dark and enabling *flu* to grow in light-dark conditions. The growth of TPR/*flu* lines under light-dark conditions was tested. WT, *flu* and TPR/*flu* lines were germinated under light-dark conditions with a daily 14h dark period. The cotyledons of *flu* and TPR/*flu* showed necrosis under light-dark conditions. Later on, the true leaves of both *flu* and TPR/*flu* were not able to develop (Figure 3.36). TPR/*flu* lines, similar to the *flu* mutant, could not accept light-dark growth. Expression of TPR(FLU) in *flu* was not able to rescue the *flu* phenotype.

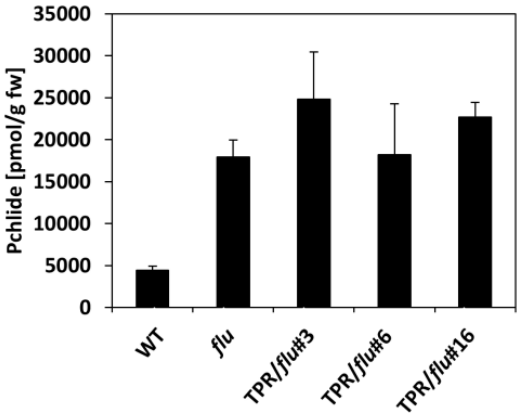

Figure 3.37 Pchlide accumulation in the dark grown TPR/*flu* lines. Plants were grown under CL for two weeks and then transferred to the dark for 12 h. Leaf material was harvested in the dark for Pchlide measurements.

The high Pchlide accumulation during darkness causes the *flu*-typical necrotic phenotype. Pchlide levels were examined in the green tissues or in the etiolated seedlings of WT, *flu* and TPR/*flu* lines in the dark. In the green tissue, leaf samples were harvested from plants grown under CL for two weeks and then transferred to the dark for 12h. Pchlide accumulation in TPR/*flu* lines was often higher in TPR/*flu* seedlings in the dark than in *flu* (Figure 3.37). Besides, Pchlide contents in the 4-day-old etiolated seedlings were also found even higher in TPR/*flu* lines than in *flu*. Interestingly, the GluTR amount was decreased in the etiolated seedlings of *flu* in comparison with WT, but this reduction in GluTR content was remedied by expressing *TPR(FLU)* (Figure 3.38).

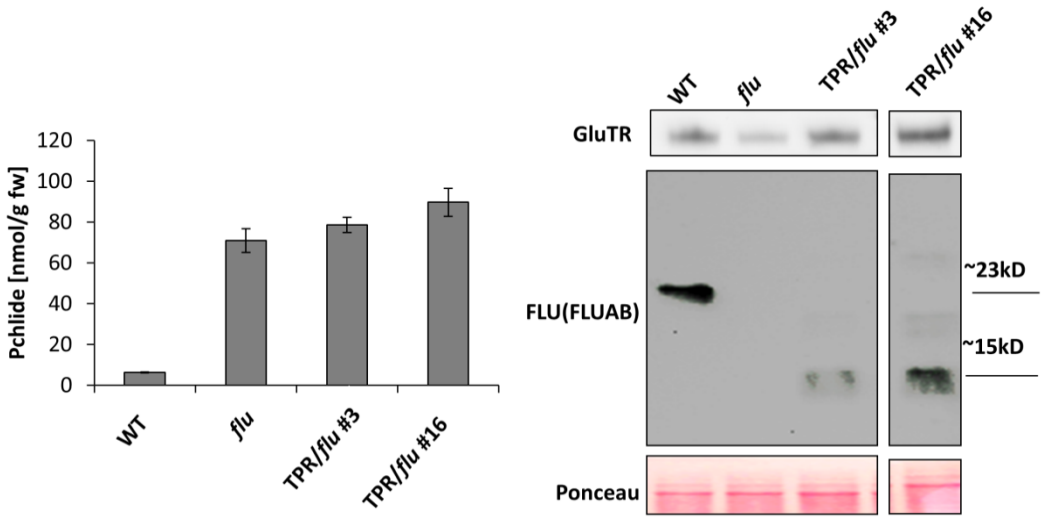

Figure 3.38 Pchlide contents or protein amounts of FLU/GluTR in the etiolated seedlings in WT, *flu* and TPR/*flu* lines. The etiolated seedlings were germinated in the dark for six days and harvested in the dark for Pchlide measurements (left panel) or western blot analysis with antibodies specific for GluTR or FLU (right panel). Ponceau indicates the Ponceau S-stained protein band of the large subunit of RuBisCo and is used for equal loading.

To re-confirm the interaction of TPR(FLU) with GluTR in vitro, pull-down experiments with recombinant proteins purified from E.coli were performed. The 6×His-tagged

GluTR (GluTR-his) was used as bait, immobilized to the Ni-NTI agarose column. The GST-tagged proteins, namely TPR(FLU)-GST, linkerTPR(FLU)-GST and the GST-tag alone were used as prey. As a negative control, both TPR(FLU)-GST and linkerTPR(FLU)-GST could not be pulled down by Ni-NTI agarose column, indicating that both TPR(FLU) and linkerTPR(FLU) could not directly bind to the Ni-NTI agarose column (Figure 3.39). Both TPR(FLU)-GST and linkerTPR(FLU)-GST were pulled down by GluTR, indicating the interactions between GluTR and these two proteins. Only a trace amount of GST-tag protein was pulled down by GluTR, which indicates a weak unspecific binding of GluTR with the GST-tag. The signal intensity of the band indicating preys and baits were quantified by a gel-analyzer and Prey/Bait/(M.W.-Prey) was used to evaluate the binding strength of prey to bait (Figure 3.39). The binding affinity of GluTR to TPR(FLU)-GST was substantially higher than the unspecific binding to the GST-tag alone, indicating that TPR(FLU)-GST interacts with GluTR. It is also important to compare the binding affinity of linkerTPR(FLU)-GST and TPR(FLU) to GluTR to determine whether the linker domain of FLU can help the interaction with GluTR. However, the accuracy of the pull-down experiment is not sufficient to estimate the exact binding $K_{D.}$

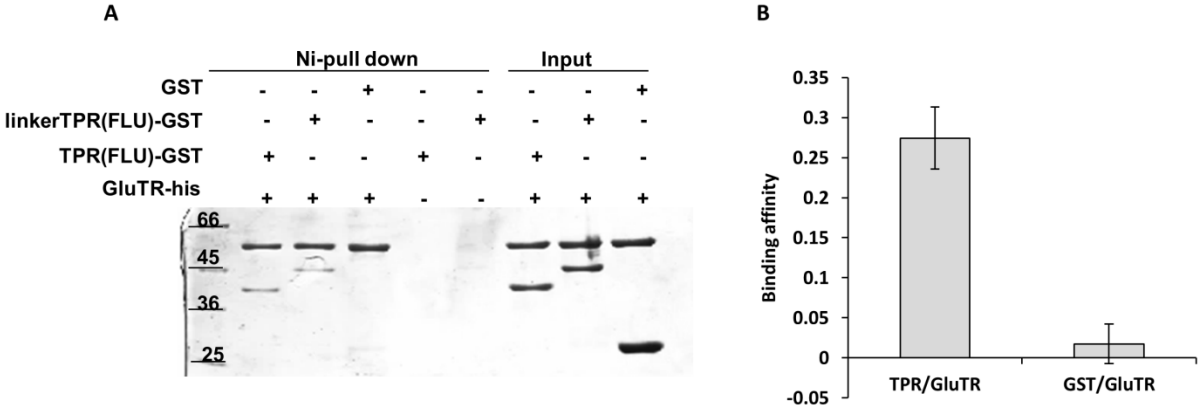

Figure 3.39 In vitro pull-down assay with the purified recombinant proteins confirms the interaction between TPR(FLU) and GluTR. (A) A coomassie blue staining of the input or elution fractions. The His-tagged GluTR was used as bait, immobilized on Ni-NTA agarose. The truncated FLU proteins with a GST tag at the N-terminal and GST tag alone were used as prey.(B) The signal intensities of protein bands representing GluTR, TPR(FLU) and GST in the first and third lanes of figure A were quantified. The ratio of the signal intensities of prey(TPR(FLU)/GST) to bait(GluTR) was calculated to estimate the binding affinity.

FLU-GluTR interaction was previously found to be the dominant factor to determine the localization of GluTR. The sub-compartmental localization of GluTR gives hints whether the binding event happened between TPR(FLU) and GluTR in vivo. Plants of WT, *flu* and TPR/*flu* were grown under CL for two weeks and then, the leaf material was harvested for the separation of the membrane and soluble fractions. Under this growth condition, GluTR was found to be approximately equally distributed among

the WT membrane and soluble fraction, while the dominant GluTR amount of *flu* was found in the soluble fraction. The TPR/*flu* lines accumulated more GluTR than *flu* and the majority of GluTR was found in the soluble fraction (Figure 3.40). The endogenous FLU protein in WT was exclusively found in the membrane fraction, while TPR(FLU), in which the TM domain was deleted, was present in the soluble fraction. The majority of GluTR and the truncated TPR(FLU) was co-localized in the soluble fraction. Interestingly, GBP also accumulated more in TPR/*flu* than in *flu* and GBP was also predominantly present in the soluble fraction (Figure 3.40).

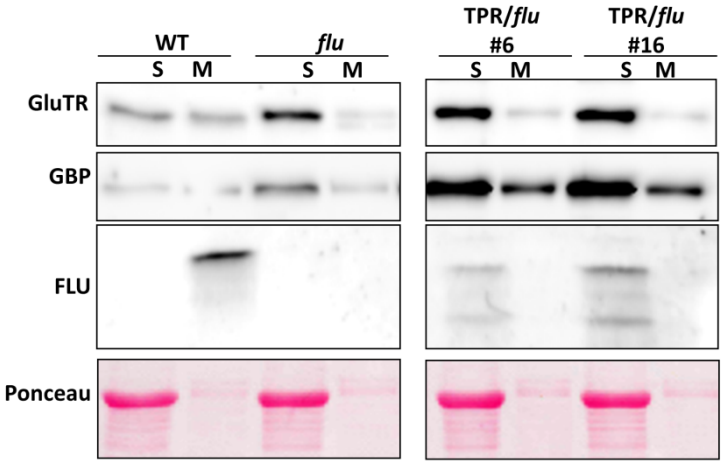

Figure 3.40 Western blot analysis of membrane-associated (M) and soluble (S) proteins involved in ALA synthesis in WT, *flu,* and TPR/*flu* lines. Plants were grown under CL for two weeks. The light intensity was 90 µmol photons $m^{-2}s^{-1}$. The membrane and soluble fractions were dissolved in equal volumes of PBS buffer. A similar volume of each fraction was loaded on the SDS-PA-gel, followed by immunoblotting analysis with specific antibodies raised against GluTR, GBP and FLU. Ponceau indicates the Ponceau S-stained protein band of RBCL and is used for equal loading.

Although TPR(FLU) interacts with GluTR, it remained to be seen whether there was enough TPR(FLU) protein to bind tightly with the bulk of accumulating GluTR. The concentration of recombinant proteins of GluTR, GSAT, or TPR(FLU) was quantified by the BCA protein assay and re-confirmed in a SDS-PAGE followed by a coomassie blue staining. The amounts of GluTR, GSAT or FLU in plants grown under CL for 2 weeks were compared with a certain amount of recombinant proteins by western blot analysis. 2.2-20 ng amounts of recombinant GluTR, GSAT, and TPR(FLU), respectively and 1mg (fresh weight, fw) of plant extract were loaded onto the SDS-PA-gel, followed by western blot analysis with specific antibodies against the three proteins. The GluTR amount in the plant extract was calculated to be less than 3.3 ng/ mg fw, but FLU amount was assessed to be around 20 ng/mg fw (Figure 3.41). Therefore, under CL growth condition, WT plants contained around 6 times more FLU than GluTR. GSAT accumulated to more than 20 ng/mg fw of the WT plant extract (Figure 3.41). This assessment indicates that the amount of GSAT does not seem to be a limiting factor for ALA synthesis in plants.

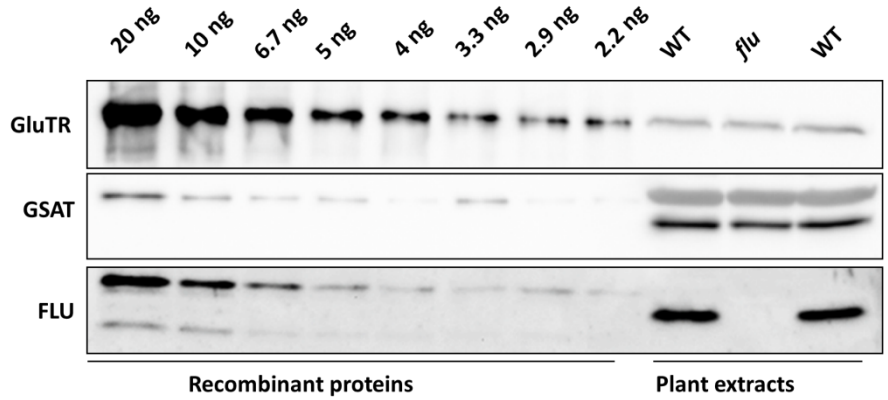

Figure 3.41 Quantifications of the absolute protein amounts of GluTR, GSAT, and FLU in plants. Western blot analysis to determine the protein amount of GluTR, GSAT and FLU in WT plant extracts by comparing the intensity of the immune signal of in planta accumulated protein with the gradually increasing amount of the respective recombinant proteins, which were purified from *E.coli* extracts. The concentration of recombinant proteins was determined by a BCA assay and verified on a SDS-PA gel, followed by a coomassie staining.

TPR/*flu* lines showed a pale-green phenotype under continuous ML. Chl and heme contents in TPR/*flu* lines were reduced by 15% and 30% compared to WT, respectively, under CL. Previously, it has been found that the ALA synthesis and steady-state levels of TBS were higher in *flu* compared with WT under CL, which indicating a higher metabolic flux of TBS in *flu* (Figure 3.1). The ALA synthesis rate (Figure 3.42A) was found to be even higher in TPR/*flu* lines than in the *flu* mutant. Porphyrins (Figure 3.42B) and Pchlide (Figure 3.42C) contents were also slightly increased compared with *flu* in TPR/*flu* lines. The metabolic flow of TBS seems to be even more increased in TPR/*flu* lines than in *flu*, which might cause more ROS generation. Under CL, two $^1O_2$ responsive genes, *AAA1* and *BAP1* already showed higher expression in the *flu* mutant compared with WT. The expression of a general ROS responsive gene, *CYP81D8*, was also induced in *flu*, while the expression of H_2O_2-induced genes, *GPX1, GPX2*, and *APX1* was not altered in *flu* (Figure 3.43). These results are consistent with the increased amounts of tetrapyrrole intermediates in *flu* (Figure 3.1). Thereby, the expression of ROS responsive genes in TPR/*flu* lines showed a similar tendency as in *flu*. *CYP81D8*, *BAP1,* and *AAA1* showed even higher expressions in TPR/*flu* lines than in the *flu* mutant (Figure 3.43).

In summary, TPR(FLU) did not rescue the *flu* phenotype under light-dark conditions. It caused an accumulation of soluble GluTR and an even increased ALA synthesis rate in *flu* in light, which might lead to a high ROS production.

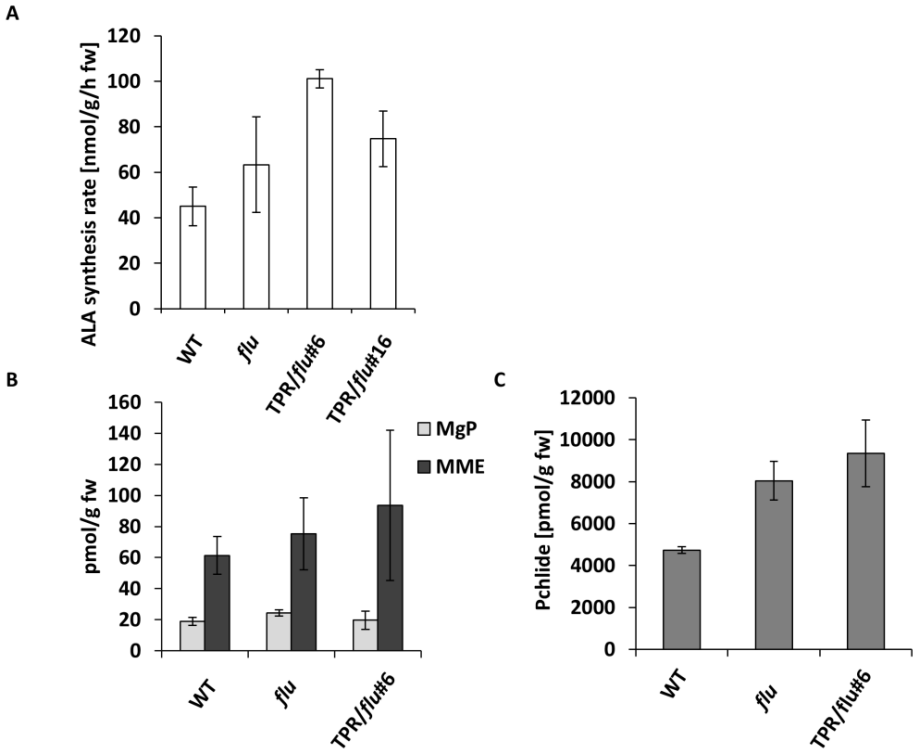

Figure 3.42 The ALA synthesis rate and steady-state levels of intermediates of TBS in WT, *flu* and TPR/*flu* lines. Plants were grown under CL for two weeks. The light intensity was 90 µmol photons $m^{-2}s^{-1}$. (A) ALA synthesis rate; (B) MgP contents; (C) Pchlide content.

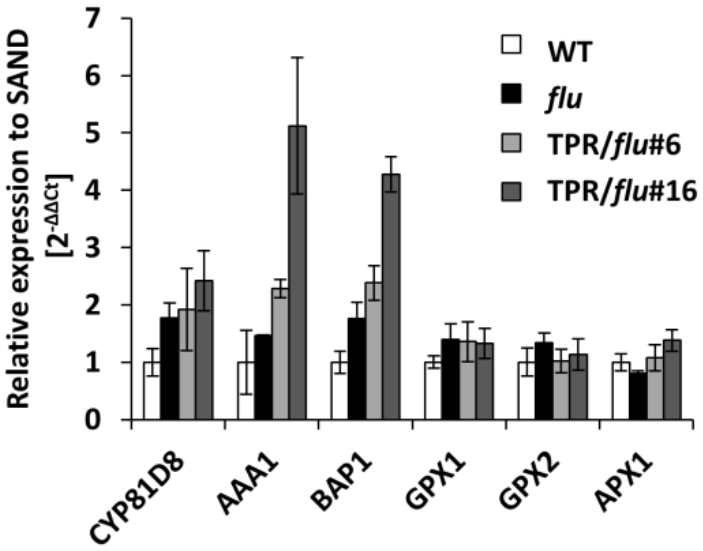

Figure 3.43 The expressions of ROS responsive marker genes in TPR/*flu* lines. Plants were grown under CL for two weeks. The light intensity is around 90 µmol photons $m^{-2}s^{-1}$. *CYP81D8* is a general ROS responsive gene; *AAA1* and *BAP1* are two $^1O_2$-responsive genes; *GPX1*, *GPX2* and *APX1* are H_2O_2-responsive genes.

3.3.2 Expressing *TPR(FLU)* in *Arabidopsis* WT plants

ALA synthesis was not suppressed in TPR/*flu* lines. On the contrary, *TPR(FLU)* expression seemed to cause an increase in ALA synthesis and TBS flow in the

transgenic lines. It was hypothesized that TPR(FLU) could compete with the endogenous FLU for binding of GluTR and might perturb the function of FLU. Then the soluble TPR(FLU) peptide should result in elevated Pchlide accumulation in the dark-grown plants even when FLU is present there. I decided to generate transgenic lines for the expression of *TPR(FLU)* in WT background. *TPR(FLU)* was transferred into *Arabidopsis* WT plants. Transgenic lines expressing *TPR(FLU)* in the WT background were designated TPR/WT#. Consistent with the observations in TPR/*flu* lines, the progenies of TPR/WT lines also showed a pale-green phenotype even under CL (Figure 3.44A). Two truncated forms of FLU could be found in TPR/WT lines in western blot analysis with the anti-TPR(FLU) antibody. The smaller variant migrated as a 15kDa peptide band and was the expected size of TPR(FLU) (Figure 3.44B). GluTR amounts also increased in TPR/WT lines as like in TPR/*flu* lines (Figure 3.44B). The amount of the endogenous FLU in TPR/WT lines was similar to that of WT.

To determine whether the expression of *TPR(FLU)* in WT compromise the expression of the endogenous *FLU*, the steady-state levels of the transcripts of both *FLU* genes were analyzed by using two primer pairs in qRT-PCR experiments. One primer pair is specific for *TPR(FLU)* and was used to determine the expression of the transgene. It was found that the expression of *TPR(FLU)* in TPR/WT lines was around 70 times higher than the expression of endogenous *FLU* in WT (Figure 3.44C). As the transgene does not contain the *TM* and *linker* motif of *FLU*, another primer pair specific for the *TM* or *linker* motif was used to determine the expression of the endogenous *FLU* but not of the transgene. The transcript amounts of endogenous *FLU* in TPR/WT lines did not significantly change compared to WT (Figure 3.44D). In summary, the transgene was highly expressed in TPR/WT lines and the expression of the transgene did not affect the expression of the endogenous *FLU* in TPR/WT lines.

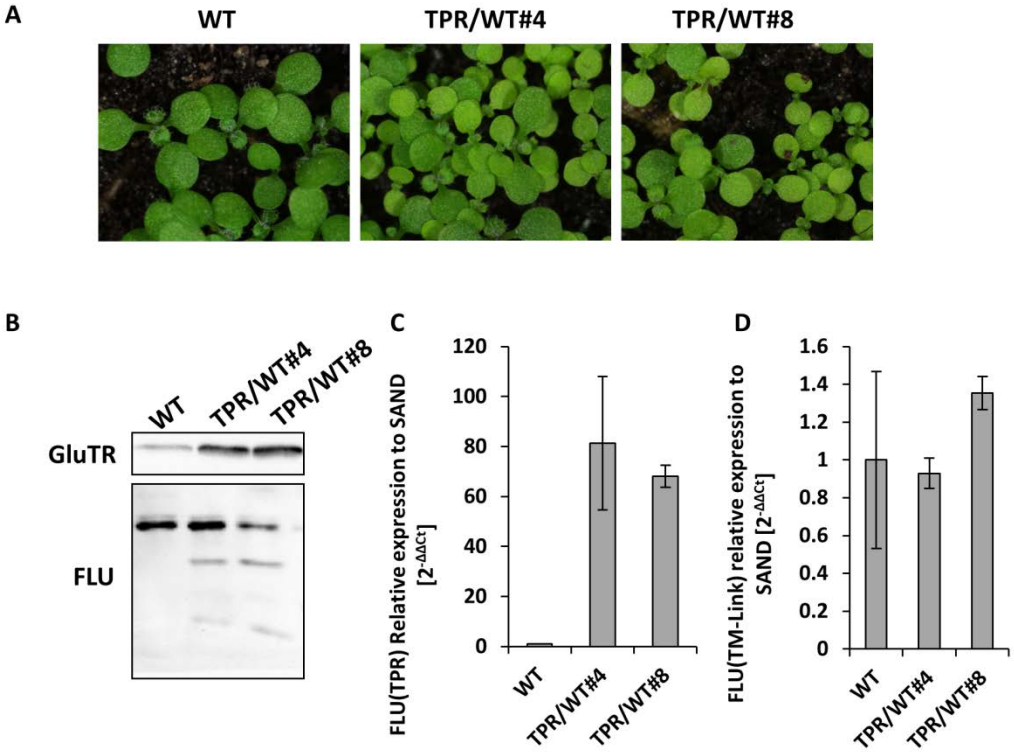

Figure 3.44 TPR/WT lines and WT under CL. (A) TPR/WT plants showed a pale-green phenotype under CL. (B) Western blot analysis of the protein amounts of GluTR and FLU in WT and TPR/WT lines. (C and D) qRT-PCR analysis of transcript levels of *FLU* in WT and TPR/WT lines using primer pairs specific for *TPR(FLU)* (C) or specific for the *TM* and *linker* motif of *FLU* (D). Plants were grown under 90 µmol photons $m^{-2}s^{-1}$ CL for one week.

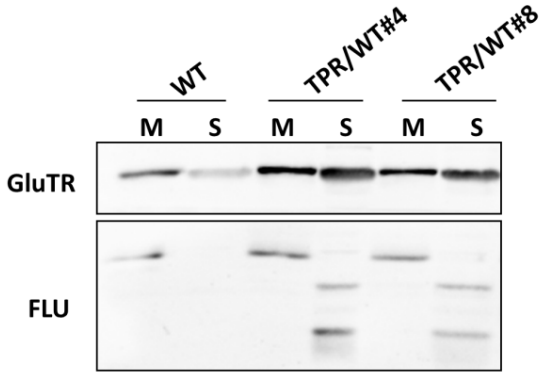

Figure 3.45 The protein amount of soluble and membrane-bound GluTR in TPR/WT lines under CL. Plants were grown under 90 µmol photons $m^{-2}s^{-1}$ CL or 120 µmol photons $m^{-2}s^{-1}$ light-dark conditions for 1 week. The pale progenies were harvested for the membrane and soluble protein analysis and probed with a specific antibody reacting with GluTR or FLU(TPR).

It was previously found that the amount of soluble GluTR increased in TPR/*flu* lines compared to *flu* (Figure 3.40). The amounts of the membrane-associated and soluble proteins were analyzed also in TPR/WT lines. Consistent with the previous results, the endogenous FLU was exclusively found in the membrane fraction while the

truncated FLU, TPR(FLU) was present in the soluble fraction due to the lack of the TM domain. The expression of TPR(FLU) caused an increased amount of GluTR relative to WT. The accumulated GluTR in TPR/WT lines was dominantly presented in the soluble fraction (Figure 3.45).

The TPR/WT plants showed a pale-green phenotype under CL. This phenotype resembles seedlings of FLUOE lines, which also showed a pale-green phenotype under CL. To compare the effects on the TBS pathway in response to overproduced FLU or TPR(FLU) in WT, one FLUOE line was additionally included to the measurements of contents of tetrapyrrole intermediates and end-products. Plants were grown under CL for two weeks. The Chl contents in TPR/WT lines were found to be 78% of the WT plants (Figure 3.46A). Heme contents in TPR/WT lines showed a similar decrease to the Chl contents under CL (Figure 3.46B). The contents of porphyrins (MgP and MME) were increased in TPR/WT lines under CL. The ALA synthesis rate was also increased in TPR/WT lines compared with WT (Figure 3.46). Although the end products of TBS decreased, the contents of intermediates for TBS pathway were slightly increased in TPR/WT lines. The FLUOE line showed a similar decrease in Chl and heme contents as the TPR/WT lines. But FLUOE lines showed reduced levels of porphyrins and Pchlide contents compared with WT (Figure 3.46C and D; Figure 3.47A). In conclusion, the metabolic flux of TBS seemed to be increased in TPR/WT lines, while it is decreased in the FLUOE line.

In the dark, FLU functions as a feedback repressor of ALA synthesis to prevent Pchlide accumulation. The *flu* mutant accumulates around 9 times more Pchlide in the dark (Meskauskiene et al., 2001). Pchlide contents in TPR/WT lines and WT seedlings were analyzed from samples harvested during light or dark exposure. Interestingly, during light exposure, Pchlide content in TPR/WT lines increased by 15% relative to WT, while in the dark, Pchlide accumulated by 67% in TPR/WT lines more than in the WT (Figure 3.47). The expression of TPR(FLU) in WT results in a higher Pchlide accumulation in the dark, which is the similar tendency as the *flu* mutant.

Pchlide content in the FLUOE line was decreased in the light but reached the same level as WT in the dark, which was consistent with previous results (Figure 3.47; Figure 3.5).

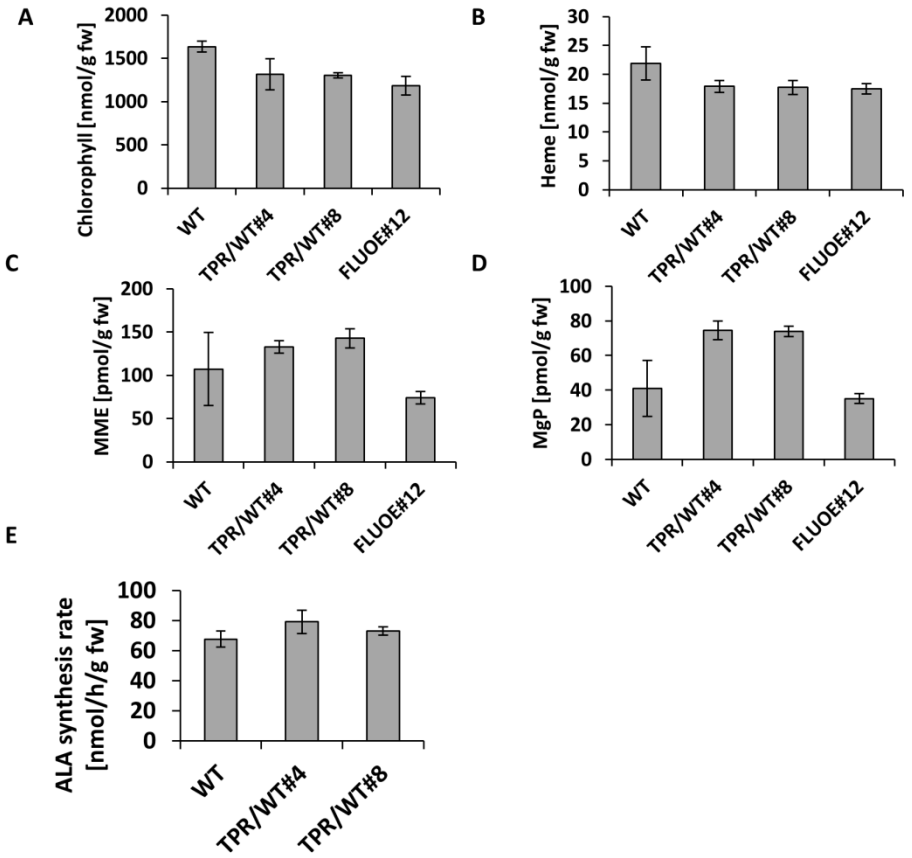

Figure 3.46 ALA synthesis rate and the contents of intermediates or end-products of TBS in TPR/WT lines grown under CL. (A) Chl contents, (B) Heme contents, (C) MgP contents, (D) MME contents, (E) Pchlide contents (F) ALA synthesis rate. Plants were grown under 90 µmol photons $m^{-2}s^{-1}$ CL or 120 µmol photons $m^{-2}s^{-1}$ during light-dark conditions for one week. T3 pale-green seedlings of TPR/WT lines were harvested for tetrapyrrole extractions.

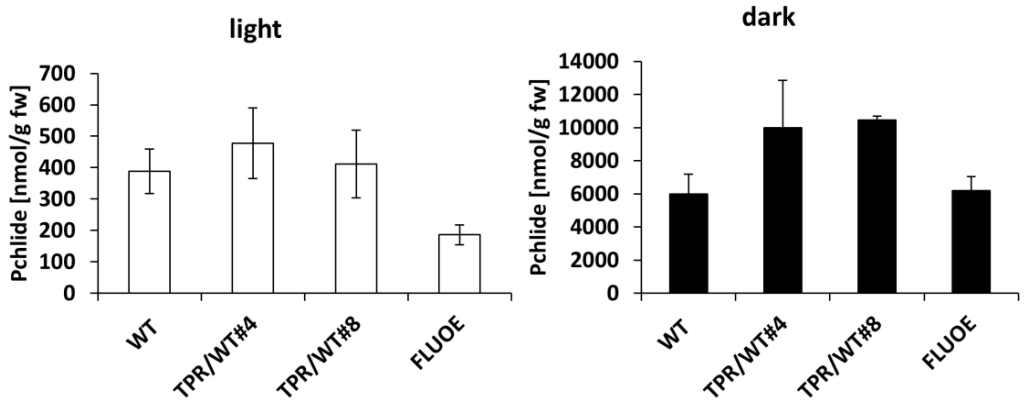

Figure 3.47 Pchlide accumulation in light and dark grown TPR/WT lines and WT. Plants were grown under light-dark conditions for two weeks. Samples were then harvested during light (light) or after 14h dark exposure (dark).

3.3.3 Expressing FLUΔlinker in *flu* with an ethanol-induced system

The gene construct for the expression of the FLUΔlinker peptide (a peptide consisting of the TPR and the TM domains of FLU) was attempted to be introduced

into *flu*, but no transgenic plants were obtained. Alternatively, an alcohol-inducible system was applied to express FLUΔlinker in the *flu* mutant. The expression of *FLUΔlinker* was under the control of a *pAlc* promoter which is induced by ethanol (Figure 3.48A). The genotype of T1 transgenic plants (pAlc_FLUΔlinker/*flu*) was determined by a PCR reaction using a primer pair specific for regions flanking the *linker* motif. As *flu* is a point mutation line, a PCR product was always amplified from the genomic DNA of both WT and mutants. Besides, an additional short PCR product was amplified from the genomic DNA of pAlc_FLUΔlinker/*flu* lines, which indicates the presence of the transgene (Figure 3.48B).

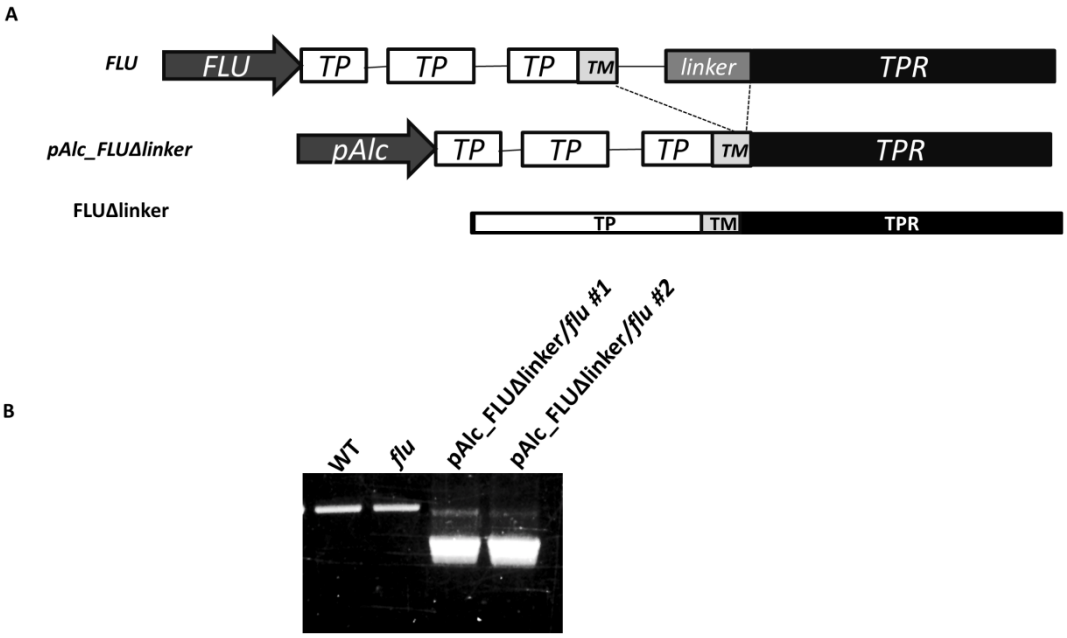

Figure 3.48 The gene construct to express FLUΔlinker in *flu* under the control of an ethanol-inducible promoter. (A) From the top to the bottom: the gene construct of the endogenous *FLU* gene; a gene construct expressing a sequence encoding a truncated FLU without the linker domain (FLUΔlinker) under the control of an ethanol-inducible promoter (pAlc); the schematic presentation of the protein domains of the FLUΔlinker peptide. (B) The confirmative genotyping to demonstrate the presence of the transgene in pAlc_FLUΔlinker/*flu* lines with the genome DNA of WT, *flu* and pAlc_FLUΔlinker/*flu* lines and a primer pair specific for *FLU*.

To verify whether FLUΔlinker peptide was produced in pAlc_FLUΔlinker/*flu* lines, 2-week-old seedlings grown under CL were subjected to ethanol induction. The procedures for ethanol induction were performed by watering the plants three 20mL 1% ethanol every 24h. Some of the progenies in the T2 generation of pAlc_FLUΔlinker/*flu* lines showed a pale-green phenotype after ethanol induction. A truncated FLU peptide migrates as an 18kDa protein in the pale-green progenies (Figure 3.49B). Therefore, the pale-green plants of pAlc_FLUΔLinker/*flu* lines after 72h ethanol induction were harvested for the following experiments.

More protein samples were harvested at different time points (0h, 12h, 24h or 72h) after ethanol induction. No specific band could be detected in a western blot analysis with the anti-TPR(FLU) antibody both in the plant samples of *flu* and pAlc_FLUΔlinker/*flu* lines without ethanol induction (0h). An immune-reacting band

at 23kDa appeared in extracts of pAlc_FLUΔlinker/*flu* 48h after ethanol induction, which has the same mobility on the SDS-PA gel as the intact FLU. An additional immune-reacting band migrated as an 18kDa protein, which is the predicted size of FLUΔlinker, appeared in the pAlc_FLUΔlinker/*flu* line 72h after ethanol induction. The immune band representing the endogenous FLU in WT migrated as a 23kDa protein and its amount did not change before or after ethanol induction. GluTR content increased in the pAlc_FLUΔlinker/*flu* line after 48h induction and even more intensively increased 72h after ethanol induction (Figure 3.50). This increased GluTR amount was accompanied by the appearance of the FLUΔlinker protein. GSAT and GBP amounts remained constant before or after ethanol induction.

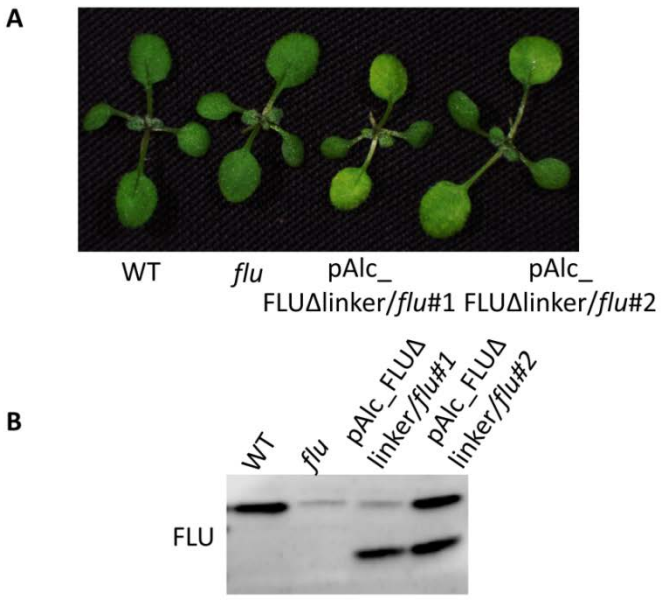

Figure 3.49 The phenotype of pAlc_FLUΔlinker/*flu* lines and western blot analysis of FLU protein 72h after ethanol induction. (A) The phenotype of pAlc_FLUΔlinker/*flu* lines 72h after ethanol induction. Plants were first grown under CL for two weeks and then induced with 1% ethanol every 24h for three times. (B) Western blot analysis of FLU protein in pAlc_FLUΔlinker/*flu* lines 72h after ethanol induction. The upper band migrates as a 23-kDa protein according to protein markers. A lower immune-reacting band shows mobility on the SDS-PA gel as an 18kDa protein. It is hypothesized that this immune signal corresponds to the truncated mature FLUΔlinker protein, while the 23kDa band corresponds to the WT FLU protein.

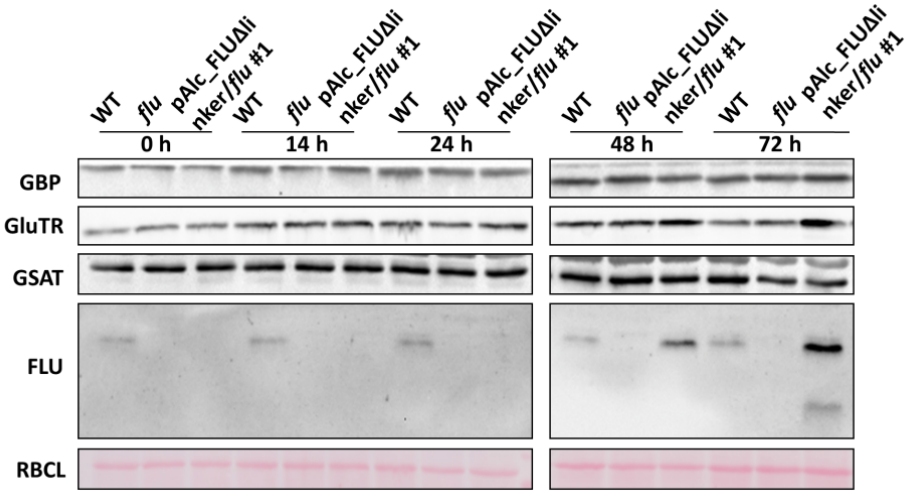

Figure 3.50 Western blot analysis of proteins involved in ALA synthesis in pAlc_FLUΔlinker/*flu* lines before or after ethanol induction. Plants were first grown under CL for two weeks and then induced with 1% ethanol every 24h for three times. Samples were harvested 0h, 14h, 24h, 48h, and 72h after ethanol induction.

The FLUΔlinker peptide contains the TM domain. Therefore, this truncated protein was expected to be localized in the membrane fraction. The localization of GluTR and FLU was analyzed in the WT, *flu* and one of the pAlc_FLUΔlinker/*flu* lines before or after the ethanol induction. Seedlings were harvested 0h and 72h after the ethanol treatment. The membrane-associated and soluble proteins were separated by methods as described in Chapter 2.4.2. The endogenous FLU was only found in the membrane fraction of WT. After 72h ethanol induction, two forms of FLU peptides with the molecular mass of 18 kDa or 23 kDa were exclusively in the membrane fraction in pAlc_FLUΔlinker/*flu* line (Figure 3.51). Before the ethanol induction, GluTR was equally distributed in the membrane fraction and soluble fraction in WT but was mainly present in the soluble fraction in *flu* and pAlc_FLUΔlinker/*flu* line. After 72h ethanol treatment, GluTR was accumulated in the pAlc_FLUΔlinker/*flu* line compared to *flu* and the majority of GluTR was found in the membrane fraction (Figure 3.51). In conclusion, the FLUΔlinker peptide is co-localized with GluTR in the membrane fraction of pAlc_FLUΔlinker/*flu* line.

To find out whether FLUΔlinker rescues the *flu* phenotype or not, the accumulation of Pchlide in the dark was analyzed after 72h ethanol induction in the pAlc_FLUΔlinker/*flu* line. *flu* accumulated around 5 times more Pchlide than WT after 14h of dark incubation. The pAlc_Δlinker/*flu* line after ethanol induction still accumulated a comparable amount of Pchlide as the flu mutant in the dark (Figure 3.52). When the ethanol-induced pAlc_Δlinker/flu plants were transferred into the dark for 14h and re-exposed to light, plants still showed necrosis phenotype as the flu mutant. Therefore, the expression of FLUΔlinker cannot rescue the flu phenotype.

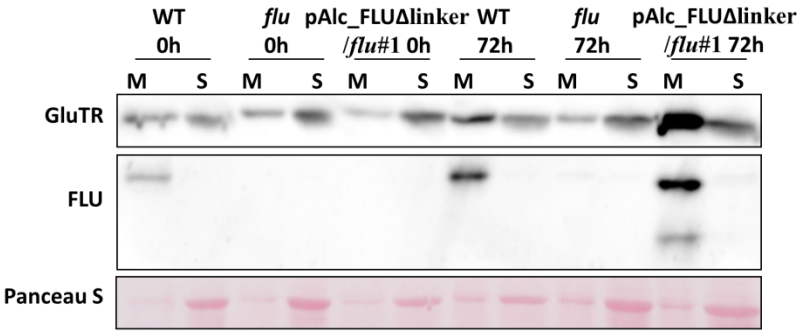

Figure 3.51 The protein amounts of membrane-bound and soluble GluTR in WT, *flu,* and the pAlc_FLUΔlinker/*flu* plants 0h or 72h after ethanol induction. Plants were first grown under CL for two weeks and then were induced with 1% ethanol every 24h for three times. Samples were harvested before the ethanol induction (0h) or 72h after the induction (72h). Ponceau indicates the Ponceau S-stained protein band of RBCL and is used for equal loading.

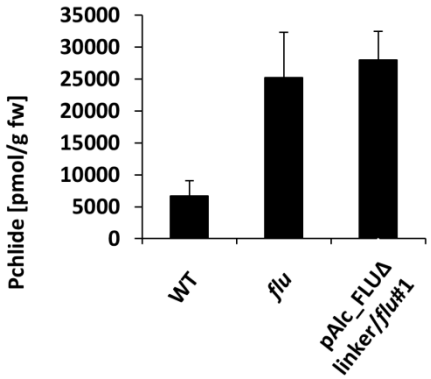

Figure 3.52 Pchlide accumulation in dark grown WT, *flu* and pAlc_FLUΔlinker/*flu* lines after ethanol induction. Plants were grown on soil under CL for two weeks and then induced with 1% ethanol every 24h for three times. Pale-green seedlings of the pAlc_FLUΔlinker/*flu* line appeared 72h after ethanol induction. WT, *flu* and the pale-green seedlings of the pAlc_FLUΔlinker/*flu* line were then transferred to darkness for 14h and were then harvested for Pchlide content measurement.

ALA synthesis in TPR/flu lines showed an increased level compared to flu (Figure 3.42A). It was hypothesized that the binding of GluTR to the membrane would help to inactivate ALA synthesis. The steady-state levels of end-products and intermediates of TBS were analyzed in the pAlc_FLUΔlinker/flu lines. After ethanol induction, Chl contents in the pAlc_FLUΔlinker/flu lines were reduced by around 20% compared with WT and flu. Heme contents were also reduced in pAlc_FLUΔlinker/flu lines. On the contrary to TPR/flu lines, The ALA synthesis rate was dramatically reduced in pAlc_FLUΔlinker/flu lines compared with flu and WT. Pchlide contents were shown to be elevated in flu relative to WT but decreased to only half of the WT in the pAlc_FLUΔlinker/flu lines (Figure 3.53). Expression of FLUΔlinker peptide seems to result in a decreased in the metabolic flux of TBS.

In summary, FLUΔlinker did not rescue the flu phenotype. FLUΔlinker caused the accumulation of membrane-associated GluTR and reduced ALA synthesis rate in light-exposed plants.

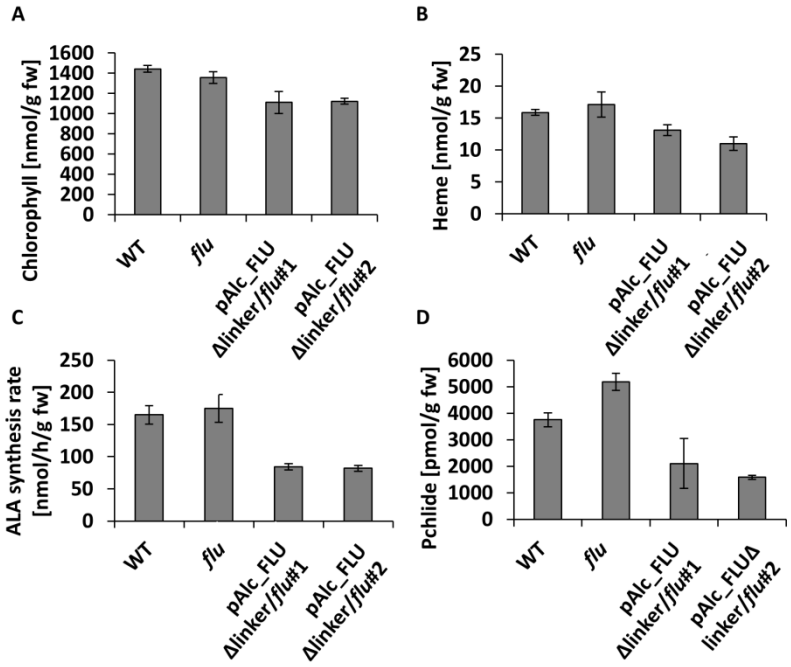

Figure 3.53 ALA synthesis rate and the steady-state levels of Chl, Pchlide and heme in WT, *flu,* and pAlc_FLUΔlinker/*flu* lines after ethanol induction. WT, *flu* and pAlc_FLUΔlinker/*flu* plants were grown under CL for two weeks and were then induced with 1% ethanol every 24h for three times. Pale-green seedlings appeared in pAlc_FLUΔlinker/*flu* lines 72h after ethanol induction. WT, *flu* and the pale-green seedlings of pAlc_FLUΔlinker/*flu* lines were then harvested for measurements.

3.3.4 The *flu* complementation line with FLUΔTM

Both the expression of TPR(FLU) and FLUΔlinker peptides in *flu* failed to rescue the *flu* phenotype. The gene construct for the expression of the FLUΔTM peptide (a peptide consisting of the linker and TPR(FLU) domains) was introduced into the *flu* mutant (Figure 3.54). The transgenic line expressing the FLUΔTM peptide was designate FLUΔTM/*flu* line.

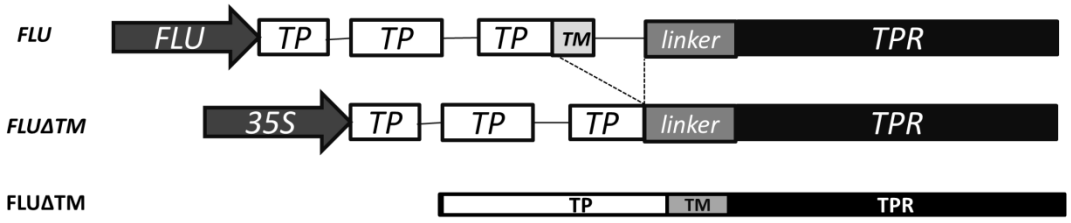

Figure 3.54 The gene construct coding for the FLUΔTM peptide. From top to bottom: *FLU*, the schematic representation of the gene construct of endogenous *FLU*; *FLUΔTM*, the gene construct for the expression of the coding sequence for the FLUΔTM peptide driven by CaMV-35S-promoter; FLUΔTM, the schematic representation of the protein domains of the FLUΔTM peptide.

WT, *flu* and FLUΔTM/*flu* plants were grown under 10h light/ 14h dark conditions. The cotyledons of *flu* were bleached, and the seedlings died later on. Some of the T2-seedlings of one FLUΔTM/*flu* line were able to grow under the light-dark conditions (Figure 3.54A). The survival rate of the FLUΔTM/*flu* seedlings was around 1/30. The rescued plants showed retarded growth and a necrotic phenotype. The necrotic phenotype was more evident in newly developing leaves than in mature leaves. However, the necrotic leaves still continued to grow. A PCR product was amplified from the genomic DNA of *flu* (CL) and the FLUΔTM/*flu* (light-dark) plants using a primer pair, which flanks the coding sequence of the TM motif. In addition, a shorter PCR product was amplified from the genomic DNA from FLUΔTM/*flu*, confirming the transgene in the FLUΔTM/*flu* plant (Figure 3.55B). By western blot analysis with the antibody specific for TPR(FLU), two specific immune-reacting protein bands were exclusively present in the soluble fraction of FLUΔTM/*flu* extracts; the fast migrating band as indicated by the arrow migrated as a 20kDa protein, which could correspond to the predicted size of FLUΔTM (Figure 3.55C), the other immune-reacting band migrated as a 30kDa protein, which is proposed to represent the precursor protein of FLUΔTM. The GluTR content was increased both in the soluble and membrane fraction of the FLUΔTM/*flu* line compared to *flu* (Figure 3.55C). In order to compare the Pchlide content of FLUΔTM/*flu* and *flu* in the dark, WT, *flu* and FLUΔTM/*flu* plants were transferred into the dark for 14h and leaf samples were then harvested in the dark for Pchlide analysis. It was found that Pchlide still accumulated more than two-times in FLUΔTM/*flu* compared with WT in the dark. However, the Pchlide accumulation of dark-grown FLUΔTM/*flu* plants was only 50% compared to dark-grown *flu* seedlings (Figure 3.55D). In summary, the expression of the FLUΔTM peptide in *flu* caused the accumulation of soluble GluTR and partially rescued the *flu* phenotype under light-dark growth conditions.

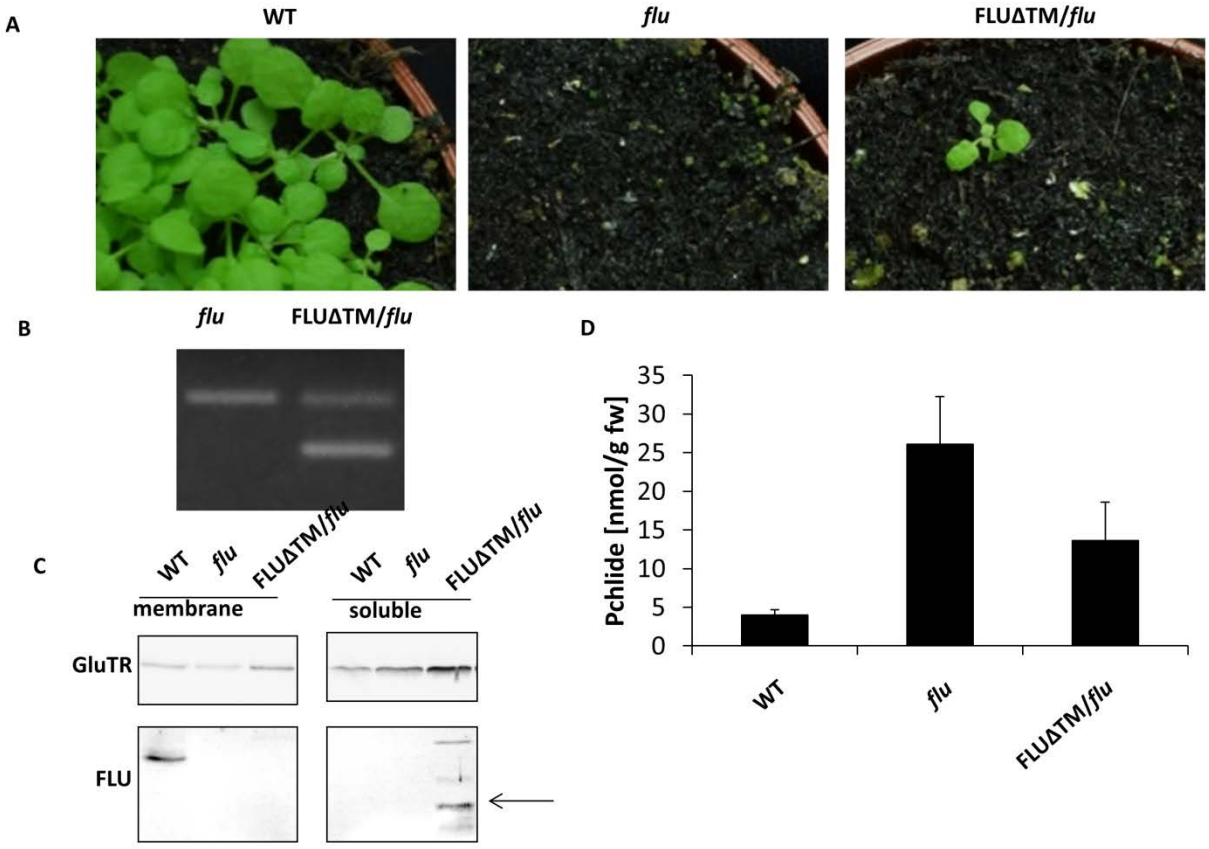

Figure 3.55 The FLUΔTM peptide partially rescued the *flu* phenotype. (A), WT, *flu* and the FLUΔTM/*flu* plants were grown under 10h light/14h dark for two weeks. (B) PCR amplification using the genomic DNA of *flu* and the FLUΔTM/*flu* line as the templates and a primer pair specific for *FLU*. The upper DNA band corresponds to the presence of the point-mutated *FLU* genes while the lower band represents the presence of the transgene. (C) Western blot analysis of membrane-bound and soluble GluTR/FLU in WT, *flu* and FLUΔTM/*flu* lines. (D) Pchlide accumulation of dark-grown WT, *flu* and the FLUΔTM/*flu* seedlings.

3.4 Interaction studies of FLU with the inactivation complex

Previous reports revealed that FLU co-migrates with the enzymes of Chl biosynthesis branch in a BN-PA gel and co-immunoprecipitation analysis (Kauss et al., 2012b). It was hypothesized that PORB, CHL27 and CHLM form a complex at the thylakoid membrane in plants. Here, this potential complex is designated the inactivation complex. This inactivation complex is proposed to be essential for a FLU-dependent regulation on ALA synthesis. To further explore the mechanism for FLU-dependent inactivation of ALA synthesis, yeast two-hybrid and BiFC assays were made to investigate the interactions between different components within the complex.

3.4.1 FLU interacts with the enzymes of Chl biosynthesis branch

The gene constructs were previously made by Maxi Rothbart to express the YFP halves fused to the target proteins, such as FLU, PORB, CHL27 or CHLM. For the BiFC assays, one construct expressing the fused protein with the N-terminal split YFP half

(G1) and one construct expressing the fused protein with the C-terminal split YFP half (G3) were transiently co-expressed in *N. benthamiana* leaves. When the fused target proteins interact with each other, the split YFP halves become physically close to each other and generate the YFP fluorescence. As a negative control, co-transformation of the single YFP halves (G1+G3) did not result in YFP fluorescence (Figure 3.56). The co-expression of FLU with PORB or CHLM with YFP halves resulted in a high YFP fluorescence, indicating an interaction between FLU and PORB or CHLM. The co-expression of FLU and CHL27 led to a low YFP fluorescence, which could be a false interaction (Figure 3.56).

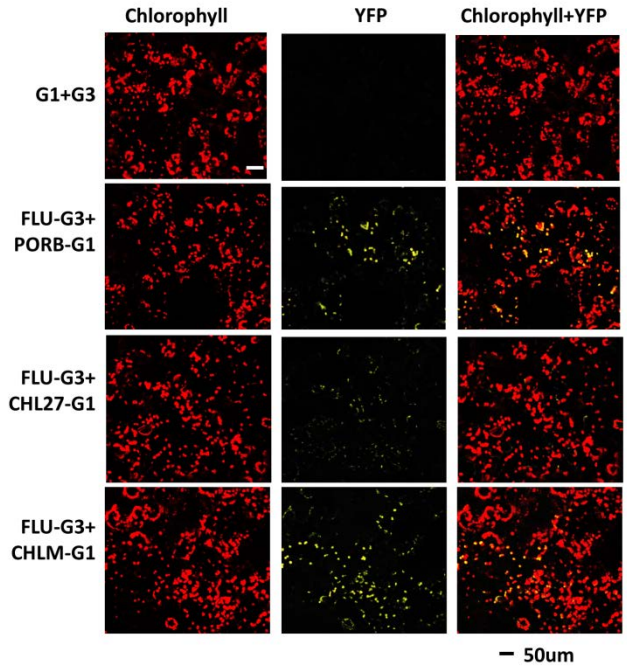

Figure 3.56 BiFC assays for the interaction of FLU with the enzymes of the Chl branch. Target proteins fused to the N- or C-terminal halves of split YFP were transiently expressed in *N. benthamiana* leaves. G1 indicates the proteins fused to the N-terminal split YFP half, whereas G3 indicates the fusion of proteins to the C-terminal split YFP half. A red signal indicates the auto-fluorescence from Chl, while a yellow signal indicates the fluorescence from YFP. Scale bar indicates 50µm.

Interactions between FLU and the enzymes of the inactivation complex were also determined by a yeast two-hybrid system. Gene constructs encoding target proteins fused to halves of ubiquitin have been previously made by Maxi Rothbart. FLU was fused to the N-terminus of ubiquitin (-NUB). The other target interaction partners were fused to the C-terminus of ubiquitin (-DHB). Cells containing NUB and DHB vector can grow on SD medium lacking leucine and tryptophan (-lt). If the target proteins interact with FLU, the ubiquitin halves were combined to a full-length ubiquitin, which would enable the yeast cells to grow on SD medium lacking histidine, uracil, leucine, and tryptophan (-hult). Cells co-expressing FLU and GluTR or CHLM were able to grow on -hult SD medium, indicating that FLU can interact with GluTR and CHLM. Cells co-expressing FLU and PORB only lead to a poor growth on -hult SD medium, which indicates a weak interaction. An interaction of FLU and CHL27 could

not be detected by the yeast two-hybrid approach (Figure 3.57). In summary, FLU interacts with PORB and CHLM both in BiFC and yeast two-hybrid assays.

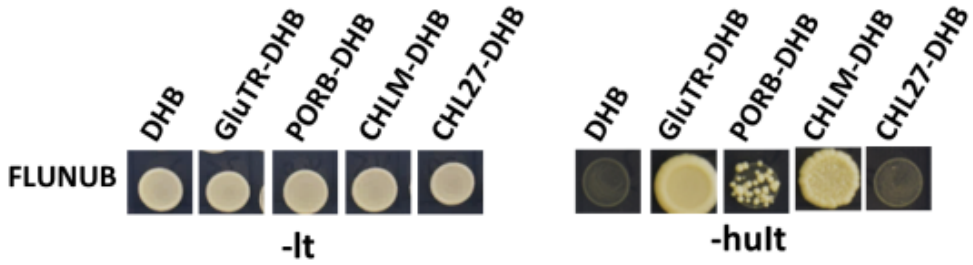

Figure 3.57 Yeast two-hybrid assays to determine the interaction of FLU with PORB, GluTR, CHLM or CHL27. GluTR, PORB, CHLM and CHL27 were fused to the C-terminal half of ubiquitin (DHB) and used as bait, while FLU was fused to the N-terminal half of ubiquitin (NUB) and used as prey. Positive interactions could be detected on SD medium without histidine, uracil, leucine and tryptophan (-hult). Co-transformed empty pDHB1MCS2 with FLU-NUB vectors was used as a negative control.

3.4.2 Identification of the binding site of FLU to the inactivation complex

The BiFC assay demonstrated that FLU interacted with PORB and CHLM. As both PORB and CHLM do not contain a TM domain, the binding site on FLU for the PORB or CHLM interaction is expected to be located in the linker or TPR(FLU) domain of FLU, which are hydrophilic. The yeast two-hybrid assay was performed to identify the binding site of PORB for interaction to FLU. cDNA sequences encoding TPR(FLU) or the linker-TPR peptide (a peptide consisting of TPR(FLU) and the linker of FLU) were sub-cloned to the pDHB-MCS2 vector. The constructs were introduced into L40ccuA cells and resulted in the expression of fusion proteins containing the truncated FLU peptides with the C-terminal half of ubiquitin. GluTR, PORB, CHLM, and CHL27 were fused to the N-terminal half of ubiquitin and expressed in L40ccuα cells. Mated cells co-expressing the truncated FLU peptides with PORB or CHLM could grow on the SD/-hult plate, indicating a direct interaction between TPR(FLU) with PORB or CHLM (Figure 3.58). However, cells co-expressing the intact FLU and PORB did not grow on SD/-hult medium. As the truncated FLU peptides are soluble proteins, while the intact FLU is a membrane protein, it seems that FLU at the membrane might compromise the interaction with PORB in the yeast two-hybrid assay. As a positive control, mated cells co-expressing GluTR and the intact FLU grew on SD/-hult medium (Figure 3.58). In conclusion, TPR(FLU) interacts with PORB and CHLM in yeast two-hybrid assays.

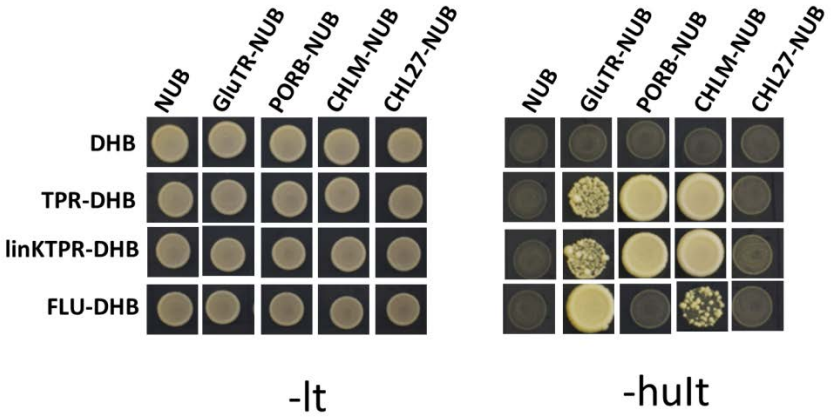

Figure 3.58 Yeast two-hybrid assay to determine the interaction of the truncated FLU peptides with PORB, GluTR, CHLM, and CHL27. FLU and its truncated version were fused to the C-terminal half of ubiquitin (DHB) and used as bait while GluTR, PORB, CHLM and CHL27 were fused to the N-terminal half of ubiquitin and used as prey. Positive interactions could be detected on medium without histidine, uracil, leucine and tryptophan (-hult).

3.4.3 GluTR interacts with the inactivation complex

Not all of the truncated forms of FLU peptides were able to fulfill already the entire function of FLU under light-dark conditions. It was hypothesized that some components of the inactivation complex might interact with GluTR and, thus, are involved in the FLU-dependent inactivation of ALA synthesis. The potential interaction between GluTR and the proteins of this protein complex were determined by both yeast two-hybrid and BiFC assays. The co-expression of GluTR and PORB or CHLM fused to the ubiquitin halves enabled the yeast cells to grow on the SD/-hult medium indicating the interaction between GluTR and CHLM, PORB. The co-expression of GluTR with the N-terminal half of ubiquitin (NUB) in yeast cells did not result in the growth on SD/-hult medium (Figure 3.59). Besides, CHL27 and YCF54 did not interact with GluTR (Figure 3.59).

In the BiFC assay, the co-expression of GluTR and PORB with the YFP halves resulted in a YFP fluorescence of the chloroplasts confirming an interaction between GluTR and PORB. In addition, the FLU and GluTR interaction was verified by the BiFC assay as a positive control. However, no signal was found upon co-expression of GluTR with CHLM or CHL27, indicating no direct interaction between GluTR and CHLM or CHL27 (Figure 3.60). In conclusion, GluTR interacts with PORB both in yeast two-hybrid and BiFC assay.

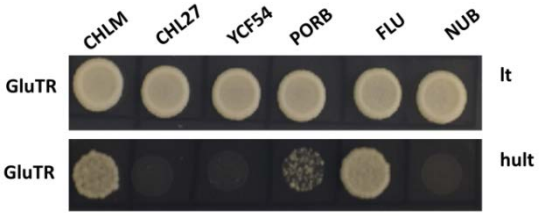

Figure 3.59 Interaction studies of GluTR with PORB, CHLM, and CHL27 by yeast two-hybrid assays. GluTR was fused to the C-terminal half of ubiquitin and used as bait while CHLM, CHL27, YCF54, PORB and FLU were fused to the N-terminal half of ubiquitin and used as prey. Positive interactions could be detected on medium without histidine, uracil, leucine and tryptophan (-hult).

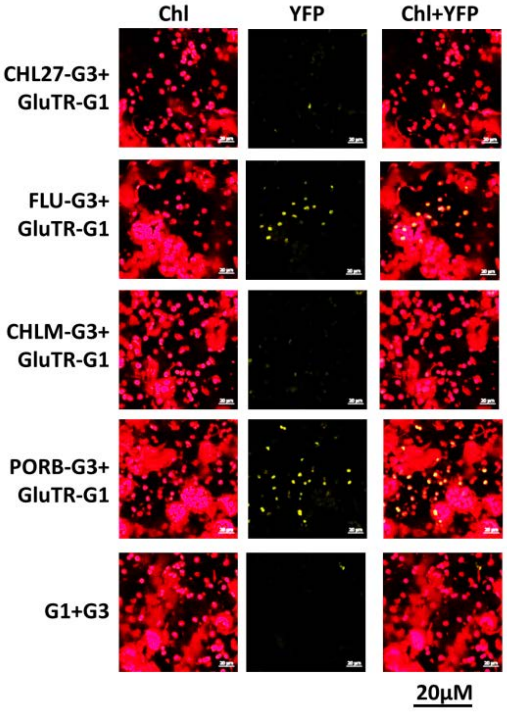

Figure 3.60 The BiFC assay shows GluTR interacting with PORB. Gen constructs of GluTR with the N-terminal half of YFP (G1) were transiently co-expressed with CHL27, FLU, CHLM or PORB fused to the C-terminal of split YFP (G3), respectively, in *N. benthamiana* leaves. Bar, 20μM.

4 Discussion

4.1 FLU controls ALA synthesis not only in the dark but also during the light exposure

High Pchlide accumulation leads to the generation of singlet oxygen, which triggers cell death (op den Camp et al., 2003). It was generally accepted that FLU acts as a negative regulator for ALA synthesis in the dark to prevent the over-accumulation of Pchlide in the dark (Meskauskiene et al., 2001; Kauss et al., 2012b). However, ALA synthesis rate in the *flu* mutant was increased not only in the dark but also during light exposure. This observation hints at the possibility that FLU also functions in light. Here, the function of FLU during light exposure was further investigated by the analyses of the *flu* mutant and FLU overexpression lines under various light conditions. Moreover, the analysis of the sub-localization of GluTR revealed that a large portion of GluTR is associated with the plastidic membranes by FLU even during light exposure.

4.1.1 The changing quantities of FLU affect the metabolic flow of TBS in plants

ALA is the first molecule committed to the TBS pathway. Thus, ALA synthesis is the valve for the metabolic flow of TBS. By modifying the amount of FLU in plants, the metabolic flow of TBS was manipulated. In the light, ALA synthesis rate was increased 44% in the *flu* mutant relative to WT (Figure 3.19). The steady-state levels of intermediates, such as Mg Proto, MME, and Pchlide, showed elevated levels in the *flu* mutant (Figure 3.1). These data indicate that the absence of FLU causes an increased metabolic flow into TBS relative to WT. Adversely, overexpression of FLU caused reduced ALA synthesis and low steady-state levels of intermediates of TBS indicating a repressed metabolic flow into TBS (Figure 3.4 and 3.5). Therefore, an exact amount of FLU in plants is essential for fine-tuning of ALA synthesis for the supply of adequate amounts of TBS end-products. However, once plants are germinated in light, both the transcript and protein amounts of *FLU*/FLU are not changed during light-dark shifts (Goslings et al., 2004). On the other hand, the expression of *HEMA1* and the accumulation of GluTR are varying under various growth conditions or in a day-night cycle (Czarnecki et al., 2011). Therefore, it is likely that ALA synthesis is strongly regulated by controlling the ratio of FLU/GluTR amounts in plants.

4.1.2 FLU' impact on ALA synthesis is dependent on light intensity

The overproduced FLU increases the binding capacity of FLU to GluTR, which leads to more membrane-associated GluTR in the FLUOE lines (Figure 3.12). Although the amount of GluTR increased, the ALA synthesis rate was reduced in FLUOE lines compared to WT, indicating that GluTR, which is associated with FLU on the thylakoid membrane, is inactivated (Figure 3.4 and Figure 3.9). FLUOE lines showed a high amount of membrane-associated GluTR and deficiency on Chl contents even under CL, indicating that FLU can also bind GluTR on the thylakoid membrane and

thereby exerting a negative regulation on Chl biosynthesis during light exposure (Figure 3.8 and Figure 3.17).

The major role of FLU is to suppress ALA synthesis in the dark (Meskauskiene et al., 2001). By a combination of co-immunoprecipitation and LC-MS analysis, GluTR was found in the dark within a FLU-containing complex, but not in light (Kauss et al., 2012b). Here, by analyzing the localization of GluTR in the light or dark, the amount of the membrane-associated GluTR in WT was increased more in the dark than in the light (Figure 3.17), indicating that FLU can bind more GluTR at the thylakoid membrane in the dark than in the light. Therefore, even standard levels of FLU are expected to exert a stronger inactivation effect on ALA synthesis in the dark than in the light. In addition, the pale-green phenotype of FLUOE lines was more severe under light-dark conditions than under CL at the same light intensity (Figure 3.2 and Figure 3.7). The dark period seems to aggravate the repression effect of FLUOE on Chl synthesis.

In the FLUOE lines, ALA synthesis was more repressed under LL than ML, which finally leads to a severer Chl reduction under LL than ML (Figure 3.2, Figure 3.4 and Figure 3.6). An excessive amount of FLU conducts stronger repression on ALA synthesis under LL than ML. It is proposed that FLU' impact on ALA synthesis varies not only in the dark and light but also under various light intensities. FLU was suggested to be in the inactivation complex with POR, CHLM, and CHL27 (Kauss et al., 2012b). Here, the protein amounts of PORB and CHL27 increased in FLUOE lines compared to WT, indicating a stabilizing effect of FLU on the inactivation complex (Figure 3.9). It is assumed that the binding affinity of this inactivation complex to GluTR changes under different light intensities, thereby exerting a stronger inactivation on ALA synthesis in the dark or LL than ML.

The GluTR amount in FLUOE lines significantly increased relative to WT but the transcript level of *HEMA1* did not change, indicating that the stability of GluTR increased when FLU is overexpressed (Figure 3.9 and Figure 3.10). GluTR is the substrate for the stroma-localized Clp protease. The N-terminus of GluTR is essential for the degradation by Clp protease as it is the binding site for some adapter proteins of Clp protease, such as ClpC, ClpS (Apitz et al., 2016). However, FLU binds to the C-terminus of GluTR. It was initially assumed that the binding of FLU to GluTR could not prevent the binding of Clp protease at the N-terminus of GluTR. One assumption to explain the increased stability of GluTR in FLUOE lines is that FLU might bind GluTR to the thylakoid membrane. This sub-compartment could reduce the possibility of GluTR to be captured by the stromal localized Clp protease.

GBP and FLU bind to the N-terminus and C-terminus of GluTR, respectively. It was previously proposed that GBP and FLU can simultaneously bind to GluTR to form a hetero-hexamer (Fang et al., 2016). The contents of GluTR and GBP increased in FLUOE lines compared to WT (Figure 3.9). This data indicates that FLU contributes to the increased stability of GluTR and GBP in vivo. This finding supports the hypothesis that a hetero-hexamer can be formed consisting of dimers of GluTR, GBP and FLU. Referring to the analysis of crystal structure, both GBP and GSAT dimers bind to the pocket area of the GluTR dimer (Moser et al., 2001; Schulze et al., 2006b; Zhao et al.,

2014). GSAT is also believed to be one of the GluTR interacting partners as the product of GluTR, GSA, is very unstable and therefore needs to be transferred to GSAT immediately. But unlike GBP, the protein amount of GSAT was not affected at the transcript and protein level in FLUOE lines (Figure 3.9). The interaction between GluTR and GSAT could not be demonstrated by pull-down assays. It is speculated that the binding of GluTR to GSAT occurs only transiently (Hennig et al., 1997; Ge et al., 2010). Thus, GBP seems to be more tightly bound to GluTR than GSAT.

4.1.3 Potential function of FLU under HL

Excess light absorption causes damage of the photosynthetic apparatus in plants (Demmig-Adams and Adams III, 1992; Graßes et al., 2001; Kimura et al., 2003). Plants have developed several quenching mechanisms against excessive light energy in response to HL stress, such as the xanthophyll cycle, ROS scavenging systems, and anthocyanins (Asada, 1996; Donahue et al., 1997; Niyogi, 1999; Mano and Kime, 2001). It was previously reported that HL could inhibit the Chl biosynthesis at the level of ALA synthesis (Aarti et al., 2007). As Chl is required for the stability of Chl-binding proteins (Apel and Kloppstech, 1980; Murray and Kohorn, 1991), it was hypothesized that plants inhibit ALA synthesis to lower the Chl supply in parallel to decrease the amounts of light-harvesting antenna complexes under HL stress.

Upon extended HL stress, FLUOE lines showed significantly diminished Chl contents than WT (Figure 3.11A). The steady-state levels of ROS responsive marker genes, especially genes responsive to $^1O_2$, are substantially less induced both under ML and HL in FLUOE lines, indicating that less amounts of ROS are generated in FLUOE lines compared to WT (Figure 3.11C and D). These facts indicate a role of FLU under HL stress. When too much light is exposed, then additional action of FLU is required to stimulate inactivation of ALA synthesis in order to reduce Chl biosynthesis. The lower Chl content results in less light energy absorption in the antenna complexes and hence reduced ROS levels in plants.

4.1.4 FLU has an important role under fluctuating light

Light conditions used in the laboratory are mostly constant light. But real light exposure is more complex in the environment (Kaiser et al., 2018; Slattery et al., 2018; Yamamoto and Shikanai, 2019). *flu* seedlings under FL growth show a pale-green phenotype, especially in the newly grown leaves, where more Chl content is required and a tight control of Chl synthesis is essential. These observations indicate that the function of FLU is essential for plants growing under FL conditions (Figure 3.22 and Figure 3.27). The contents of intermediates of Chl synthesis, such as porphyrins and Pchlide, were increased in *flu* relative to WT at the end of the LL period (Figure 3.24), which can lead to the generation of ROS, especially $^1O_2$. The expression of $^1O_2$-responsive genes showed elevated levels in *flu* under FL. This could be interpreted with the accumulation of $^1O_2$ (Figure 3.26). High levels of $^1O_2$ are generated when *flu is* transferred from dark to light. The subsequent photo-oxidation causes PCD (op den Camp et al., 2003). The levels of accumulating

$^1O_2$ in *flu* under FL are not high enough to trigger PCD, but they might cause impairment of the chloroplast activities.

Moreover, the knockout of the *EX1* gene blocks the $^1O_2$-dependent signaling pathway (Wagner et al., 2004). The growth of *flu/ex1* under FL is suggested to be investigated in future in order to clarify whether the pale-green phenotype of *flu* under FL is explained by the partial function of the $^1O_2$-dependent signaling pathway.

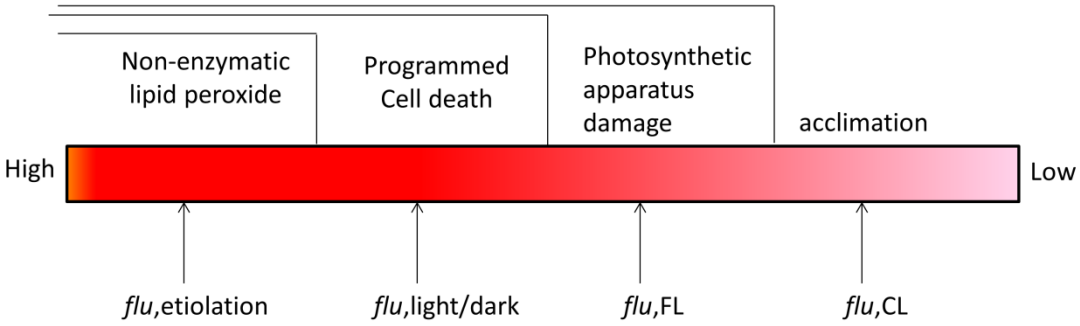

Figure 4.1 The dose-dependent effects of $^1O_2$ on plants. The depth of color in the bar indicates the concentration of $^1O_2$. The more intensive the color, the higher the concentration. Arrows below the bar indicate the relative concentration of $^1O_2$ in *flu* under various growth conditions from left to right. Etiolation, 4-day-old etiolated seedlings re-exposed to light for 8h; light-dark, light-exposed *flu* plants treated with 8 h of darkness and re-illuminated to light for 8h; FL, 30min LL/30min ML; CL, continuously ML. Upper part indicates various effects on plants in dependency to the amount of $^1O_2$. The detailed explanation of the model is found in the text.

The *flu* mutant accumulates different $^1O_2$ levels under various growth conditions, which causes different effects on plants (Figure 4.1). The minimum amount of $^1O_2$ is accumulated in *flu* under CL. Under this condition, the expression of genes responsive to $^1O_2$ such as *AAA1* and *BAP1* showed elevated levels in *flu* compared to WT under CL (Figure 3.43), indicating the higher generation of $^1O_2$ in *flu* in contrast to WT. However, *flu* grows as well as WT under CL (Meskauskiene et al., 2001). It is likely that CL-grown *flu* is sufficiently acclimated and can cope with the generated level of $^1O_2$ accumulation. It is assumed that the accumulation of various antioxidants, such as ascorbate (vitamin C) and α-tocopherol (vitamin E) are adequate (Hernández et al., 2009). It is expected that the *flu* mutant grown under FL accumulates a greater amount of $^1O_2$ compared with *flu* under CL. This amount of $^1O_2$ causes a detrimental photosensitization, which impairs the photosynthetic apparatus. The *flu* mutant grown under 8h dark and 16h light cycle accumulates an even greater amount of $^1O_2$ than *flu* under FL. This level of $^1O_2$ triggers the expression of genes involved in $^1O_2$-dependent PCD, which leads to cell death (op den Camp et al., 2003). The highest level of accumulation of $^1O_2$ is taken place in the etiolated seedling of *flu* exposure to light. This level of $^1O_2$ causes non-enzymatic lipid peroxide (Przybyla et al., 2008).

4.1.5 FLU controls the sub-compartmental localization of GluTR

It was previously suggested that ALA synthesis activity occurs in the stroma fraction (Kannangara and Gough, 1977). In the same line, it was previously thought that

GluTR is exclusively localized in the stroma (Eckhardt et al., 2004). However, a portion of GluTR was recently reported to be found in the thylakoid membrane. Using certain protocols, even GSAT was found in the margin area of thylakoids (Czarnecki and Grimm, 2012; Wang et al., 2016). The localization of GluTR was verified and the question further addressed in this thesis, how this localization affects the enzyme activity of GluTR.

The lengthy and sophisticated methods of chloroplast preparations might give a false view on the allocation of proteins, and so yielded in an artificial or false pattern of protein distribution within the plastids. Here, a crude but fast method was applied to separate total proteins in plants into a membrane-localized and a soluble fraction. The thylakoid-associated and stromal proteins were previously normalized according to the total amounts of proteins in each fraction (Czarnecki et al., 2011; Wang et al., 2016). However, the total amount of protein differs in membrane and stroma fractions (Figure 3.12). It is only comparable when the stroma and membrane proteins were dissolved in the same volume of buffer and the same volume of each fraction was applied for protein analysis on PA-gels. Moreover, this crude method provides a fast and material-saving way to evaluate the sub-compartmental localization of proteins which are exclusively in chloroplasts.

GluTR was found to be dominantly present in the soluble fraction under conditions where more ALA synthesis is expected, for example, in the newly developing leaves, in the middle of the day or the de-etiolated seedlings (Figure 3.14; Figure 3.15 and Figure 3.20). These observations are consistent with previous ideas that the stromal GluTR supports TBS for ALA synthesis (Kannangara and Gough, 1977). Furthermore, the soluble GluTR was more abundant in *flu,* while it was less abundant in FLUOE lines (Figure 3.16). In consistency, the ALA synthesis rate was increased in *flu* and decreased in FLUOE lines. Thus, the ALA synthesis corresponds to the contents of soluble GluTR in the *flu* and FLUOE lines (Figure 3.19).

But anyway, in light-grown WT plants, a large portion of GluTR was found in the membrane fraction (Figure 3.17 and Figure 3.18). When FLU is absent, the predominant portion of GluTR is always soluble (Figure 3.17 and Figure 3.18), indicating that a bulk of GluTR is associated with the membrane by FLU even during light exposure. Conversely, overexpression of FLU leads to the accumulation of membrane-associated GluTR and to lower amounts in the soluble fraction (Figure 3.12; Figure 3.17 and Figure 3.18). The content of membrane-associated GluTR is in proportion with the amount of FLU. It is concluded that the localization of GluTR is primarily dependent on FLU-GluTR interaction.

The impairment of the stromal-localized Clp protease substantially increases the stability of GluTR in the dark (Apitz et al., 2016; Figure 3.21A). Soluble GluTR is expected to be more accessible for the degradation by Clp protease. The degradation rate of GluTR in FLUOE seedlings in the dark was lower than in WT (Figure 3.21B). The association of GluTR to the membrane by FLU might prevent the degradation of GluTR by Clp protease.

But, a small portion of GluTR is present in the membrane even in the *flu* mutant (Figure 3.17). This portion of membrane-associated GluTR seemed to be independent of FLU binding and was found to be present in a high molecular weight complex by a 2D-BN-PAGE analysis (Yanyu Yang, 2018, master thesis). It is proposed that a combination of BN-PAGE and mass spectrometry, the interaction partners of GluTR within this complex might be revealed in the future.

The stromal GluTR contributes to the bulk of ALA synthesis activity (Kannangara and Gough, 1977). Maintenance of the appropriate amount of soluble GluTR under various conditions is essential for a fine-tuned supply of ALA for TBS. Three pathways were suggested to control the amount of soluble GluTR (Figure 4.2). Firstly, the amount of newly synthesized GluTR has to be imported into plastids and allocated to the stroma. Secondly, Clp protease degrades the stromal GluTR. Thirdly, FLU in the inactivation complex maintains a large portion of inactive GluTR at the thylakoid membrane. When plants are exposed to light, a small portion of GluTR is released into the stroma from the thylakoids membrane. When plants are exposed to growth conditions that require less Chl synthesis, e.g. under LL, or no Chl synthesis, as during darkness, more GluTR can be associated to thylakoid membrane by interaction with proteins of the inactivation complex. The interaction of GluTR with the inactivation complex might be triggered by binding of Pchlide to this complex (Kauss et al, 2012).

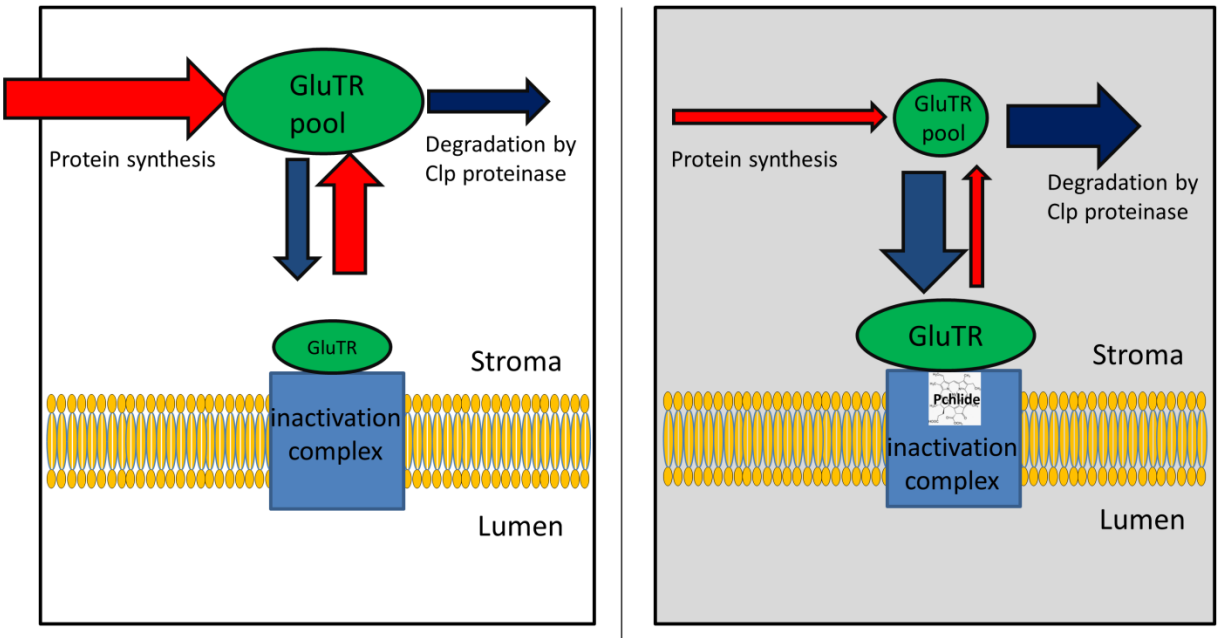

Figure 4.2 A model for the control of soluble GluTR in plastids. White background indicates standard growth conditions while grey background indicates dark, LL or stress conditions. The area of the green-labeled GluTR indicates its amount. Red arrows indicate the flux of GluTR to increase the amount of the soluble part, while blue arrows indicate the way to decline the amount of soluble GluTR. Details of the model are explained in the main text.

4.1.6 FLU also functions in the light to fine-tune ALA for Chl biosynthesis

Chlamydomonas contains a DPOR and is able to convert Pchlide to Chlide even in the dark. Then, in algae, it is not vital to suppress ALA rapidly to avoid the accumulation of Pchlide in the dark (Falciatore et al., 2005). The appearance of FLP in *Chlamydomonas* might be important for regulating ALA synthesis in light.

In the field, light intensity changes frequently and dramatically. Then, it is a challenge for plants to maintain an optimal TBS flow to provide adequate substrates and also to avoid the accumulation of tetrapyrrole intermediates. The control of TBS at the ALA synthesis step is an economical and safe way for TBS regulation. The post-translational control of ALA synthesis mediated by FLU allows a fast response to environmental changes. Unlike the previous model that FLU function only in the dark to suppress ALA synthesis (Kauss et al., 2012b), here, it is proposed that FLU enables plants to maintain an excessive amount of GluTR at the thylakoid membrane to balance rapidly the content of active GluTR under various light conditions.

4.2 Characterization of functions of two cysteines in FLU

Redox control to regulate the stability or the enzyme activity of key enzymes involved in TBS has been previously reported in several publications (Richter et al., 2016; Da et al., 2017; Richter et al., 2018; Wittmann et al., 2018). The FLU protein in *Arabidopsis* contains two conserved cysteines. The cysteine residue119 is at the N-terminus of FLU near the TM and the other one, cysteine292, localized in the TPR(FLU) domain. Both cysteine residues are highly conserved in angiosperms (Figure S2). It was hypothesized that the cysteines of FLU are involved in the inter-molecular formation of the FLU homodimers or FLU-GluTR heterodimers. Therefore, the *flu* complementation lines with cysteines-substituted-FLU lines were generated to identify a potential redox reactive cysteine in FLU.

Under the non-reducing condition, FLU in WT plants migrated as a 45kDa protein, the predicted size of the FLU homodimer. This finding demonstrates that FLU forms a homodimer through an intermolecular disulfide bond in plants (Figure 3.28). No monomers were found in non-reducing gels from plants extracts of samples harvested in the light, dark, or cold stress conditions indicating that the intermolecular disulfide bonds of FLU homodimers were not disrupted under these growth conditions (Figure S1). This disulfide bond formation of FLU homodimers seems to be an intrinsic structure but is unlikely to be involved in the redox-dependent regulation of ALA synthesis under various growth conditions. Unlike FLU, the dominant content of GluTR migrates as a monomer under the non-reducing condition on SDS-PA-gels (Figure 3.28). GluTR in WT might form a homodimer through its interaction domain at the C-terminus, but likely not through the intermolecular disulfide bond between two GluTR proteins (Moser et al., 2001; Zhang et al., 2015).

The substitution of cysteine119 into a serine that results only in the swap of a sulfur atom with an oxygen atom, prevents disulfide bonding of FLU homodimers as seen in non-reducing gels. However, the substitution of cysteine292 did not affect the dimer formation of FLU (Figure 3.30). Therefore, the disulfide bonding of homodimeric FLU

in plants is dependent on the cysteine residue119 but not cysteine292. However, the dimer or monomer of FLU, examined here, were detected under the denaturing condition in the SDS-PA gel. It needs to be clarified in future experiments whether those mutants contain native FLU homodimers.

Although two FLUC119S does not form a stable dimer in the SDS-PA gel, FLUC119S still rescues the *flu* phenotype. As a GluTR homodimer is a functional unit for ALA synthesis (Moser et al., 2001), the FLU dimer is thought to facilitate the formation of FLU-GluTR tetramer for GluTR inactivation. Surprisingly, FLUC119S seemed to suppress ALA synthesis even more efficiently. Firstly, the ALA synthesis rate was reduced in the FLUC119S lines in the light-grown plants compared to the FLU(WT) lines (Figure 3.29). Secondly, Pchlide accumulated to lower extent in light or darkness in FLUC119S lines relative to the FLU(WT) lines (Figure S3). The cysteine292 is positioned close to the dimerization domain of GluTR, which could be involved in the interaction and inactivation of GluTR (Zhang et al., 2015). But, FLUC292S fully complements the *flu* knockout mutant, demonstrating that cysteine 292 of FLU was not essential for the FLU-GluTR interaction dependent repression of ALA synthesis in the dark (Figure 3.29).

4.3 Analysis of the role of functional domains of FLU in the repression of ALA synthesis

Three domains were previously suggested in the FLU protein, TPR(FLU), TM domain and linker domain. It was reported that TPR(FLU) inactivates ALA synthesis alone in vitro (Zhang et al.,2015). The TM domain enables FLU to anchor GluTR into the thylakoid membrane. The linker domain is a typical domain for protein-protein interaction, which was previously proposed to be involved in the interaction with the inactivation complex (Zhang et al.,2015). Three different series of *flu* complementation lines were established, which express always a different truncated FLU peptide, namely TPR(FLU), FLUΔlinker, FLUΔTM. These complementation lines were generated to explore the in vivo function of each domain.

4.3.1 Transit peptide of the precursor protein of FLU

The integration of thylakoid proteins into the membrane is conducted by multiple pathways. The insertion of LHCa/b into thylakoid membrane relies on the interaction with cpSRP proteins as well as ALB3, FTSY proteins (Lamppa, 1988). Some thylakoids proteins contain a bipartite transit peptide to be targeted into the plastidic stroma and further into the lumen. One example is the integration of photosystem II reaction center protein W (PsbW) into the thylakoid membrane. PsbW contains a bipartite transit peptide comprising an envelope transit peptide followed by a hydrophobic signal-type peptide (Robinson et al., 2001). Translocation across the envelope will remove the envelope transit peptide in the stroma. After integration of the intermediate precursor of PsbW into the thylakoid membrane, the hydrophobic signal-type peptide will be cleaved by the thylakoidal processing peptidase (TPP) to form the mature protein (Robinson et al., 2001). Another example is the subunit II of the membrane-embedded CF0 (CF0II) assembly of the plastidic ATP synthase. CF0II

also contains a bipartite transit peptide. To process CF0II, cleavage of the precursor protein is also required in the thylakoid membrane by the TPP (Michl et al., 1994). FLU is a membrane protein exclusively localized in the thylakoid membrane (Meskauskiene et al., 2001). However, how FLU is integrated into thylakoid membrane is not clear.

The transient expression of a DNA sequence coding for a fused protein consisting of the predicted transit peptide of FLU (described in chapter 3.3) and a GFP protein resulted in a GFP-fluorescence in the chloroplast (Figure S4), which demonstrated that the intact transit peptide sequence is within the predicted transit peptide of FLU. The lines expressing the truncated FLU peptides always showed not only the immune band at the target size but also a higher protein band, which indicated a 5 kDa larger protein than the predicted protein (Figure 3.33 and Figure 3.49). The extra immune-reacting band could correspond to the precursor protein. But this band migrated faster than the expected precursor protein as the transit peptide is predicted to be 11 kDa. Another possibility is that the transit peptide of FLU forms a bipartite transit peptide, which consists of an “envelope transit” and “thylakoid transfer” signal in tandem. The 5 kDa larger truncated FLU form could indicate an intermediate pre-protein without the envelope transit peptide but still contained the 'thylakoid transfer' signal peptide. Loss of linker or TM domain would decrease the cleavage efficiency of the 'thylakoid transfer' signal peptide. To further verify this hypothesis in future, the exact cleavage site for the transit peptide has to be identified in future.

4.3.2 TPR(FLU) caused the accumulation of GluTR

Evidence was shown previously that TPR(FLU) alone could interact with the dimerization domain of GluTR in vitro (Zhang et al., 2015). Here, by in vitro pull-down experiments, the interaction between TPR(FLU) and GluTR was confirmed (Figure 3.39). Moreover, by analysis of GluTR and FLU in the membrane and soluble fractions, it was shown that GluTR accumulates mainly in the same fraction with the truncated FLU peptide in the *flu* complementation lines (Figure 3.40; Figure 3.45 and Figure 3.55). The TPR/*flu*, TPR/WT and FLUΔTM/*flu* lines contained a soluble truncated FLU peptide and the majority of GluTR in these lines was present in the soluble part (Figure 3.40; Figure 3.45 and Figure 3.55) while in the pAlc_FLUΔLinker/*flu* lines, the major portion of GluTR was associated in the membrane (Figure 3.51). These data also indicate that all truncated FLU peptides interact with GluTR in plants when they contain the TPR(FLU) domain. Interestingly, GluTR amounts were strongly increased in all of the complementation lines containing the truncated FLU peptides compared to WT or *flu*. The accumulation of GluTR is not due to the stimulated expression of the *HemA1* gene (Figure 3.34 and Figure 3.35). The binding of truncated FLU peptides to GluTR perhaps block the proteolysis of GluTR. GluTR degradation was previously found to be conducted by the stromal localized Clp protease. The N-terminus of GluTR is the recognition site for Clp protease (Apitz et al., 2015). However, TPR(FLU) binds to the C-terminus of GluTR (Zhang et al., 2015). At a first glance, binding of TPR(FLU) to the C-terminus of GluTR should not impair the binding of Clp-selector proteins to GluTR. However, it is

not excluded that the C-terminus of GluTR is also required for the degradation process. Moreover, there could also be another degradation mechanism of GluTR, for which the C-terminus of GluTR is perhaps required.

It was recently reported that heme triggers the degradation of GluTR (Richter et al., 2019). Conversely, reduced content of heme might increase the stability of GluTR. As the heme contents were reduced in the *flu* complementation lines with the truncated FLU peptides (Figure 3.46 and Figure 3.53), it is not excluded that the reduced heme levels in the mutants contribute to the increased stability of GluTR.

The overexpression of the intact FLU also led to the accumulation of GluTR (Figure 3.2 and Figure 3.9). However, 30 times more intact FLU relative to the WT level resulted in around 3 times more GluTR accumulation in FLUOE lines while a WT-like amount of TPR(FLU), caused already more than 6 times GluTR accumulation compared to *flu* (Figure 3.35). The truncated FLU peptides resulted in a higher GluTR accumulation than endogenous expression of intact FLU in plants. It is assumed that the interaction of TPR(FLU) to GluTR blocks its proteolysis. Then TPR(FLU) seems to be more accessible for the interaction with GluTR than the intact FLU. It is hypothesized that the intact FLU has a higher tendency to form a dimer of TPR(FLU) than the “free” TPR(FLU) peptide, which has a disadvantage for the interaction with GluTR.

4.3.3 TPR(FLU) alone does not rescue the *flu* phenotype

flu shows a high ALA synthesis rate and high levels of Pchlide accumulation in the dark, which subsequently causes the generation of $^1O_2$ and triggers cell death upon light exposure (Meskausine et al., 2001; Kauss et al., 2003). TPR(FLU) inactivates the enzyme activity of GluTR in an in vitro experiment (Zhang et al., 2015). It was hypothesized that TPR(FLU) could suppress the ALA synthesis and prevent the accumulation of Pchlide and therefore rescue *flu*. However, Pchlide, both in the light-exposed leaves and in the etiolated seedlings of TPR/*flu* lines, accumulated even more compared to *flu* (Figure 3.42, Figure 3.37 and Figure 3.38). TPR(FLU) cannot fulfill the function of intact FLU to repress ALA synthesis in plants. Moreover, the analysis of TPR/WT lines confirmed this conclusion. Pchlide slightly increased in TPR/WT lines compared to WT in light but increased more significantly in the dark period (Figure 3.47). In the dark, soluble GluTR in WT needs to be inactivated by FLU. TPR(FLU) in TPR/WT lines might compete for the binding of soluble GluTR with the endogenous FLU. It is proposed that the interaction of TPR(FLU) with GluTR does not completely inactivate the enzyme activity of GluTR, thereby resulting in the accumulation of Pchlide in the TPR/WT lines in the dark. Therefore, the expression of TPR(FLU) in WT is proposed to impair the function of endogenous FLU in the dark.

Although six times more GluTR accumulated in TPR/*flu* lines compared to *flu*, the ALA synthesis rate was only 50% higher (Figure 3.42). It is speculated that a large portion of GluTR was partially inactivated in the TPR/*flu* lines. TPR(FLU) could function as a negative regulator for ALA synthesis but the inactivation effect is not high enough to minimize the Pchlide accumulation in the dark. On the other hand,

the expression of the FLUΔTM peptide in *flu* partially rescues the *flu* phenotype (Figure 3.55). It is assumed that the linker domain is also involved in the interaction with GluTR and can strengthen the affinity to GluTR. However, as Pchlide content only decreased to half of the *flu* content in the dark, FLUΔTM did not result in full complementation of *flu*, indicating that the function of the TM domain of FLU is also required for the entire inactivation of ALA synthesis in the dark.

4.3.4 The binding of GluTR to the thylakoid membrane is essential to tightly inactivate ALA synthesis

Several attempts to express FLUΔlinker in *flu* mutants failed to obtain stable transgenic plants. The FLUΔlinker peptide was found to be more stable than the soluble formed truncated FLU peptides in a transient transformation to *N. benthamiana* leaves (Figure S5). FLUΔlinker was successfully expressed in *flu* using an ethanol-inducible promoter-gene construct. However, this truncated FLU peptide with a TM was still not able to rescue the *flu* phenotype, indicating that the linker domain is indispensable in the inactivation of ALA synthesis.

Although FLUΔlinker was not able to suppress the Pchlide accumulation in *flu* in dark, its effects on ALA synthesis in light-exposed plants were different from TPR(FLU). A higher amount of GluTR also accumulated in pAlc_FLUΔlinker/*flu* lines compared to WT and *flu*. But the increasing amounts of GluTR in pAlc_FLUΔlinker/*flu* lines did not result in a higher ALA synthesis rate as in the TPR/*flu* lines (Figure 3.50 and Figure 3.53). On the contrary, the ALA synthesis and Pchlide content in the pAlc_FLUΔlinker/*flu* lines were reduced, indicating that the FLUΔlinker peptide has a stronger inactivation effect of ALA synthesis than TPR(FLU) (Figure 3.53). As soluble GluTR has been suggested to be the active form for ALA synthesis in plants (Schmied et al., 2018), the TM domain of FLU might function in anchoring GluTR to the membrane, thereby decreasing the ALA synthesis.

The TM domain might not only function as an anchor but also function in interacting with some components of the inactivation complex. To answer this question, a fused protein with the TM of APX (Takahashi et al., 2014) and FLUΔTM is proposed to be expressed in *flu* to find out whether this fused protein exerts the same inactivation effect on ALA synthesis as the native FLU.

4.3.5 Mechanisms involved in a proper inactivation of ALA synthesis mediated by FLU

The major role of FLU is to repress ALA synthesis in the dark and thereby preventing Pchlide accumulation in the dark. By studying the *flu* complementation lines with the truncated FLU peptides, the mechanisms for FLU-dependent inactivation of GluTR were further explored. Some mechanisms for the inactivation of ALA synthesis by FLU are proposed.

A schematic model of the truncated FLU peptides and their effects on inactivation of ALA synthesis is proposed based on results in this study (Figure 4.3). It is generally

accepted with the current model that TPR(FLU)-GluTR interaction prevents the binding of glutamyl-tRNA to GluTR, thereby inactivating ALA synthesis (Zhang et al., 2015). However, the inactivation effect of TPR(FLU) on ALA synthesis is not sufficient to prevent the Pchlide accumulation of *flu* in the dark and therefore cannot rescue the *flu* phenotype (Figure 3.36 and Figure 3.37). FLUΔlinker that contains the TM domain of FLU helps to anchor GluTR to the thylakoid membrane, which might decrease the chance for binding of GluTR to the soluble glutamyl-tRNA. Therefore, FLUΔlinker has a higher inactivation effect on ALA synthesis than TPR(FLU). However, this inactivation effect is still not sufficient to rescue the *flu* phenotype in the dark (Figure 3.52). FLUΔTM achieves a stronger inactivation effect on ALA synthesis than TPR(FLU) and FLUΔlinker because FLUΔTM can partially suppress the Pchlide accumulation of *flu* in the dark (Figure 3.55). It is hypothesized that the linker domain of FLU might also be involved in the binding of GluTR. Therefore the FLUΔTM peptide is more tightly associated with GluTR than TPR(FLU), thereby can more efficiently prevent the binding of GluTR to glutamyl-tRNA. Therefore, it is proposed that all three domains of FLU are contributed to a tight inactivation of ALA synthesis. Moreover, GluTR was found to interact not only with FLU but also with PORB and CHLM (Figure 3.59; Figure 3.60). FLU within the inactivation complex might have a higher affinity to GluTR than the single FLU, hence conducts an even stronger inactivation on ALA synthesis than the single FLU.

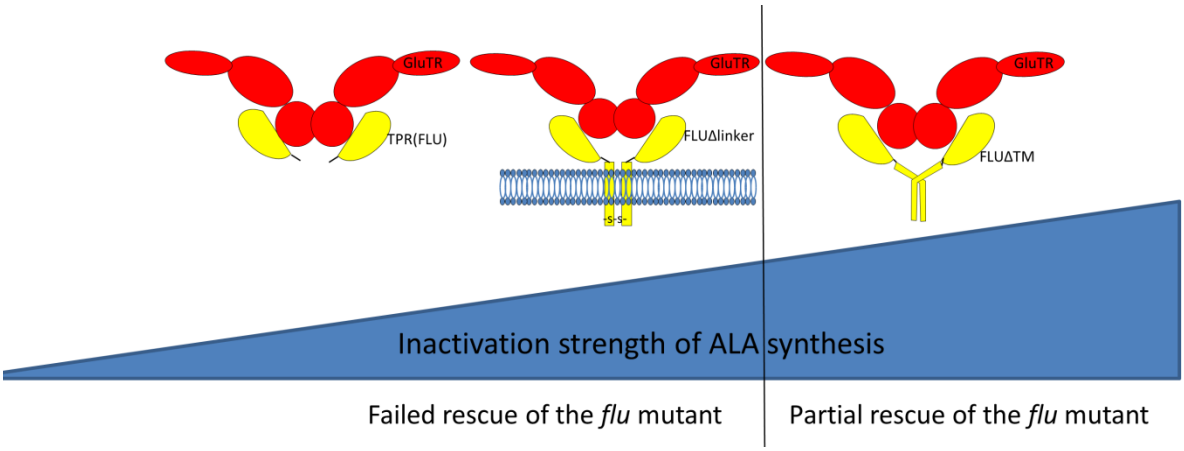

Figure 4.3: A schematic association of truncated FLU peptides with ALA synthesis activity. Red cartoons indicate the domains of GluTR, and yellow cartoons indicate the domains of FLU. The intact FLU contains 3 domains, TPR(FLU), linker and TM domain. FLUΔlinker, TM plus TPR domains of FLU; FLUΔTM, linker plus TPR domain. The blue triangle indicates the strength of repression on ALA synthesis depending on the interaction between truncated FLU peptides and GluTR.

The FLU-GluTR interaction was previously proposed to be driven by the binding of Pchlide to the inactivation complex (Kauss et al., 2012). The interactions between FLU and CHLM/PORB were verified by BiFC and yeast two-hybrid assays (Figure 3.56 and Figure 3.57). TPR(FLU) alone showed also a strong interaction with PORB and CHLM in the yeast two-hybrid assay (Figure 3.58). Based on a previous model and results in this study, a modified hypothetical model is proposed to explain the dark repression of ALA synthesis relying on the FLU-GluTR interaction that is dependent on the Pchlide binding to POR (Figure 4.4). TPR(FLU) and linker might interact simultaneously with the inactivation complex and GluTR. In light, FLU forms a

homodimer within the inactivation complex. In this state, the two TPR(FLU) units are close to each other and do not interact with GluTR. When Pchlide is accumulated in the dark and associated with PORB, it causes a conformational change of the inactivation complex. This conformational change opens the TPR(FLU) homodimer, and ease the interaction with GluTR, thereby triggers inactivation of ALA synthesis in the dark.

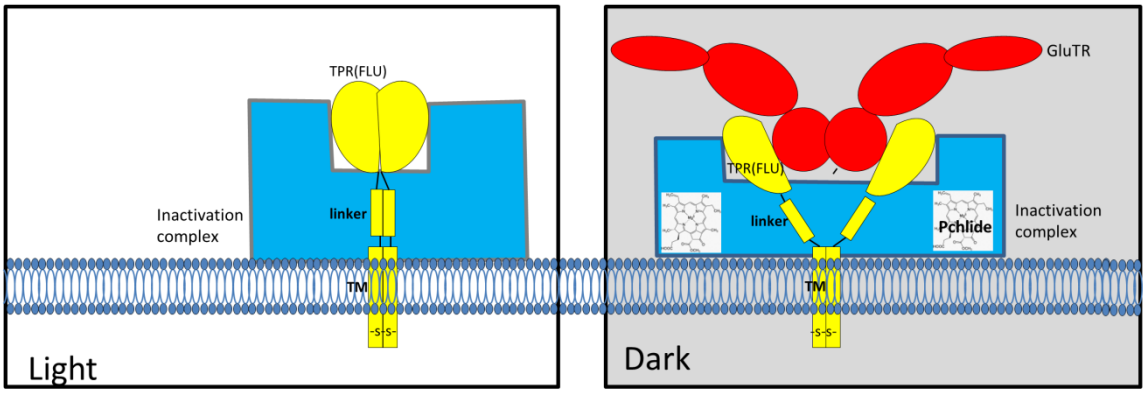

Figure 4.4: A hypothetical mechanism of FLU-mediated dark repression of ALA synthesis. FLU interacts with the inactivation complex with its TPR and linker domains.In the light,TPR(FLU) forms a homodimer that do not interact with GluTR. In the dark, Pchlide bound to the inactivation complex, resulting in a conformational change of theinactivation complex which facilitates the binding of GluTR to FLU.

Both PORB and PORC are present in the inactivation complex and they share a high sequence identity (Kauss et al., 2012b). Therefore, it is likely that both forms could be involved in the feedback regulation of ALA synthesis. *PORA* is expressed at the early stage of plant development during etiolation (Matsumoto et al., 2004). GluTR is highly associated with the membrane in the etiolated seedlings (Figure 3.20). PORA might be involved in the inactivation of ALA synthesis in the etiolated seedlings. CHL27, CHLG and geranylgeranyl reductase (CHLP) were also previously found to assemble with FLU (Kauss et al., 2012b). But the direct interaction of CHL27 and FLU was not detected by BiFC and yeast two-hybrid assays (Figure 3.56 and Figure 3.57). Additional protein(s) in the inactivation complex might be required for binding of CHL27. Furthermore, one of the light-harvesting-like (LIL) proteins, LIL3, interacts with CHLP and PORB and was suggested to function in the organization of the late steps in Chl biosynthesis (Hey et al., 2017). Moreover, it has been also shown that FeCh2 is tightly associated with POR through its CAB domain (Fan, 2019). It is hypothesized that a huge complex containing enzymes involved in late steps of TBS contribute to the control of ALA synthesis for the adequate synthesis of different TBS end-products.

4 References

Aarti, D., Tanaka, R., Ito, H., and Tanaka, A. (2007). High light inhibits chlorophyll biosynthesis at the level of 5 ‐ aminolevulinate synthesis during de ‐ etiolation in cucumber (Cucumis sativus) cotyledons. Photochemistry and Photobiology **83,** 171-176.

Adhikari, N.D., Froehlich, J.E., Strand, D.D., Buck, S.M., Kramer, D.M., and Larkin, R.M. (2011). GUN4-porphyrin complexes bind the ChlH/GUN5 subunit of Mg-Chelatase and promote chlorophyll biosynthesis in Arabidopsis. The Plant Cell **23,** 1449-1467.

Alonso, J.M., Stepanova, A.N., Leisse, T.J., Kim, C.J., Chen, H., Shinn, P., Stevenson, D.K., Zimmerman, J., Barajas, P., and Cheuk, R. (2003). Genome-wide insertional mutagenesis of Arabidopsis thaliana. Science 301, 653-657.

Andersen, A.N., and Burbidge, A.H. (1992). An overview of the ant fauna of Cape Arid. Journal of the Royal Society of Western Australia **75,** 2.

Apel, K., and Kloppstech, K. (1980). The effect of light on the biosynthesis of the light-harvesting chlorophyll a/b protein. Planta **150,** 426-430.

Apitz, J., Schmied, J., Lehmann, M.J., Hedtke, B., and Grimm, B. (2014). GluTR2 complements a hema1 mutant lacking glutamyl-tRNA reductase 1, but is differently regulated at the post-translational level. Plant and Cell Physiology **55,** 645-657.

Apitz, J., Nishimura, K., Schmied, J., Wolf, A., Hedtke, B., van Wijk, K.J., and Grimm, B. (2016). Posttranslational control of ALA synthesis includes GluTR degradation by Clp protease and stabilization by GluTR-binding protein. Plant physiology **170,** 2040-2051.

Asada, K. (1996). Radical production and scavenging in the chloroplasts. In Photosynthesis and the Environment (Springer), pp. 123-150.

Baier, M., and Dietz, K.-J. (2005). Chloroplasts as source and target of cellular redox regulation: a discussion on chloroplast redox signals in the context of plant physiology. Journal of Experimental Botany **56,** 1449-1462.

Balsera, M., Uberegui, E., Schuermann, P., and Buchanan, B.B. (2014). Evolutionary development of redox regulation in chloroplasts. Antioxidants & redox signaling **21,** 1327-1355.

Bang, W.Y., Jeong, I.S., Kim, D.W., Im, C.H., Ji, C., Hwang, S.M., Kim, S.W., Son, Y.S., Jeong, J., and Shiina, T. (2008). Role of Arabidopsis CHL27 protein for photosynthesis, chloroplast development and gene expression profiling. Plant and cell physiology **49,** 1350-1363.

Baruah, A., Šimková, K., Apel, K., and Laloi, C. (2009a). Arabidopsis mutants reveal multiple singlet oxygen signaling pathways involved in stress response and development. Plant molecular biology **70,** 547-563.

Baruah, A., Šimková, K., Hincha, D.K., Apel, K., and Laloi, C. (2009b). Modulation of 1O2 ‐ mediated retrograde signaling by the PLEIOTROPIC RESPONSE LOCUS 1 (PRL1) protein, a central integrator of stress and energy signaling. The Plant Journal **60,** 22-32.

Battersby, A.R. (2000). Tetrapyrroles: the pigments of life. Natural product reports **17,** 507-526.

Beale, S., and Weinstein, J. (1990). Biosynthesis of heme and chlorophylls. by HA Dailey, McGraw-Hill, New York**,** 287-391.

Beale, S.I. (1993). Biosynthesis of phycobilins. Chemical reviews **93,** 785-802.

Beevers, H. (1961). Respiratory Metabolism in Plants, Row Peterson. Evanston, Illinois.

Bougri, O., and Grimm, B. (1996). Members of a low ‐ copy number gene family encoding glutamyl ‐ tRNA reductase are differentially expressed in barley. The Plant Journal **9,** 867-878.

Bruch, E.M., Rosano, G.L., and Ceccarelli, E.A. (2012). Chloroplastic Hsp100 chaperones ClpC2 and ClpD interact in vitro with a transit peptide only when it is located at the N-terminus of a protein. BMC plant biology **12,** 57.

Brzezowski, P., Schlicke, H., Richter, A., Dent, R.M., Niyogi, K.K., and Grimm, B. (2014). The GUN 4 protein plays a regulatory role in tetrapyrrole biosynthesis and chloroplast ‐ to ‐ nucleus signalling in C hlamydomonas reinhardtii. The Plant Journal **79,** 285-298.

Buchanan, B.B., and Balmer, Y. (2005). Redox regulation: a broadening horizon. Annu. Rev. Plant Biol. **56,** 187-220.

Chang, C.C., Ślesak, I., Jordá, L., Sotnikov, A., Melzer, M., Miszalski, Z., Mullineaux, P.M., Parker, J.E., Karpińska, B., and Karpiński, S. (2009). Arabidopsis chloroplastic glutathione peroxidases play a role in cross talk between photooxidative stress and immune responses. Plant Physiology 150, 670-683.

Chen, M., Schliep, M., Willows, R.D., Cai, Z.-L., Neilan, B.A., and Scheer, H. (2010). A red-shifted chlorophyll. Science 329, 1318-1319.

Chow, K.S., Singh, D.P., Walker, A.R., and Smith, A.G. (1998). Two different genes encode ferrochelatase in Arabidopsis: mapping, expression and subcellular targeting of the precursor proteins. The Plant Journal **15,** 531-541.

Clough, S.J., and Bent, A.F. (1998). Floral dip: a simplified method for Agrobacterium ‐ mediated transformation of Arabidopsis thaliana. The plant journal **16,** 735-743.

Czarnecki, O., and Grimm, B. (2012). Post-translational control of tetrapyrrole biosynthesis in plants, algae, and cyanobacteria. Journal of experimental botany **63,** 1675-1687.

Czarnecki, O., Hedtke, B., Melzer, M., Rothbart, M., Richter, A., Schröter, Y., Pfannschmidt, T., and Grimm, B. (2011). An Arabidopsis GluTR binding protein mediates spatial separation of 5-aminolevulinic acid synthesis in chloroplasts. The Plant Cell **23,** 4476-4491.

Da, Q., Wang, P., Wang, M., Sun, T., Jin, H., Liu, B., Wang, J., Grimm, B., and Wang, H.-B. (2017). Thioredoxin and NADPH-dependent thioredoxin reductase C regulation of tetrapyrrole biosynthesis. Plant physiology **175,** 652-666.

Danon, A., Miersch, O., Felix, G., op den Camp, R.G., and Apel, K. (2005). Concurrent activation of cell death‐regulating signaling pathways by singlet oxygen in Arabidopsis thaliana. The Plant Journal **41,** 68-80.

Das, A.K., Cohen, P.T., and Barford, D. (1998). The structure of the tetratricopeptide repeats of protein phosphatase 5: implications for TPR‐mediated protein‐protein interactions. The EMBO journal **17,** 1192-1199.

Davis, S.J., Kurepa, J., and Vierstra, R.D. (1999). The Arabidopsis thaliana HY1 locus, required for phytochrome-chromophore biosynthesis, encodes a protein related to heme oxygenases. Proceedings of the National Academy of Sciences **96,** 6541-6546.

Day, I.S., Golovkin, M., and Reddy, A. (1998). Cloning of the cDNA for glutamyl-tRNA synthetase from Arabidopsis thaliana. Biochimica et Biophysica Acta (BBA)-Gene Structure and Expression **1399,** 219-224.

Demmig-Adams, B., and Adams Iii, W. (1992). Photoprotection and other responses of plants to high light stress. Annual review of plant biology **43,** 599-626.

Dietz, K.-J., Jacob, S., Oelze, M.-L., Laxa, M., Tognetti, V., de Miranda, S.M.N., Baier, M., and Finkemeier, I. (2006). The function of peroxiredoxins in plant organelle redox metabolism. Journal of experimental botany **57,** 1697-1709.

Dogra, V., Li, M., Singh, S., Li, M., and Kim, C. (2019). Oxidative post-translational modification of EXECUTER1 is required for singlet oxygen sensing in plastids. Nature Communications **10,** 2834.

Dogra, V., Duan, J., Lee, K.P., Lv, S., Liu, R., and Kim, C. (2017). FtsH2-dependent proteolysis of EXECUTER1 is essential in mediating singlet oxygen-triggered retrograde signaling in Arabidopsis thaliana. Frontiers in plant science **8,** 1145.

Donahue, J.L., Okpodu, C.M., Cramer, C.L., Grabau, E.A., and Alscher, R.G. (1997). Responses of antioxidants to paraquat in pea leaves (relationships to resistance). Plant physiology **113,** 249-257.

Duggan, J., and Gassman, M. (1974). Induction of porphyrin synthesis in etiolated bean leaves by chelators of iron. Plant physiology **53,** 206-215.

Eckhardt, U., Grimm, B., and Hörtensteiner, S. (2004). Recent advances in chlorophyll biosynthesis and breakdown in higher plants. Plant molecular biology **56,** 1-14.

Espinas, N.A., Kobayashi, K., Takahashi, S., Mochizuki, N., and Masuda, T. (2012). Evaluation of unbound free heme in plant cells by differential acetone extraction. Plant and Cell Physiology **53,** 1344-1354.

Everingham, M., Zisserman, A., Williams, C.K., Van Gool, L., Allan, M., Bishop, C.M., Chapelle, O., Dalal, N., Deselaers, T., and Dorkó, G. (2005). The 2005 pascal visual object classes challenge. In Machine Learning Challenges Workshop (Springer), pp. 117-176.

Falciatore, A., Merendino, L., Barneche, F., Ceol, M., Meskauskiene, R., Apel, K., and Rochaix, J.-D. (2005). The FLP proteins act as regulators of chlorophyll synthesis in response to light and plastid signals in Chlamydomonas. Genes & development **19,** 176-187.

Fan, T. (2019). Control and function of two ferrochelatase isoforms in Arabidopsis thaliana.

Fang, Y., Zhao, S., Zhang, F., Zhao, A., Zhang, W., Zhang, M., and Liu, L. (2016). The Arabidopsis glutamyl-tRNA reductase (GluTR) forms a ternary complex with FLU and GluTR-binding protein. Scientific reports **6,** 19756.

Foyer, C.H., and Shigeoka, S. (2011). Understanding oxidative stress and antioxidant functions to enhance photosynthesis. Plant physiology **155,** 93-100.

Freist, W., Gauss, D.H., Soll, D., and Lapointe, J. (1997). Glutamyl-tRNA synthetase. Biological chemistry **378,** 1313-1330.

Frick, G., Su, Q., Apel, K., and Armstrong, G.A. (2003). An Arabidopsis porB porC double mutant lacking light‐dependent NADPH: protochlorophyllide oxidoreductases B and C is highly chlorophyll‐deficient and developmentally arrested. The Plant Journal **35,** 141-153.

Furuya, M., and Schäfer, E. (1996). Photoperception and signalling of induction reactions by different phytochromes. Trends in Plant Science **1,** 301-307.

Ge, H., Lv, X., Fan, J., Gao, Y., Teng, M., and Niu, L. (2010). Crystal structure of Glutamate1-semialdehyde aminotransferase from Bacillus subtilis with bound pyridoxamine-5′-phosphate. Biochemical and biophysical research communications **402,** 356-360.

Gendron, J.M., Pruneda-Paz, J.L., Doherty, C.J., Gross, A.M., Kang, S.E., and Kay, S.A. (2012). Arabidopsis circadian clock protein, TOC1, is a DNA-binding transcription factor. Proceedings of the National Academy of Sciences **109,** 3167-3172.

Gibson, L., Willows, R.D., Kannangara, C.G., von Wettstein, D., and Hunter, C.N. (1995). Magnesium-protoporphyrin chelatase of Rhodobacter sphaeroides:

reconstitution of activity by combining the products of the bchH,-I, and-D genes expressed in Escherichia coli. Proceedings of the National Academy of Sciences **92,** 1941-1944.

Gorchein, A. (1972). Magnesium protoporphyrin chelatase activity in Rhodopseudomonas spheroides. Studies with whole cells. Biochemical Journal **127,** 97-106.

Goslings, D., Meskauskiene, R., Kim, C., Lee, K.P., Nater, M., and Apel, K. (2004). Concurrent interactions of heme and FLU with Glu tRNA reductase (HEMA1), the target of metabolic feedback inhibition of tetrapyrrole biosynthesis, in dark‐and light‐grown Arabidopsis plants. The Plant Journal **40,** 957-967.

Gough, S.P., and Kannangara, C.G. (1979). Biosynthesis of δ-aminolevulinate in greening barley leaves III: The formation of δ-aminolevulinate intigrina mutants of barley. Carlsberg Research Communications **44,** 403.

Graßes, T., Grimm, B., Koroleva, O., and Jahns, P. (2001). Loss of α-tocopherol in tobacco plants with decreased geranylgeranyl reductase activity does not modify photosynthesis in optimal growth conditions but increases sensitivity to high-light stress. Planta **213,** 620-628.

Granick, S. (1959). Magnesium porphyrins formed by barley seedling treated with δ-aminolevulinic acid. Plant Physiol. **34,** XIII.

Grimm, B. (1998). Novel insights in the control of tetrapyrrole metabolism of higher plants. Current opinion in plant biology **1,** 245-250.

Grimm, B. (2003). Regulatory mechanisms of eukaryotic tetrapyrrole biosynthesis. In The porphyrin handbook (Elsevier), pp. 1-32.

Grimm, B., Porra, R.J., Rüdiger, W., and Scheer, H. (2007). Chlorophylls and bacteriochlorophylls: biochemistry, biophysics, functions and applications. (Springer Science & Business Media).

Hamilton, J.W., Bement, W.J., Sinclair, P.R., Sinclair, J.F., Alcedo, J.A., and Wetterhahn, K.E. (1991). Heme regulates hepatic 5-aminolevulinate synthase mRNA expression by decreasing mRNA half-life and not by altering its rate of transcription. Archives of biochemistry and biophysics **289,** 387-392.

Hansson, M., and Kannangara, C.G. (1997). ATPases and phosphate exchange activities in magnesium chelatase subunits of Rhodobacter sphaeroides. Proceedings of the National Academy of Sciences **94,** 13351-13356.

Hartel, H., Kruse, E., and Grimm, B. (1997). Restriction of chlorophyll synthesis due to expression of glutamate 1-semialdehyde aminotransferase antisense RNA does not reduce the light-harvesting antenna size in tobacco. Plant physiology **113,** 1113-1124.

Heinemann, I.U., Jahn, M., and Jahn, D. (2008). The biochemistry of heme biosynthesis. Archives of biochemistry and biophysics **474,** 238-251.

Hennig, M., Grimm, B., Contestabile, R., John, R.A., and Jansonius, J.N. (1997). Crystal structure of glutamate-1-semialdehyde aminomutase: an α2-dimeric vitamin B6-dependent enzyme with asymmetry in structure and active site reactivity. Proceedings of the National Academy of Sciences **94,** 4866-4871.

Herman, C.A., Im, C.-s., and Beale, S.I. (1999). Light-regulated expression of the gsa gene encoding the chlorophyll biosynthetic enzyme glutamate 1-semialdehyde aminotransferase in carotenoid-deficient Chlamydomonas reinhardtii cells. Plant molecular biology **39,** 289-297.

Hermann, S. (2006). Tricine-SDS-PAGE. Nat Protoc **1,** 16-22.

Hernández, I., Alegre, L., Van Breusegem, F., and Munné-Bosch, S. (2009). How relevant are flavonoids as antioxidants in plants? Trends in plant science **14,** 125-132.

Hey, D., Rothbart, M., Herbst, J., Wang, P., Müller, J., Wittmann, D., Gruhl, K., and Grimm, B. (2017). LIL3, a light-harvesting complex protein, links terpenoid and tetrapyrrole biosynthesis in Arabidopsis thaliana. Plant physiology **174,** 1037-1050.

Hinchigeri, S.B., Hundle, B., and Richards, W.R. (1997). Demonstration that the BchH protein of Rhodobacter capsulatus activates S‐adenosyl‐l‐methionine: magnesium protoporphyrin IX methyltransferase. FEBS letters **407,** 337-342.

Hou, S., Reynolds, M.F., Horrigan, F.T., Heinemann, S.H., and Hoshi, T. (2006). Reversible binding of heme to proteins in cellular signal transduction. Accounts of chemical research **39,** 918-924.

Hu, Q., Miyashita, H., Iwasaki, I., Kurano, N., Miyachi, S., Iwaki, M., and Itoh, S. (1998). A photosystem I reaction center driven by chlorophyll d in oxygenic photosynthesis. Proceedings of the National Academy of Sciences **95,** 13319-13323.

Huang, L., Bonner, B.A., and Castelfranco, P.A. (1989). Regulation of 5-Aminolevulinic Acid (ALA) Synthesis in Developing Chloroplasts: II. Regulation of ALA-Synthesizing Capacity by Phytochrome. Plant physiology **90,** 1003-1008.

Ilag, L.L., Kumar, A.M., and Söll, D. (1994). Light regulation of chlorophyll biosynthesis at the level of 5-aminolevulinate formation in Arabidopsis. The Plant Cell **6,** 265-275.

Järvi, S., Suorsa, M., Paakkarinen, V., and Aro, E.-M. (2011). Optimized native gel systems for separation of thylakoid protein complexes: novel super-and mega-complexes. Biochemical Journal **439,** 207-214.

Jacobs, J.M., and Jacobs, N.J. (1987). Oxidation of protoporphyrinogen to protoporphyrin, a step in chlorophyll and haem biosynthesis. Purification and partial

characterization of the enzyme from barley organelles. Biochemical journal **244,** 219-224.

Jung, H.-S., Okegawa, Y., Shih, P.M., Kellogg, E., Abdel-Ghany, S.E., Pilon, M., Sjölander, K., Shikanai, T., and Niyogi, K.K. (2010). Arabidopsis thaliana PGR7 encodes a conserved chloroplast protein that is necessary for efficient photosynthetic electron transport. PLoS One **5,** e11688.

Juszczak, I., Rudnik, R., Pietzenuk, B., and Baier, M. (2012). Natural genetic variation in the expression regulation of the chloroplast antioxidant system among Arabidopsis thaliana accessions. Physiologia plantarum **146,** 53-70.

Kaiser, E., Morales, A., and Harbinson, J. (2018). Fluctuating light takes crop photosynthesis on a rollercoaster ride. Plant Physiology **176,** 977-989.

Kannangara, C.G., and Gough, S.P. (1977). Synthesis of δ-aminolevulinic acid and chlorophyll by isolated chloroplasts. Carlsberg Research Communications **42,** 441.

Kasemir, H. (1983). Light control of chlorophyll accumulation in higher plants. In Photomorphogenesis (Springer), pp. 662-686.

Kauss, D., Bischof, S., Steiner, S., Apel, K., and Meskauskiene, R. (2012a). FLU, a negative feedback regulator of tetrapyrrole biosynthesis, is physically linked to the final steps of the Mg++ ‐ branch of this pathway. FEBS letters **586,** 211-216.

Kauss, D., Bischof, S., Steiner, S., Apel, K., and Meskauskiene, R. (2012b). FLU, a negative feedback regulator of tetrapyrrole biosynthesis, is physically linked to the final steps of the Mg++-branch of this pathway. FEBS letters **586,** 211-216.

Kendrick, R.E., and Kronenberg, G.H. (2012). Photomorphogenesis in plants. (Springer Science & Business Media).

Kikuchi, G., and Hayashi, N. (1981). Regulation by heme of synthesis and intracellular translocation of δ-aminolevulinate synthase in the liver. Molecular and cellular biochemistry **37,** 27-41.

Kilian, J., Whitehead, D., Horak, J., Wanke, D., Weinl, S., Batistic, O., D’ Angelo, C., Bornberg ‐ Bauer, E., Kudla, J., and Harter, K. (2007). The AtGenExpress global stress expression data set: protocols, evaluation and model data analysis of UV ‐ B light, drought and cold stress responses. The Plant Journal 50, 347-363.

Kimura, M., Yamamoto, Y.Y., Seki, M., Sakurai, T., Sato, M., Abe, T., Yoshida, S., Manabe, K., Shinozaki, K., and Matsui, M. (2003). Identification of Arabidopsis Genes Regulated by High Light–Stress Using cDNA Microarray¶. Photochemistry and Photobiology **77,** 226-233.

Kobayashi, K., and Masuda, T. (2016). Transcriptional regulation of tetrapyrrole biosynthesis in Arabidopsis thaliana. Frontiers in plant science **7,** 1811.

Kohchi, T., Mukougawa, K., Frankenberg, N., Masuda, M., Yokota, A., and Lagarias, J.C. (2001). The Arabidopsis HY2 gene encodes phytochromobilin synthase, a ferredoxin-dependent biliverdin reductase. The Plant Cell **13,** 425-436.

Koski, V.M., and Smith, J.H. (1948). The isolation and spectral absorption properties of protochlorophyll from etiolated barley seedlings. Journal of the American Chemical Society **70,** 3558-3562.

Kovacheva, S., Bédard, J., Patel, R., Dudley, P., Twell, D., Ríos, G., Koncz, C., and Jarvis, P. (2005). In vivo studies on the roles of Tic110, Tic40 and Hsp93 during chloroplast protein import. The Plant Journal **41,** 412-428.

Kruse, E., Grimm, B., Beator, J., and Kloppstech, K. (1997). Developmental and circadian control of the capacity for δ-aminolevulinic acid synthesis in green barley. Planta **202,** 235-241.

Kubota, Y., Nomura, K., Katoh, Y., Yamashita, R., Kaneko, K., and Furuyama, K. (2016). Novel mechanisms for heme-dependent degradation of ALAS1 protein as a component of negative feedback regulation of heme biosynthesis. Journal of Biological Chemistry **291,** 20516-20529.

Kumar, A.M., and Söll, D. (2000). Antisense HEMA1 RNA expression inhibits heme and chlorophyll biosynthesis in Arabidopsis. Plant physiology **122,** 49-56.

Kumar, A.M., Schaub, U., Söll, D., and Ujwal, M.L. (1996). Glutamyl-transfer RNA: at the crossroad between chlorophyll and protein biosynthesis. Trends in Plant Science **1,** 371-376.

Laloi, C., and Havaux, M. (2015). Key players of singlet oxygen-induced cell death in plants. Frontiers in plant science **6,** 39.

Lamppa, G.K. (1988). The chlorophyll a/b-binding protein inserts into the thylakoids independent of its cognate transit peptide. Journal of Biological Chemistry **263,** 14996-14999.

Larkin, R.M., Alonso, J.M., Ecker, J.R., and Chory, J. (2003). GUN4, a regulator of chlorophyll synthesis and intracellular signaling. Science **299,** 902-906.

Lauriére, M. (1993). A semidry electroblotting system efficiently transfers both high-and low-molecular-weight proteins separated by SDS-PAGE. Analytical biochemistry **212,** 206-211.

Lebedev, N., Van Cleve, B., Armstrong, G., and Apel, K. (1995). Chlorophyll synthesis in a deetiolated (det340) mutant of Arabidopsis without NADPH-Protochlorophyllide (Pchlide) oxidoreductase (POR) A and photoactive Pchlide-F655. The Plant Cell **7,** 2081-2090.

Ledford, H.K., and Niyogi, K.K. (2005). Singlet oxygen and photo‐oxidative stress management in plants and algae. Plant, Cell & Environment **28,** 1037-1045.

Lee, K.P., Kim, C., Lee, D.W., and Apel, K. (2003). TIGRINA d, required for regulating the biosynthesis of tetrapyrroles in barley, is an ortholog of the FLU gene of Arabidopsis thaliana 1. Febs Letters **553,** 119-124.

Legnaioli, T., Cuevas, J., and Mas, P. (2009). TOC1 functions as a molecular switch connecting the circadian clock with plant responses to drought. The EMBO journal **28,** 3745-3757.

Leister, D., and Kleine, T. (2016). Definition of a core module for the nuclear retrograde response to altered organellar gene expression identifies GLK overexpressors as gun mutants. Physiologia plantarum **157,** 297-309.

Leivar, P., and Quail, P.H. (2011). PIFs: pivotal components in a cellular signaling hub. Trends in plant science **16,** 19-28.

Lermontova, I., Kruse, E., Mock, H.-P., and Grimm, B. (1997). Cloning and characterization of a plastidal and a mitochondrial isoform of tobacco protoporphyrinogen IX oxidase. Proceedings of the National Academy of Sciences **94,** 8895-8900.

Levicán, G., Katz, A., De Armas, M., Núñez, H., and Orellana, O. (2007). Regulation of a glutamyl-tRNA synthetase by the heme status. Proceedings of the National Academy of Sciences **104,** 3135-3140.

Lister, R., Chew, O., Rudhe, C., Lee, M.-N., and Whelan, J. (2001). Arabidopsis thaliana ferrochelatase‐I and‐II are not imported into Arabidopsis mitochondria. FEBS letters **506,** 291-295.

Luo, T., Fan, T., Liu, Y., Rothbart, M., Yu, J., Zhou, S., Grimm, B., and Luo, M. (2012). Thioredoxin redox regulates ATPase activity of magnesium chelatase CHLI subunit and modulates redox-mediated signaling in tetrapyrrole biosynthesis and homeostasis of reactive oxygen species in pea plants. Plant Physiology **159,** 118-130.

Mano, M.M., and Kime, C.R. (2001). Logic and Computer Design Fundamentals 2nd Edition Updated. (Chapter).

Masuda, T., Ohta, H., Shioi, Y., Tsuji, H., and Takamiya, K.-i. (1995). Stimulation of glutamyl-tRNA reductase activity by benzyladenine in greening cucumber cotyledons. Plant and cell physiology **36,** 1237-1243.

Masuda, T., Suzuki, T., Shimada, H., Ohta, H., and Takamiya, K. (2003a). Subcellular localization of two types of ferrochelatase in cucumber. Planta **217,** 602-609.

Masuda, T., Fusada, N., Oosawa, N., Takamatsu, K.i., Yamamoto, Y.Y., Ohto, M., Nakamura, K., Goto, K., Shibata, D., and Shirano, Y. (2003b). Functional analysis of isoforms of NADPH: protochlorophyllide oxidoreductase (POR), PORB and PORC, in Arabidopsis thaliana. Plant and cell physiology 44, 963-974.

Matsumoto, F., Obayashi, T., Sasaki-Sekimoto, Y., Ohta, H., Takamiya, K.-i., and Masuda, T. (2004). Gene expression profiling of the tetrapyrrole metabolic pathway in Arabidopsis with a mini-array system. Plant Physiology **135,** 2379-2391.

McCormac, A.C., and Terry, M.J. (2002). Light‐signalling pathways leading to the co‐ordinated expression of HEMA1 and Lhcb during chloroplast development in Arabidopsis thaliana. The Plant Journal **32,** 549-559.

McCormac, A.C., Fischer, A., Kumar, A.M., Söll, D., and Terry, M.J. (2001). Regulation of HEMA1 expression by phytochrome and a plastid signal during de‐etiolation in Arabidopsis thaliana. The Plant Journal **25,** 549-561.

Meskauskiene, R., and Apel, K. (2002). Interaction of FLU, a negative regulator of tetrapyrrole biosynthesis, with the glutamyl‐tRNA reductase requires the tetratricopeptide repeat domain of FLU. FEBS letters **532,** 27-30.

Meskauskiene, R., Nater, M., Goslings, D., Kessler, F., op den Camp, R., and Apel, K. (2001). FLU: a negative regulator of chlorophyll biosynthesis in Arabidopsis thaliana. Proceedings of the national academy of sciences **98,** 12826-12831.

Michalska, J., Zauber, H., Buchanan, B.B., Cejudo, F.J., and Geigenberger, P. (2009). NTRC links built-in thioredoxin to light and sucrose in regulating starch synthesis in chloroplasts and amyloplasts. Proceedings of the National Academy of Sciences **106,** 9908-9913.

Michl, D., Robinson, C., Shackleton, J.B., Herrmann, R.G., and Klösgen, R. (1994). Targeting of proteins to the thylakoids by bipartite presequences: CFoII is imported by a novel, third pathway. The EMBO journal **13,** 1310-1317.

Moon, J., Zhu, L., Shen, H., and Huq, E. (2008). PIF1 directly and indirectly regulates chlorophyll biosynthesis to optimize the greening process in Arabidopsis. Proceedings of the National Academy of Sciences **105,** 9433-9438.

Moser, J., Schubert, W.D., Beier, V., Bringemeier, I., Jahn, D., and Heinz, D.W. (2001). V‐shaped structure of glutamyl‐tRNA reductase, the first enzyme of tRNA‐dependent tetrapyrrole biosynthesis. The EMBO journal **20,** 6583-6590.

Muramoto, T., Tsurui, N., Terry, M.J., Yokota, A., and Kohchi, T. (2002). Expression and biochemical properties of a ferredoxin-dependent heme oxygenase required for phytochrome chromophore synthesis. Plant Physiology **130,** 1958-1966.

Murray, D.L., and Kohorn, B.D. (1991). Chloroplasts of Arabidopsis thaliana homozygous for the ch-1 locus lack chlorophyll b, lack stable LHCPII and have stacked thylakoids. Plant molecular biology **16,** 71-79.

Nagai, D., Kravtsov, A.V., and Vikhlinin, A. (2007). Effects of galaxy formation on thermodynamics of the intracluster medium. The Astrophysical Journal **668,** 1.

Narita, S.-i., Tanaka, R., Ito, T., Okada, K., Taketani, S., and Inokuchi, H. (1996). Molecular cloning and characterization of a cDNA that encodes protoporphyrinogen oxidase of Arabidopsis thaliana. Gene **182,** 169-175.

Nielsen, O.F. (1974). Macromolecular physiology of plastids XII. Tigrina mutants in barley: genetic, spectroscopic and structural characterization. Hereditas **76,** 269-303.

Nishimura, K., Kato, Y., and Sakamoto, W. (2016). Chloroplast proteases: updates on proteolysis within and across suborganellar compartments. Plant Physiology **171,** 2280-2293.

Nishimura, K., Kato, Y., and Sakamoto, W. (2017). Essentials of proteolytic machineries in chloroplasts. Molecular plant **10,** 4-19.

Nishimura, K., Asakura, Y., Friso, G., Kim, J., Oh, S.-h., Rutschow, H., Ponnala, L., and van Wijk, K.J. (2013). ClpS1 is a conserved substrate selector for the chloroplast Clp protease system in Arabidopsis. The Plant Cell **25,** 2276-2301.

Niyogi, K.K. (1999). Photoprotection revisited: genetic and molecular approaches. Annual review of plant biology **50,** 333-359.

Oñate-Sánchez, L., and Vicente-Carbajosa, J. (2008). DNA-free RNA isolation protocols for Arabidopsis thaliana, including seeds and siliques. BMC research notes **1,** 93.

Olinares, P.D.B., Kim, J., and van Wijk, K.J. (2011). The Clp protease system; a central component of the chloroplast protease network. Biochimica Et Biophysica Acta (BBA)-Bioenergetics **1807,** 999-1011.

op den Camp, R.G., Przybyla, D., Ochsenbein, C., Laloi, C., Kim, C., Danon, A., Wagner, D., Hideg, É., Göbel, C., and Feussner, I. (2003). Rapid induction of distinct stress responses after the release of singlet oxygen in Arabidopsis. The Plant Cell 15, 2320-2332.

Pérez-Ruiz, J.M., Spínola, M.C., Kirchsteiger, K., Moreno, J., Sahrawy, M., and Cejudo, F.J. (2006). Rice NTRC is a high-efficiency redox system for chloroplast protection against oxidative damage. The Plant Cell **18,** 2356-2368.

Paddock, T., Lima, D., Mason, M.E., Apel, K., and Armstrong, G.A. (2012). Arabidopsis light-dependent protochlorophyllide oxidoreductase A (PORA) is essential for normal plant growth and development. Plant molecular biology **78,** 447-460.

Papenbrock, J., Mock, H.-P., Tanaka, R., Kruse, E., and Grimm, B. (2000). Role of magnesium chelatase activity in the early steps of the tetrapyrrole biosynthetic pathway. Plant Physiology **122,** 1161-1170.

Pazderník, M., Mareš, J., Pilný, J., and Sobotka, R. (2019). The antenna-like domain of the cyanobacterial ferrochelatase can bind chlorophyll and carotenoids in an energy-dissipative configuration. Journal of Biological Chemistry**,** jbc. RA119. 008434.

Pfannschmidt, T. (2003). Chloroplast redox signals: how photosynthesis controls its own genes. Trends in plant science **8,** 33-41.

Plumley, G., and Schmidt, G.W. (1995). Light-harvesting chlorophyll a/b complexes: interdependent pigment synthesis and protein assembly. The Plant Cell **7,** 689-704.

Ponka, P. (1997). Tissue-specific regulation of iron metabolism and heme synthesis: distinct control mechanisms in erythroid cells. Blood **89,** 1-25.

Pontoppidan, B., and Kannangara, C.G. (1994). Purification and partial characterisation of barley glutamyl‐tRNAGlu reductase, the enzyme that directs glutamate to chlorophyll biosynthesis. European journal of biochemistry **225,** 529-537.

Porra, R., Thompson, W., and Kriedemann, P. (1989). Determination of accurate extinction coefficients and simultaneous equations for assaying chlorophylls a and b extracted with four different solvents: verification of the concentration of chlorophyll standards by atomic absorption spectroscopy. Biochimica et Biophysica Acta (BBA)-Bioenergetics **975,** 384-394.

Przybyla, D., Göbel, C., Imboden, A., Hamberg, M., Feussner, I., and Apel, K. (2008). Enzymatic, but not non‐enzymatic, 1O2‐mediated peroxidation of polyunsaturated fatty acids forms part of the EXECUTER1‐dependent stress response program in the flu mutant of Arabidopsis thaliana. The Plant Journal **54,** 236-248.

Quail, P.H., Boylan, M.T., Parks, B.M., Short, T.W., Xu, Y., and Wagner, D. (1995). Phytochromes: photosensory perception and signal transduction. Science **268,** 675-680.

Rüdiger, W. (1997). Chlorophyll metabolism: from outer space down to the molecular level. Phytochemistry **46,** 1151-1167.

Ratinaud, M.H., Thomes, J.C., and Julien, R. (1983). Glutamyl-tRNA synthetases from wheat. Isolation and characterization of three dimeric enzymes. European journal of biochemistry **135,** 471-477.

Reinbothe, S., Reinbothe, C., Apel, K., and Lebedev, N. (1996). Evolution of chlorophyll biosynthesis—the challenge to survive photooxidation. Cell **86,** 703-705.

Richter, A., and Grimm, B. (2019). The multifaceted regulation of 5-aminolevulinic acid synthesis. Numerous ways to control glutamyl-tRNA reductase. Metabolism, Structure and Function of Plant Tetrapyrroles: Control Mechanisms of Chlorophyll Biosynthesis and Analysis of Chlorophyll-Binding Proteins**,** 69.

Richter, A., Peter, E., Pörs, Y., Lorenzen, S., Grimm, B., and Czarnecki, O. (2010). Rapid dark repression of 5-aminolevulinic acid synthesis in green barley leaves. Plant and cell physiology **51,** 670-681.

Richter, A.S., and Grimm, B. (2013). Thiol-based redox control of enzymes involved in the tetrapyrrole biosynthesis pathway in plants. Frontiers in plant science **4,** 371.

Richter, A.S., Wang, P., and Grimm, B. (2016). Arabidopsis Mg-protoporphyrin IX methyltransferase activity and redox regulation depend on conserved cysteines. Plant and Cell Physiology **57,** 519-527.

Richter, A.S., Banse, C., and Grimm, B. (2019). The GluTR-binding protein is the heme-binding factor for feedback control of glutamyl-tRNA reductase. eLife **8,** e46300.

Richter, A.S., Pérez‐Ruiz, J.M., Cejudo, F.J., and Grimm, B. (2018). Redox‐control of chlorophyll biosynthesis mainly depends on thioredoxins. FEBS letters **592,** 3111-3115.

Richter, A.S., Peter, E., Rothbart, M., Schlicke, H., Toivola, J., Rintamäki, E., and Grimm, B. (2013). Posttranslational influence of NADPH-dependent thioredoxin reductase C on enzymes in tetrapyrrole synthesis. Plant physiology **162,** 63-73.

Rieble, S., and Beale, S.I. (1991). Separation and partial characterization of enzymes catalyzing δ-aminolevulinic acid formation in Synechocystis sp. PCC 6803. Archives of biochemistry and biophysics **289,** 289-297.

Robinson, C., Thompson, S.J., and Woolhead, C. (2001). Multiple pathways used for the targeting of thylakoid proteins in chloroplasts. Traffic **2,** 245-251.

Rogers, K.C., and Söll, D. (1995). Divergence of glutamate and glutamine aminoacylation pathways: providing the evolutionary rationale for mischarging. Journal of molecular evolution **40,** 476-481.

Rosano, G.L., Bruch, E.M., and Ceccarelli, E.A. (2011). Insights into the Clp/HSP100 chaperone system from chloroplasts of Arabidopsis thaliana. Journal of Biological Chemistry **286,** 29671-29680.

Salome, P.A., Oliva, M., Weigel, D., and Krämer, U. (2013). Circadian clock adjustment to plant iron status depends on chloroplast and phytochrome function. The EMBO journal **32,** 511-523.

Sangwan, I., and O'Brian, M.R. (1999). Expression of a soybean gene encoding the tetrapyrrole-synthesis enzyme glutamyl-tRNA reductase in symbiotic root nodules. Plant physiology **119,** 593-598.

Santana, M.A., Tan, F.-C., and Smith, A.G. (2002). Molecular characterisation of coproporphyrinogen oxidase from Glycine max and Arabidopsis thaliana. Plant Physiology and Biochemistry **40,** 289-298.

Schmied, J., Hedtke, B., and Grimm, B. (2011). Overexpression of HEMA1 encoding glutamyl-tRNA reductase. Journal of plant physiology **168,** 1372-1379.

Schmied, J., Hou, Z., Hedtke, B., and Grimm, B. (2018). Controlled partitioning of glutamyl-tRNA reductase in stroma-and membrane-associated fractions affects the synthesis of 5-aminolevulinic acid. Plant and Cell Physiology **59,** 2204-2213.

Schulze, J.O., Schubert, W.-D., Moser, J., Jahn, D., and Heinz, D.W. (2006a). Evolutionary relationship between initial enzymes of tetrapyrrole biosynthesis. Journal of molecular biology **358,** 1212-1220.

Schulze, J.O., Masoumi, A., Nickel, D., Jahn, M., Jahn, D., Schubert, W.-D., and Heinz, D.W. (2006b). Crystal structure of a non-discriminating glutamyl-tRNA synthetase. Journal of molecular biology **361,** 888-897.

Shen, Y.-Y., Wang, X.-F., Wu, F.-Q., Du, S.-Y., Cao, Z., Shang, Y., Wang, X.-L., Peng, C.-C., Yu, X.-C., and Zhu, S.-Y. (2006). The Mg-chelatase H subunit is an abscisic acid receptor. Nature 443, 823.

Shin, J., Kwon, Y.D., Kwon, O., Lee, H.S., and Kim, P. (2007). 5-Aminolevulinic acid biosynthesis in Escherichia coli coexpressing NADP-dependent malic enzyme and 5-aminolevulinate synthase. Journal of microbiology and biotechnology **17,** 1579.

Slattery, R.A., Walker, B.J., Weber, A.P., and Ort, D.R. (2018). The impacts of fluctuating light on crop performance. Plant physiology **176,** 990-1003.

Smith, A.G., Marsh, O., and Elder, G.H. (1993). Investigation of the subcellular location of the tetrapyrrole-biosynthesis enzyme coproporphyrinogen oxidase in higher plants. Biochemical Journal **292,** 503-508.

Sobotka, R., Tichy, M., Wilde, A., and Hunter, C.N. (2011). Functional assignments for the carboxyl-terminal domains of the ferrochelatase from Synechocystis PCC 6803: the CAB domain plays a regulatory role, and region II is essential for catalysis. Plant physiology **155,** 1735-1747.

Song, Y., Pu, H., Jiang, T., Zhang, L., and Ouyang, M. (2016). Crystal structure of glutamate-1-semialdehyde-2, 1-aminomutase from Arabidopsis thaliana. Acta Crystallographica Section F: Structural Biology Communications **72,** 448-456.

Stange-Thomann, N., Thomann, H.-U., Lloyd, A.J., Lyman, H., and Söll, D. (1994). A point mutation in Euglena gracilis chloroplast tRNA (Glu) uncouples protein and chlorophyll biosynthesis. Proceedings of the National Academy of Sciences **91,** 7947-7951.

Stephenson, P.G., and Terry, M.J. (2008). Light signalling pathways regulating the Mg-chelatase branchpoint of chlorophyll synthesis during de-etiolation in Arabidopsis thaliana. Photochemical & Photobiological Sciences **7,** 1243-1252.

Stobart, A.K., and Ameen-Bukhari, I. (1986). Photoreduction of protochlorophyllide and its relationship to δ-aminolaevulinic acid synthesis in the leaves of dark-grown barley (Hordeum vulgare) seedlings. Biochemical journal **236,** 741-748.

Strain, H.H., Thomas, M.R., and Katz, J.J. (1963). Spectral absorption properties of ordinary and fully deuteriated chlorophylls a and b. Biochimica et biophysica acta **75,** 306-311.

Su, Q., Frick, G., Armstrong, G., and Apel, K. (2001). POR C of Arabidopsis thaliana: a third light-and NADPH-dependent protochlorophyllide oxidoreductase that is differentially regulated by light. Plant molecular biology **47,** 805-813.

Suzuki, H., Tashiro, S., Hira, S., Sun, J., Yamazaki, C., Zenke, Y., Ikeda‐Saito, M., Yoshida, M., and Igarashi, K. (2004). Heme regulates gene expression by triggering Crm1‐dependent nuclear export of Bach1. The EMBO journal **23,** 2544-2553.

Suzuki, J.Y., Bollivar, D.W., and Bauer, C.E. (1997). Genetic analysis of chlorophyll biosynthesis. Annual review of genetics **31,** 61-89.

Suzuki, T., Masuda, T., Singh, D.P., Tan, F.-C., Tsuchiya, T., Shimada, H., Ohta, H., Smith, A.G., and Takamiya, K.-i. (2002). Two types of ferrochelatase in photosynthetic and nonphotosynthetic tissues of cucumber their difference in phylogeny, gene expression, and localization. Journal of Biological Chemistry **277,** 4731-4737.

Takahashi, K., Takabayashi, A., Tanaka, A., and Tanaka, R. (2014). Functional analysis of light-harvesting-like protein 3 (LIL3) and its light-harvesting chlorophyll-binding motif in Arabidopsis. Journal of biological chemistry **289,** 987-999.

Tanaka, R., and Tanaka, A. (2007). Tetrapyrrole biosynthesis in higher plants. Annu. Rev. Plant Biol. **58,** 321-346.

Tanaka, R., Kobayashi, K., and Masuda, T. (2011). Tetrapyrrole metabolism in Arabidopsis thaliana. The Arabidopsis book/American Society of Plant Biologists **9**.

Tanaka, R., Yoshida, K., Nakayashiki, T., Masuda, T., Tsuji, H., Inokuchi, H., and Tanaka, A. (1996). Differential expression of two hemA mRNAs encoding glutamyl-tRNA reductase proteins in greening cucumber seedlings. Plant physiology **110,** 1223-1230.

Terry, M.J., and Kendrick, R.E. (1996). The aurea and yellow-green-2 mutants of tomato are deficient in phytochrome chromophore synthesis. Journal of Biological Chemistry **271,** 21681-21686.

Terry, M.J., and Kendrick, R.E. (1999). Feedback Inhibition of Chlorophyll Synthesis in the Phytochrome Chromophore-Deficient aurea andyellow-green-2 Mutants of Tomato. Plant Physiology **119,** 143-152.

Thomas, J., and Weinstein, J.D. (1990). Measurement of heme efflux and heme content in isolated developing chloroplasts. Plant physiology **94,** 1414-1423.

Toyokura, K., Yamaguchi, K., Shigenobu, S., Fukaki, H., Tatematsu, K., and Okada, K. (2015). Mutations in plastidial 5-aminolevulinic acid biosynthesis genes suppress a

pleiotropic defect in shoot development of a mitochondrial gaba shunt mutant in Arabidopsis. Plant and Cell Physiology **56,** 1229-1238.

Ujwal, M., McCormac, A.C., Goulding, A., Kumar, A.M., Söll, D., and Terry, M.J. (2002). Divergent regulation of the HEMA gene family encoding glutamyl-tRNA reductase in Arabidopsis thaliana: expression of HEMA2 is regulated by sugars, but is independent of light and plastid signalling. Plant molecular biology **50,** 81-89.

Van Lis, R., Atteia, A., Nogaj, L.A., and Beale, S.I. (2005). Subcellular localization and light-regulated expression of protoporphyrinogen IX oxidase and ferrochelatase in Chlamydomonas reinhardtii. Plant physiology **139,** 1946-1958.

Vasileuskaya, Z., Oster, U., and Beck, C.F. (2005). Mg-protoporphyrin IX and heme control HEMA, the gene encoding the first specific step of tetrapyrrole biosynthesis, in Chlamydomonas reinhardtii. Eukaryotic cell **4,** 1620-1628.

von Gromoff, E.D., Alawady, A., Meinecke, L., Grimm, B., and Beck, C.F. (2008). Heme, a plastid-derived regulator of nuclear gene expression in Chlamydomonas. The Plant Cell **20,** 552-567.

Von Wettstein, D., Gough, S., and Kannangara, C.G. (1995). Chlorophyll biosynthesis. The Plant Cell **7,** 1039.

Von Wettstein, D., Kahn, A., Nielsen, O.F., and Gough, S. (1974). Genetic regulation of chlorophyll synthesis analyzed with mutants in barley. Science **184,** 800-802.

Vothknecht, U.C., Kannangara, C.G., and Von Wettstein, D. (1996). Expression of catalytically active barley glutamyl tRNAGlu reductase in Escherichia coli as a fusion protein with glutathione S-transferase. Proceedings of the National Academy of Sciences **93,** 9287-9291.

Vothknecht, U.C., Kannangara, C.G., and von Wettstein, D. (1998). Barley glutamyl tRNAGlu reductase: mutations affecting haem inhibition and enzyme activity. Phytochemistry **47,** 513-519.

Wagner, D., Przybyla, D., op den Camp, R., Kim, C., Landgraf, F., Lee, K.P., Würsch, M., Laloi, C., Nater, M., and Hideg, E. (2004). The genetic basis of singlet oxygen–induced stress responses of Arabidopsis thaliana. Science 306, 1183-1185.

Walter, M., Chaban, C., Schütze, K., Batistic, O., Weckermann, K., Näke, C., Blazevic, D., Grefen, C., Schumacher, K., and Oecking, C. (2004). Visualization of protein interactions in living plant cells using bimolecular fluorescence complementation. The Plant Journal 40, 428-438.

Wang, L., Kim, C., Xu, X., Piskurewicz, U., Dogra, V., Singh, S., Mahler, H., and Apel, K. (2016). Singlet oxygen-and EXECUTER1-mediated signaling is initiated in grana margins and depends on the protease FtsH2. Proceedings of the National Academy of Sciences **113,** E3792-E3800.

Wang, P., Liang, F.-C., Wittmann, D., Siegel, A., Shan, S.-o., and Grimm, B. (2018). Chloroplast SRP43 acts as a chaperone for glutamyl-tRNA reductase, the rate-limiting enzyme in tetrapyrrole biosynthesis. Proceedings of the National Academy of Sciences **115,** E3588-E3596.

Waters, M.T., Wang, P., Korkaric, M., Capper, R.G., Saunders, N.J., and Langdale, J.A. (2009). GLK transcription factors coordinate expression of the photosynthetic apparatus in Arabidopsis. The Plant Cell **21,** 1109-1128.

Wellburn, A. (1975). δ-Aminolaevulinic acid formation in greening Avena laminae. Phytochemistry **14,** 699-701.

Wientjes, E., Oostergetel, G.T., Jansson, S., Boekema, E.J., and Croce, R. (2009). The role of Lhca complexes in the supramolecular organization of higher plant photosystem I. Journal of Biological Chemistry **284,** 7803-7810.

Williams, P., Hardeman, K., Fowler, J., and Rivin, C. (2006). Divergence of duplicated genes in maize: evolution of contrasting targeting information for enzymes in the porphyrin pathway. The Plant Journal **45,** 727-739.

Willows, R.D., Kannangara, C.G., and Pontoppidan, B. (1995). Nucleotides of tRNA (Glu) involved in recognition by barley chloroplast glutamyl-tRNA synthetase and glutamyl-tRNA reductase. Biochimica et Biophysica Acta (BBA)-Gene Structure and Expression **1263,** 228-234.

Willows, R.D., Gibson, L.C., Kanangara, C.G., Hunter, C.N., and Von Wettstein, D. (1996). Three separate proteins constitute the magnesium chelatase of Rhodobacter sphaeroides. European journal of biochemistry **235,** 438-443.

Wind, J.J., Peviani, A., Snel, B., Hanson, J., and Smeekens, S.C. (2013). ABI4: versatile activator and repressor. Trends in plant science **18,** 125-132.

Wittmann, D., Kløve, S., Wang, P., and Grimm, B. (2018). Towards Initial Indications for a Thiol-Based Redox Control of Arabidopsis 5-Aminolevulinic Acid Dehydratase. Antioxidants **7,** 152.

Woodson, J.D., Perez-Ruiz, J.M., and Chory, J. (2011). Heme synthesis by plastid ferrochelatase I regulates nuclear gene expression in plants. Current Biology **21,** 897-903.

Yamamoto, H., and Shikanai, T. (2019). PGR5-dependent cyclic electron flow protects photosystem I under fluctuating light at donor and acceptor sides. Plant physiology **179,** 588-600.

Yaronskaya, E., Vershilovskaya, I., Poers, Y., Alawady, A.E., Averina, N., and Grimm, B. (2006). Cytokinin effects on tetrapyrrole biosynthesis and photosynthetic activity in barley seedlings. Planta **224,** 700-709.

Zavgorodnyaya, A., Papenbrock, J., and Grimm, B. (1997). Yeast 5‐aminolevulinate synthase provides additional chlorophyll precursor in transgenic tobacco. The Plant Journal **12,** 169-178.

Zhang, D.W., Yuan, S., Xu, F., Zhu, F., Yuan, M., Ye, H.X., Guo, H.Q., Lv, X., Yin, Y., and Lin, H.H. (2016). Light intensity affects chlorophyll synthesis during greening process by metabolite signal from mitochondrial alternative oxidase in A rabidopsis. Plant, cell & environment **39,** 12-25.

Zhang, M., Zhang, F., Fang, Y., Chen, X., Chen, Y., Zhang, W., Dai, H.-E., Lin, R., and Liu, L. (2015). The non-canonical tetratricopeptide repeat (TPR) domain of fluorescent (FLU) mediates complex formation with glutamyl-tRNA reductase. Journal of Biological Chemistry **290,** 17559-17565.

Zhao, A., and Han, F. (2018). Crystal structure of Arabidopsis thaliana glutamyl-tRNA Glu reductase in complex with NADPH and glutamyl-tRNA Glu reductase binding protein. Photosynthesis research **137,** 443-452.

Zhao, A., Fang, Y., Chen, X., Zhao, S., Dong, W., Lin, Y., Gong, W., and Liu, L. (2014). Crystal structure of Arabidopsis glutamyl-tRNA reductase in complex with its stimulator protein. Proceedings of the National Academy of Sciences **111,** 6630-6635.

Supplemental Figures

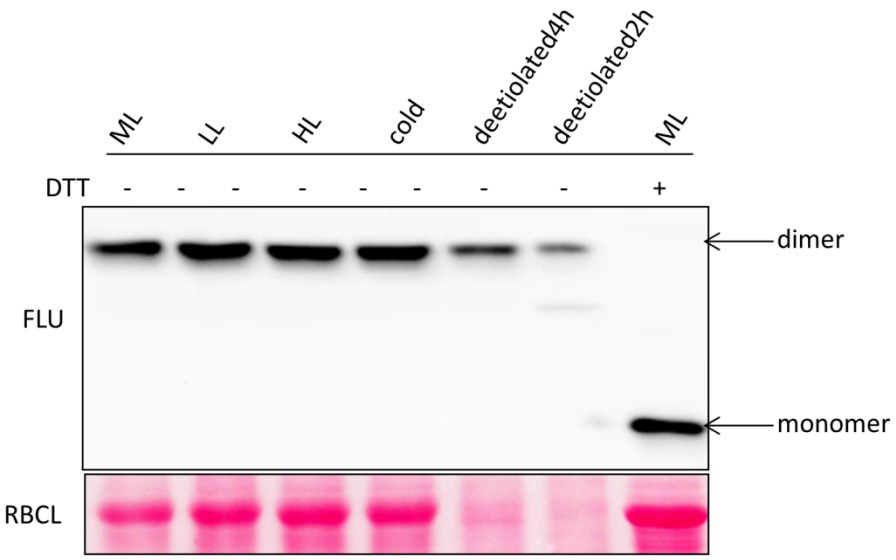

Figure S1: Western blot analysis of the disulfide-dependent FLU dimer in WT plants under various growth conditions or in the etiolated seedlings. Plants were grown under ML (120 µmol photons $m^{-2}s^{-1}$) light-dark conditions for 3 weeks and then transferred to LL (20 µmol photons $m^{-2}s^{-1}$), HL (500 µmol photons $m^{-2}s^{-1}$) or cold (4°C). De-etiolated seedlings were 4-day-old etiolated seedlings exposed to light for 4 hours or 2 hours. Total proteins were extracted under non-reducing condition (-DTT) or under reducing condition (+DTT). Arrows indicate the protein migrating at 45 kDa (the size of FLU dimer) or migrating at 23 kDa (the size of FLU monomer).

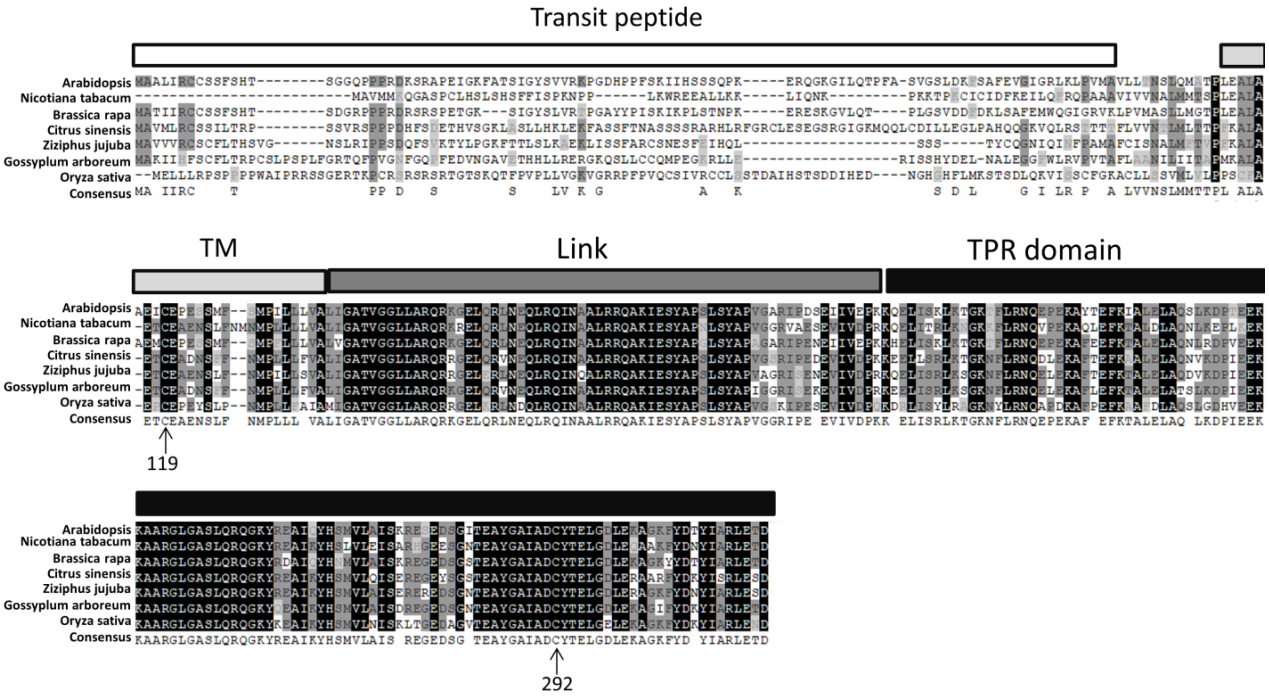

Figure S2 The alignment of FLU homologs in angiosperms. Arabidopsis (NM_001202959.1); Nicotiana tabacum (XM_016592932.1); Brassica rapa (XM_009148165.2); Citrus sinensis (XM_006465817.3); Ziziphus jujube (XM_016046254.2); Gossyplum arboretum (XM_017750835.1); Oryza sativa (XM_015769044.2). The presentations on the top of the sequences indicate the protein motifs of FLU. Arrows indicate the conserved cysteines in FLU.

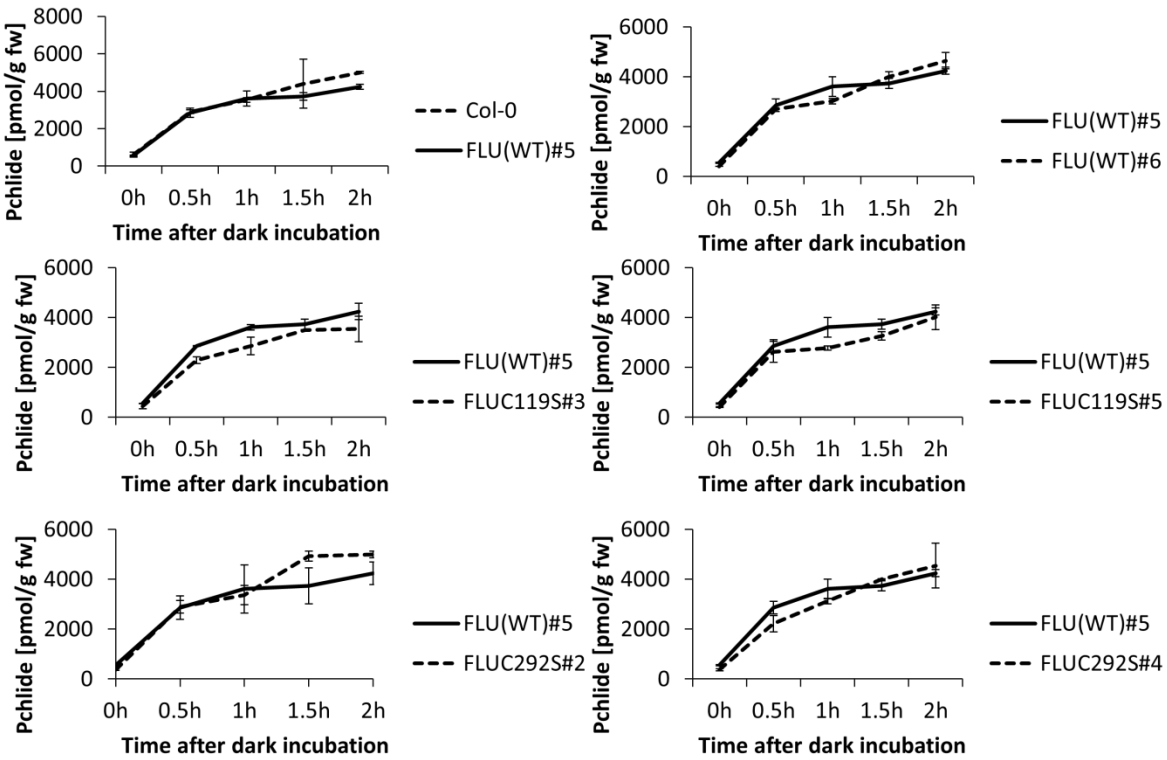

Figure S3: Pchlide accumulation in FLU(WT)#5 and FLUC119S#3 in the dark. Plants were grown under light-dark conditions for 3 weeks and then transferred to dark for 0h, 0.5h, 1h, 1.5h or 2h. FLU(WT)#5 is a *flu* complementation line by expressing the WT FLU sequence. FLUC119S#5 is a *flu* complementation line expressing a site-mutated FLU, in which the cysteine 119 is substituted with a serine.

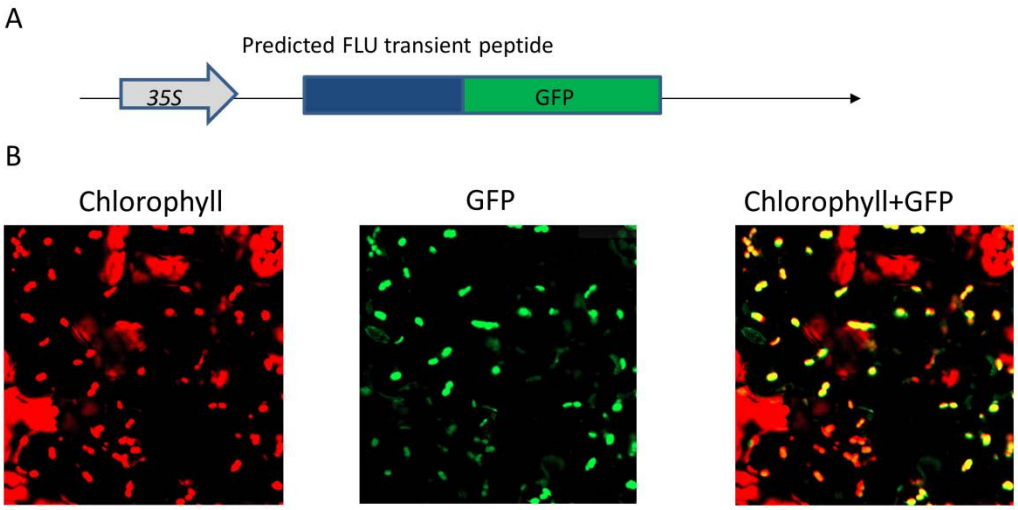

Figure S4: Transient expression of GFP fused with the N-terminus of FLU in *Nicotiana tabacum* resulted a GFP fluorescence in chloroplasts. (A) The schematic presentation showed the motifs and promoter to expressing a GFP fused protein with the predicted transit peptide of FLU (the sequence of 100 amino acids at the N-terminus of the pre-sequence of FLU). (B) The GFP fluorescence was obtained in the chloroplasts.

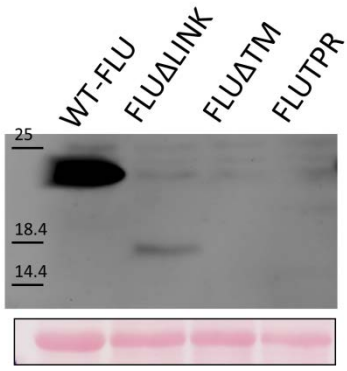

Figure S5: Western blot analysis of FLU contents in *Nicotiana tabacum* leaves transiently expressing the truncated FLU peptides or intact FLU. pGL1 indicates the transformation with the empty vector. FLUΔlink, FLUΔTM, TPR(FLU) and WT-FLU indicated that the protein samples were harvested from tabacco leaves which transiently expressing FLUΔlink, FLUΔTM, TPR(FLU) or the intact FLU from *Arabidopsis thaliana* under the control of CaMV-35S promoter.

Acknowledgement

First and foremost, I would like to express my sincere gratitude to Prof. Dr. Bernhard Grimm for offering the opportunity to carry out the experimental work in his group and for the valuable suggestions and comments on experimental design and thesis corrections. His diligence and wisdom in scientific work impressed me so much and would definitely cause a positive impact on my academic career.

I would like to give special thanks to Dr. Boris Hedtke for technical support when I started the work in the lab and also for a lot of wonderful ideas and suggestions on planning of experiments.

Thank all my colleagues and also friends in our group. They were always ready to help others and care about others. Many thanks to Yanyu Yang and Xiaoqing Pang. They cooperated with me on other projects about the regulation of ALA synthesis. Some of the conclusions in this study were also reconfirmed in their researches. I extend my sincere thanks to Dr. Peng Wang, Tingting Fan, Shuiling Ji who always enthusiastic to share their research experience with me, which has benefited me a lot. I appreciate Janina Apitz and Judith Schmied who provided me a lot of mutant lines. Many thanks also to Kersten Träder who generated the FLU overexpressing lines. A special thanks to Josephine Herbst, Daniel Wittmann, Patrick Schall, Daniel Hey who helped a lot on experiments and also on the daily life in Berlin.

I would also like to convey special thanks to Prof. Christian Schmitz-Linneweber and Prof. Dr. Thomas Pfannschmidt for reviewing my dissertation and I also thank my committee members, Prof. Kurt Zoglauer, and Dr. Christina Kühn for their willingness to assess my PhD work.

Finally, I would like to thank my fiancee, Hong Zhou and all of my family membranes. They were extremely loving and supportive, and I could not achieve anything without them.

Selbständigkeitserklärung

Hiermit erkläre ich, Zhiwei Hou, die vorliegende Arbeit selbstständig verfasst zu haben und nur unter Verwendung der angegebenen Hilfen und Hilfsmittel angefertigt zu haben. Die Dissertation wurde in dieser oder ähnlicher Form bei keiner anderen Prüfungsbehörde vorgelegt.

Zhiwei Hou

Berlin, October 2019